

PROTEIN PHOSPHATASE INHIBITOR-1 AND CDK5:  
OF MOLECULES AND MEMORY

APPROVED BY SUPERVISORY COMMITTEE

James A. Bibb, Ph.D.

---

Ilya Bezprozvanny, Ph.D.

---

Margaret A. Phillips, Ph.D.

---

Donald C. Cooper, Ph.D.

---

## DEDICATION

I would like to thank the members of my Graduate Committee and my family and friends for their support, understanding, and encouragement.

PROTEIN PHOSPHATASE INHIBITOR-1 AND CDK5:  
OF MOLECULES AND MEMORY

by

BAOCHAN NGUYEN

DISSERTATION

Presented to the Faculty of the Graduate School of Biomedical Sciences

The University of Texas Southwestern Medical Center at Dallas

In Partial Fulfillment of the Requirements

For the Degree of

DOCTOR OF PHILOSOPHY

The University of Texas Southwestern Medical Center at Dallas

Dallas, Texas

April, 2007

Copyright

by

Baochan Nguyen, 2007

All Rights Reserved

PROTEIN PHOSPHATASE INHIBITOR-1 AND CDK5:  
OF MOLECULES AND MEMORY

Baochan Nguyen, Ph.D.

The University of Texas Southwestern Medical Center at Dallas, 2007

James A. Bibb, Ph.D.

Protein phosphatase inhibitor-1 and cyclin-dependent kinase 5 (Cdk5) have been independently implicated in synaptic plasticity, learning, and memory. We began our studies with the identification, confirmation, and characterization of a novel Cdk5-dependent phosphorylation site (Ser6) on inhibitor-1. In the striatum, basal *in vivo* phosphorylation and dephosphorylation of Ser6 were mediated by Cdk5 and protein phosphatases 2A (PP-2A) and 1 (PP-1), respectively. Additionally, protein phosphatase 2B (PP-2B) contributed to dephosphorylation under conditions of high  $\text{Ca}^{2+}$ . Functionally, Cdk5-dependent phosphorylation of inhibitor-1 intramolecularly impaired dephosphorylation and deactivation of the protein, placing the activities of Cdk5 and protein kinase A (PKA) in synergism in the negative regulation of PP-1.

These studies uncovered a potential new regulatory mechanism for Cdk5. Investigation revealed that depolarization differentially regulates the Cdk5-dependent sites of inhibitor-1 and its homologue dopamine- and cAMP-regulated phosphoprotein (DARPP-32) in a cofactor- and N-methyl-D-aspartate (NMDA)

receptor-independent manner. Effects on DARPP-32 were  $\text{Ca}^{2+}$ -mediated and PP-2A-dependent, while effects on inhibitor-1 were nonselectively cation-mediated and either partially PP-2B-dependent or independent of the major serine/threonine phosphatases, depending on the site.

Given the uncertain role of inhibitor-1 in learning and memory, we next focused on identifying behaviors and substrates impacted by inhibitor-1 function. Mice constitutively lacking inhibitor-1 displayed enhanced neurogenesis and mildly impaired habituation, but normal contextual fear and novelty learning. Furthermore, levels of hippocampal inhibitor-1 were increased by voluntary wheel running, a stimulus for neurogenesis. Thus, inhibitor-1 may function in an anti-neurogenic mechanism and be more important in the direct or indirect modulation of dopamine-dependent behaviors than in the mnemonic functions of the hippocampus.

Using a whole-cell patch clamp approach, we also attempted to identify electrical properties of dentate granule cells that might be affected by Cdk5-dependent phosphorylation of inhibitor-1. Most promising among the results was a reduction in the ability of granule cells lacking inhibitor-1 to faithfully respond to high-frequency trains of stimuli. Granule cell excitability was also increased by pharmacological inhibition of Cdk5 with roscovitine. Finally, in a related study, we helped firmly establish a role for Cdk5 in hippocampal synaptic plasticity by demonstrating that conditional loss of Cdk5 enhances NMDA receptor-mediated currents, particularly of the NR2B type.

## TABLE OF CONTENTS

PRIOR PUBLICATIONS .....	xi
LIST OF FIGURES .....	xii
LIST OF ABBREVIATIONS .....	xv
<b>CHAPTER ONE.....</b>	<b>1</b>
INTRODUCTION .....	1
<b>CHAPTER TWO.....</b>	<b>7</b>
REGULATION OF PROTEIN PHOSPHATASE INHIBITOR-1 BY CYCLIN-DEPENDENT KINASE 5 .....	7
<i>Summary</i> .....	7
<i>Introduction</i> .....	8
<i>Experimental Procedures</i> .....	11
Chemicals and enzymes .....	11
Subcloning .....	13
Site-directed mutagenesis .....	13
Purification of inhibitor-1 .....	14
In vitro protein phosphorylation reactions .....	15
In vitro protein dephosphorylation reactions .....	16
Phosphopeptide maps and phosphoamino acid analysis.....	19
Phosphorylation site identification by mass spectrometry.....	19
Generation of phosphorylation state-specific antibodies .....	20
Immunohistochemistry .....	20
Preparation and incubation of acute slices.....	21
Transfection of PC12 cells.....	22
Immunoblot analysis of cell and tissue homogenates.....	23
Nuclear magnetic resonance .....	24
Data analysis .....	25

<i>Results</i> .....	25
Discovery, identification, and confirmation of Ser6 as a novel Cdk5 site of inhibitor-1.....	25
Demonstration of the in vivo phosphorylation of inhibitor-1 at Ser6.....	28
In vivo phosphorylation of inhibitor-1 by Cdk5 at Ser6.....	29
In vivo dephosphorylation of inhibitor-1 by PP-2A, PP-1, and calcineurin at Ser6.....	31
Functional significance of Cdk5-dependent phosphorylation of inhibitor-1 in vitro.....	34
Functional significance of Cdk5-dependent phosphorylation of inhibitor-1 in vivo .....	36
Structural effects of phosphomimetic mutation of inhibitor-1 at the Cdk5 sites.....	39
<i>Discussion</i> .....	39
<b>CHAPTER THREE .....</b>	<b>64</b>
DIFFERENTIAL REGULATION OF THE CDK5-DEPENDENT PHOSPHORYLATION SITES OF INHIBITOR-1 AND DARPP-32 BY DEPOLARIZATION.....	64
<i>Summary</i> .....	64
<i>Introduction</i> .....	65
<i>Experimental Procedures</i> .....	69
Drugs.....	69
Preparation and incubation of acute striatal slices.....	69
Immunoblots and data analysis.....	70
<i>Results</i> .....	70
Dose-dependent reduction of three Cdk5-dependent phosphorylation sites by NMDA, independent of changes in levels of p35 and p25 .....	70



Evaluation of the role of Cdk5-activating cofactors .....	71
Evaluation of the role of protein phosphatases .....	73
Evaluation of potential modulation by dopamine .....	75
Evaluation of the roles of calpain and PKC .....	76
Similar effects on the three Cdk5-dependent sites by other ionotropic glutamate receptor agonists and by direct depolarization .....	76
Evaluation of the role of NMDA receptors .....	78
Evaluation of the role of voltage-gated Ca <sup>2+</sup> channels .....	79
Evaluation of the role of cations .....	79
<i>Discussion</i> .....	82
<b>CHAPTER FOUR .....</b>	<b>100</b>
LOSS OF PROTEIN PHOSPHATASE INHIBITOR-1 ALTERS LEARNING AND RUNNING-INDUCED NEUROGENESIS .....	100
<i>Summary</i> .....	100
<i>Introduction</i> .....	101
<i>Experimental Procedures</i> .....	104
Subjects .....	104
Contextual fear conditioning .....	105
Immunoblots .....	106
Voluntary wheel running .....	106
Neurogenesis .....	107
Open field habituation .....	108
Novel location and object recognition .....	108
Locomotor activity .....	109
Data analysis .....	110
<i>Results</i> .....	110
Contextual fear conditioning .....	110

Voluntary wheel running and neurogenesis.....	111
Novel location and object recognition .....	112
Habituation.....	113
Biochemical targets of PP-1 and inhibitor-1.....	114
<i>Discussion</i> .....	116
<b>CHAPTER FIVE.....</b>	<b>127</b>
ELECTROPHYSIOLOGICAL CHARACTERIZATION OF MICE	
LACKING INHIBITOR-1 AND CDK5.....	127
<i>Summary</i> .....	127
<i>Introduction</i> .....	128
<i>Experimental Procedures</i> .....	130
Drugs and reagents.....	130
Slice preparation .....	130
Current-clamp recordings .....	131
Voltage-clamp recordings .....	132
Data analysis .....	133
<i>Results</i> .....	134
Characterization of dentate GCs from inhibitor-1 knockout mice.....	134
Effects of Cdk5 inhibition on GC excitability .....	137
Examination of EPSC components in CA1 pyramidal neurons from conditional Cdk5 knockout mice .....	137
<i>Discussion</i> .....	138
<b>APPENDIX A .....</b>	<b>149</b>
DATAPRO MACROS FOR USE IN IGOR .....	149
<b>BIBLIOGRAPHY .....</b>	<b>164</b>

## PRIOR PUBLICATIONS

- Wei FY, Tomizawa K, Ohshima T, Asada A, Saito T, **Nguyen C**, Bibb JA, Ishiguro K, Kulkarni AB, Pant HC, Mikoshiba K, Matsui H, Hisanaga S. (2005). Control of cyclin-dependent kinase 5 (Cdk5) activity by glutamatergic regulation of p35 stability. *J Neurochem* 93(2):502-12.
- Kansy JW, Daubner SC, Nishi A, Sotogaku N, Lloyd MD, **Nguyen C**, Lu L, Haycock JW, Hope BT, Fitzpatrick PF, Bibb JA. (2004) Identification of tyrosine hydroxylase as a physiological substrate for Cdk5. *J Neurochem* 91(2):374-84.
- Nguyen C**, Bibb JA. (2003) Cdk5 and the mystery of synaptic vesicle endocytosis. *J Cell Biol* 163(4):697-9.
- Turner RT 3rd, Loy JA, **Nguyen C**, Devasamudram T, Ghosh AK, Koelsch G, Tang J. (2002). Specificity of memapsin 1 and its implications on the design of memapsin 2 ( $\beta$ -secretase) inhibitor selectivity. *Biochemistry* 41(27):8742-6.
- Ghosh AK, Bilcer G, Harwood C, Kawahama R, Shin D, Hussain KA, Hong L, Loy JA, **Nguyen C**, Koelsch G, Ermolieff J, Tang J. (2001). Structure-based design: potent inhibitors of human brain memapsin 2 ( $\beta$ -secretase). *J Med Chem* 44(18):2865-8.

## LIST OF FIGURES

Figure 2.1. Discovery of a novel Cdk5 site on inhibitor-1 .....	47
Figure 2.2. Identification of Ser6 as the novel Cdk5 site of inhibitor-1 .....	48
Figure 2.3. Confirmation of Ser6 as the novel Cdk5 site of inhibitor-1 .....	49
Figure 2.4. Demonstration of the <i>in vivo</i> phosphorylation of inhibitor-1 at Ser6 .....	50
Figure 2.5. <i>In vivo</i> phosphorylation of inhibitor-1 by Cdk5 at Ser6.....	51
Figure 2.6. Comparison of Cdk5-dependent phosphorylation of inhibitor-1 at Ser6 and Ser67 in the hippocampus and the striatum .....	52
Figure 2.7. <i>In vivo</i> dephosphorylation of inhibitor-1 by PP-2A, PP-1, and calcineurin at Ser6 .....	53
Figure 2.8. Functional significance of Cdk5-dependent phosphorylation of inhibitor-1 <i>in vitro</i> .....	54
Figure 2.9. Functional significance of Cdk5-dependent phosphorylation of inhibitor-1 <i>in vivo</i> .....	55
Figure 2.10. Analysis of the structural effects of phosphomimetic mutation of inhibitor-1 by 2D NMR .....	56
Supplemental Figure 2.1. Disulfide-bond reduction of recombinant rat inhibitor-1 .....	57
Supplemental Figure 2.2. Specificity of antisera against phospho-Ser6 inhibitor-1 .....	58
Supplemental Figure 2.3. Immunostain for phospho-Ser6 inhibitor-1 .....	59
Supplemental Figure 2.4. Reduction in levels of phospho-Ser67 inhibitor-1 by indolinone A .....	60
Supplemental Figure 2.5. Enhancement of phosphorylation of PKA- dependent site of inhibitor-1 by roscovitine .....	61

Supplemental Figure 2.6. Effects of washout of forskolin on PKA-dependent sites of DARPP-32 and inhibitor-1 and Cdk5-dependent sites of inhibitor-1 .....	62
Supplemental Figure 2.7. Forskolin-induced changes in levels of total inhibitor-1 and phospho-Ser51 eIF2 $\alpha$ in PC12 cells .....	63
Figure 3.1. Reduction in phosphorylation of three Cdk5 sites by NMDA .....	86
Figure 3.2. Evaluation of the role of Cdk5-activating cofactors.....	87
Figure 3.3. Evaluation of the role of protein phosphatases.....	88
Figure 3.4. Evaluation of potential modulation by dopamine .....	89
Figure 3.5. Similar reductions in phosphorylation of three Cdk5 sites by AMPA, kainate, and KCl.....	90
Figure 3.6. Evaluation of the role of NMDA receptors .....	91
Figure 3.7. Evaluation of the role of voltage-gated Ca <sup>2+</sup> channels.....	92
Figure 3.8. Evaluation of the role of intracellular Ca <sup>2+</sup> .....	93
Figure 3.9. Evaluation of the role of extracellular cations.....	94
Supplemental Figure 3.1. Levels of phospho-Ser67 inhibitor-1 in the hippocampus of juvenile wild-type and p35 knockout mice .....	95
Supplemental Figure 3.2. Levels of phospho-Ser6 and phospho-Ser67 inhibitor-1 in the striatum after chronic cocaine.....	96
Supplemental Figure 3.3. Evaluation of the roles of PKC and calpain .....	97
Supplemental Figure 3.4. Levels of phospho-Ser6 inhibitor-1 in the hippocampus after seizures .....	98
Supplemental Figure 3.5. Evaluation of the roles of NMDA and AMPA receptors in the effect of KCl.....	99
Figure 4.1. Fear conditioning.....	121
Figure 4.2. Voluntary wheel running and neurogenesis .....	122
Figure 4.3. Novel location and object recognition.....	123
Figure 4.4. Habituation .....	124

Figure 4.5. Biochemical targets of PP-1 and inhibitor-1 .....	125
Supplemental Figure 4.1. Open field behavior .....	126
Figure 5.1. Input resistance .....	141
Figure 5.2. Action potential properties .....	142
Figure 5.3. Train frequency breakpoint .....	143
Figure 5.4. Membrane potential oscillations.....	144
Figure 5.5. Voltage-dependent amplification of responses to simulated synaptic input.....	145
Figure 5.6. Effects of roscovitine on GC excitability .....	146
Figure 5.7. Effects of loss of Cdk5 on NMDA receptor currents .....	147
Supplemental Figure 5.1. Biocytin stains of dentate granule cells .....	148

## LIST OF ABBREVIATIONS

2D NMR, two-dimensional nuclear magnetic resonance

μcystin, microcystin

ACSF, artificial cerebrospinal fluid

AMPA, α-amino-3-hydroxy-5-methyl-4-isoxazolepropionic acid

ANOVA, analysis of variance

AP5, 2-amino-5-phosphonopentanoic acid

ATP, adenosine triphosphate

BAPTA-AM, 1,2-bis(2-aminophenoxy)ethane-*N,N,N',N'*-tetraacetic acid-acetomethylester

BrdU, 5-bromo-2-deoxyuridine

Brij, Polyoxyethyleneglycol dodecyl ether

BSA, bovine serum albumin

butyro, butyrolactone

CA, cornu ammonis

calptn, calpeptin

calyA, calyculin A

CaMKII, Ca<sup>2+</sup>/calmodulin-dependent protein kinase II

Cdk, cyclin-dependent kinase

CKI, casein kinase I

cont, control

CREB, cAMP response element-binding protein

cyA, cyclosporin A

D32, DARPP-32

DAPI, 4'-6-diamidino-2-phenylindole

DARPP-32, dopamine- and cAMP-regulated phosphoprotein, *M*<sub>r</sub> 32,000

DMSO, dimethyl sulfoxide

DNQX, dinitroquinoxaline-2,3-dione  
 DTT, dithiothreitol  
 EDTA, ethylenediamine tetraacetic acid  
 EGTA, ethylene glycol-bis(2-aminoethyl ether)-N,N,N',N'-tetraacetic acid  
 eIF2 $\alpha$ , eukaryotic translation initiation factor 2 $\alpha$   
 EPSC, excitatory postsynaptic current  
 ERC, entorhinal cortex  
 forsk, forskolin  
 fostr, fostreicin  
 GC, (dentate) granule cell  
 GSK3, glycogen synthase kinase 3  
 HEPES, 4-(2-hydroxyethyl)-1-piperazineethanesulfonic acid  
 HPLC, high performance liquid chromatography  
 HSQC, heteronuclear single quantum correlation  
 I-1, protein phosphatase inhibitor-1  
 ifen, ifenprodil  
 indo, indolinone  
 inhibitor-1, protein phosphatase inhibitor-1  
 IPTG, isopropyl- $\beta$ -D-thiogalactopyranoside  
 ko, knockout  
 LTD, long-term depression  
 LTP, long-term potentiation  
 MALDI-TOF MS, matrix-assisted laser desorption ionization time-of-flight mass  
     spectrometry  
 MAPK, mitogen-activated protein kinase  
 MK, MK801  
 Mol, molecular layer of the dentate gyrus  
 MOPS, 3-(N-morpholino)-propanesulfonic acid



Nim, nimodipine  
NMDA, N-methyl-D-aspartate  
OGL, outer granular layer of the dentate gyrus  
quin, quinpirole  
PBS, phosphate-buffered saline  
PKA, cAMP-dependent protein kinase, protein kinase A  
PKC, protein kinase C  
PP-1, protein phosphatase 1  
PP-2A, protein phosphatase 2A  
PP-2B, protein phosphatase 2B, Ca<sup>2+</sup>/calmodulin-dependent protein phosphatase,  
calcineurin  
OA, okadaic acid  
RO, Ro-32-0432  
rosc, roscovitine  
SDS-PAGE, sodium dodecyl sulfate polyacrylamide gel electrophoresis  
sEPSC, simulated EPSC  
SGZ, subgranular zone of the dentate gyrus  
SKF, SKF81297  
TBS, Tris-buffered saline  
TBS-T, TBS-Tween  
wt, wild-type

# **CHAPTER ONE**

## **INTRODUCTION**

The reversible phosphorylation of proteins is one of the most common signaling modalities available to living cells, representing by far the most prevalent form of posttranslational modification. Phosphorylation cascades control virtually every aspect of biology, and novel phosphorylation sites are being identified at increasing rates with the advent of mass spectrometric technologies (Campbell and Morrice, 2002). While the phosphorylation state of a protein is dictated by the balance between the kinase and phosphatase activities that act upon it, recognition of the importance of phosphatases has generally fallen behind that of kinases.

Protein kinases have long dominated the world of intracellular signaling, in part because they outnumber protein phosphatases by about three-fold. Even more striking, serine/threonine kinases outnumber serine/threonine phosphatases by about twenty-fold (Bollen, 2001). In the past decade, an explosion in the discovery of phosphatase regulatory subunits has led to the conclusion that phosphatases, though fewer in number, are just as highly regulated. Traditionally regarded as passive regulators that function in homeostasis, phosphatases are increasingly being recognized for their roles in the activation and amplification of particular signals.

One of the earliest such examples came with the discovery of protein phosphatase inhibitor-1. An inhibitor of protein phosphatase 1 (PP-1), inhibitor-1 is remarkable in its absolute dependence on cAMP-dependent protein kinase (PKA) activity for its function (Endo et al., 1996; Foulkes et al., 1983; Huang and Glinsmann, 1976). Reversal of PKA-dependent phosphorylation of inhibitor-1 at Thr35 by calcineurin (PP-2B, or  $\text{Ca}^{2+}$ /calmodulin-dependent protein phosphatase) (Ingebritsen and Cohen, 1983) inactivates inhibitor-1, preventing it from further inhibiting PP-1. Thus, inhibitor-1 represents one mechanism whereby PKA can amplify cAMP signals by preventing the dephosphorylation of sites shared with PP-1. In this manner, inhibitor-1 served as one of the first of an undoubted many examples of cross-talk between kinases and phosphatases.

In 2001, cyclin-dependent kinase 5 (Cdk5) joined the fray of cross-talk on inhibitor-1, when it was shown to phosphorylate inhibitor-1 at a different site, Ser67 (Bibb et al., 2001b). The phenomenon of multi-site phosphorylation by one or more kinases is not uncommon and provides great potential for signal integration (Cohen, 2000; Holmberg et al., 2002; Yang, 2005). A relatively recently discovered proline-directed serine/threonine kinase, Cdk5 has been implicated in numerous aspects of neuronal function and dysfunction. Included in its broad list of substrates are proteins involved in synaptic vesicle recycling, cytoskeletal dynamics, and dopaminergic signaling (Dhavan and Tsai, 2001). Cdk5 is broadly expressed but its activity is predominantly localized to the brain,

where its requisite cofactors p35 (Lew et al., 1994; Tsai et al., 1994) and p39 (Tang and Wang, 1996; Tang et al., 1995) are expressed. Efforts at characterizing the regulation of Cdk5 activity have been limited, with the majority of studies focusing on downstream pathways. Pharmacologic inhibition of Cdk5, although not without caveats, suggests an important role for Cdk5 in synaptic plasticity (Li et al., 2001) and learning (Fischer et al., 2002, 2003). However, the importance of Cdk5 to neurodevelopment, evidenced by the perinatal lethality of mice lacking the gene (Ohshima et al., 1996), has hampered direct investigation into this and other aspects of Cdk5 function.

Phosphorylation and dephosphorylation cascades, though important to a variety of biological processes, are known to be especially important for synaptic plasticity, particularly long-term potentiation (LTP) and long-term depression (LTD). These terms incorporate a heterogeneous group of phenomena, the most well-characterized of which is the Schaffer collateral type. In general, phosphorylation favors LTP, and dephosphorylation favors LTD. The induction of LTP, classically by high frequency stimulation (100 Hz for 1-2 s), involves a transient increase in PKA activity (Roberson and Sweatt, 1996) followed by a decrease in PP-1 activity (Blitzer et al., 1998; Brown et al., 2000; Woo et al., 2002), while the induction of LTD, classically by low frequency stimulation (1 Hz for 10 min), involves an increase in calcineurin activity (Mulkey et al., 1994). Salient biochemical models of plasticity have not only incorporated the changes

in these activities, but also explained how potentiation and depression—two seemingly opposite processes—could both depend on the activation of N-methyl-D-aspartate (NMDA) receptors and the elevation of intracellular  $\text{Ca}^{2+}$  levels.

In 1989 John Lisman proposed a model that would dominate the field of long-term synaptic plasticity at the biochemical level for the next decade (Lisman, 1989; Winder and Sweatt, 2001). He proposed that the magnitude of the rise in  $\text{Ca}^{2+}$  would determine whether the synapse was strengthened or weakened. As a substrate whose function relies on the balance of activity between PKA and calcineurin, both of which are known to be important to the long-term modification of synaptic strength, inhibitor-1 became incorporated into this model as a critical switch between potentiation and depression. The dependence of inhibitor-1 function on PKA activity served as a useful theoretical link between the increase in PKA activity and the decrease in PP-1 activity found during LTP, whereas the antagonistic effects of PKA and calcineurin on inhibitor-1 function provided the theoretical basis for a  $\text{Ca}^{2+}$  sensor.

In Lisman's model, low-frequency NMDA receptor stimulation results in a slight elevation of intracellular  $\text{Ca}^{2+}$  levels, which leads to the activation of calcineurin. In contrast, intense NMDA receptor stimulation results in a larger elevation of intracellular  $\text{Ca}^{2+}$  levels sufficient to activate  $\text{Ca}^{2+}$ /calmodulin-dependent adenylyl cyclase, which in turn activates PKA by raising cAMP levels. The balance between these processes determines the phosphorylation state of

inhibitor-1 and thus its inhibitory activity against PP-1. PP-1 regulates the phosphorylation state and activity of  $\text{Ca}^{2+}$ /calmodulin-dependent protein kinase II (CaMKII) (Strack et al., 1997) and a number of other substrates thought to be important in mediating changes in synaptic strength, including NMDA (Blank et al., 1997; Snyder et al., 1998) and  $\alpha$ -amino-3-hydroxy-5-methyl-4-isoxazolepropionic acid (AMPA) (Yan et al., 1999) receptors and cAMP response element-binding protein (CREB) (Bito et al., 1996; Hagiwara et al., 1992). Decreased PP-1 activity allows CaMKII to autophosphorylate on Thr286 (Kwiatkowski et al., 1988) and to enhance AMPA receptor conductance and/or insertion (Lisman and Zhabotinsky, 2001). Thus, PP-1 activity contributes to the induction of LTD (Mulkey et al., 1994), and inhibition of PP-1 promotes LTP (Blitzer et al., 1998; Blitzer et al., 1995).

In keeping with Lisman's model, a multitude of studies purportedly link inhibitor-1 to hippocampal plasticity, learning, and memory. However, most of these studies have employed exogenous inhibitor-1 to bring about a change in plasticity or learning (Blitzer et al., 1998; Brown et al., 2000; Genoux et al., 2002; Morishita et al., 2001; Mulkey et al., 1994), thereby truly implicating PP-1 and not inhibitor-1. Furthermore, the few studies that have specifically examined the function of endogenous inhibitor-1 have been conducted in the CA1 region of the hippocampus (Blitzer et al., 1998; Brown et al., 2000), which possesses negligible amounts of inhibitor-1 (Allen et al., 2000). Inhibitor-1 knockout mice display

normal LTP and LTD in the Schaffer collateral pathway and perform normally in the Morris water maze (Allen et al., 2000). Thus, despite the prominent position inhibitor-1 has come to occupy as a regulator of PP-1 in biochemical models of Schaffer collateral plasticity, the actual contribution of inhibitor-1 to hippocampal learning and memory is questionable.

We began our studies with the characterization of a novel Cdk5-dependent phosphorylation site on inhibitor-1, followed by an assessment of its functional implications. These studies uncovered a potential new regulatory mechanism for Cdk5, which we had hoped would link Cdk5-dependent phosphorylation of inhibitor-1 to plasticity, learning, and memory. However, given the uncertain role of inhibitor-1 in these processes, we instead focused on identifying behaviors and substrates impacted by inhibitor-1 function. Using a whole-cell patch clamp approach, we also attempted to identify electrical properties of dentate granule cells that might be affected by inhibitor-1 function. Finally, in a related study we helped firmly establish a role for Cdk5 in hippocampal synaptic plasticity by evaluating the effects of conditional loss of Cdk5 on NMDA receptor currents as an explanation for the observed enhancement in LTP and learning.

## CHAPTER TWO

### REGULATION OF PROTEIN PHOSPHATASE INHIBITOR-1

#### BY CYCLIN-DEPENDENT KINASE 5

##### Summary

Inhibitor-1, the first identified endogenous inhibitor of protein phosphatase 1 (PP-1), was previously reported to be a substrate for cyclin-dependent kinase 5 (Cdk5) at Ser67. Further investigation has revealed the presence of an additional Cdk5 site identified by mass spectrometry and confirmed by site-directed mutagenesis as Ser6. Basal levels of phospho-Ser6 inhibitor-1, as detected by a phosphorylation-state specific antibody against the site, existed in specific regions of the brain and varied with age. In the striatum, basal *in vivo* phosphorylation and dephosphorylation of Ser6 were mediated by Cdk5 and protein phosphatase 2A (PP-2A) and PP-1, respectively. Additionally, calcineurin contributed to dephosphorylation under conditions of high  $\text{Ca}^{2+}$ . In biochemical assays the function of Cdk5-dependent phosphorylation of inhibitor-1 at Ser6 and Ser67 was demonstrated to be an intramolecular impairment of the ability of inhibitor-1 to be dephosphorylated at Thr35; this effect was recapitulated in two systems *in vivo*. Dephosphorylation of inhibitor-1 at Thr35 is equivalent to inactivation of the protein, as inhibitor-1 only serves as an inhibitor of PP-1 when phosphorylated by cAMP-dependent kinase (PKA) at



Thr35. Thus, inhibitor-1 serves as a critical junction between kinase and phosphatase signaling pathways, linking PP-1 to not only PKA and calcineurin, but also Cdk5.

## **Introduction**

Phosphatases are now recognized as important players in processes ranging from muscle contraction to synaptic plasticity. Protein phosphatase inhibitor-1 (I-1)<sup>1</sup>, was identified from rabbit skeletal muscle in 1976 as an inhibitor of PP-1 and a regulator of glycogen metabolism (Huang and Glinesmann, 1976). In recent years, interest in the protein has focused on its role in heart failure and neuronal plasticity. In the brain, inhibitor-1 can be found in many areas including the olfactory bulb, neostriatum, cerebral cortex, and the dentate gyrus of the hippocampus. The level of inhibitor-1 in the rest of the hippocampus is a matter of some debate; reports range from little or none to moderate amounts (Allen et al., 2000; Barbas et al., 1993; Gustafson et al., 1991; Lowenstein et al., 1995; Sakagami et al., 1994) .

Inhibitor-1 is a heat-stable 19 kDa protein that possesses little ordered structure and a preponderance of glutamic acid and proline in its amino acid sequence (Nimmo and Cohen, 1978). As a regulator of one of the three major serine/threonine phosphatases in mammalian cells that can itself be regulated by a

major kinase, inhibitor-1 occupies an important position in neuronal signal transduction cascades. Only when phosphorylated by PKA at Thr35 does inhibitor-1 become a potent ( $IC_{50} = 1$  nM) and selective inhibitor of PP-1 (Endo et al., 1996; Foulkes et al., 1983; Huang and Glinsmann, 1976). Through its action on inhibitor-1, PKA can amplify cAMP signals by preventing the dephosphorylation of sites it shares with PP-1. That calcineurin (PP-2B, or  $Ca^{2+}$ /calmodulin-dependent protein phosphatase) can inactivate I-1 by dephosphorylating the PKA site (Cohen, 1989; Mulkey et al., 1994; Shenolikar and Nairn, 1991) provides an added layer of complexity, as well as a point of integration for cAMP- and  $Ca^{2+}$ -dependent second messenger systems. The ability of inhibitor-1 to link the actions of PKA and calcineurin to PP-1 has allowed it to occupy a central position in molecular models of synaptic plasticity.

In 2001, inhibitor-1 was found to be phosphorylated at another residue (Ser67) by Cdk5, a proline-directed serine/threonine kinase (Bibb et al., 2001b). This phosphorylation did not have an effect on the ability of phospho-Thr35 inhibitor-1 to inhibit PP-1 and had only a mild effect on the ability of PKA to phosphorylate inhibitor-1 at Thr35. Despite its name, Cdk5 is not cyclin-dependent. Furthermore, unlike all other cyclin-dependent kinases, Cdk5 is most active in postmitotic neurons due to its requirement for the relatively neuron-specific cofactor p35 (Lew et al., 1994; Tsai et al., 1994), or its homologue p39 (Tang and Wang, 1996; Tang et al., 1995).

While early studies focused on its ability to hyperphosphorylate tau and its relationship to Alzheimer's disease (Baumann et al., 1993), Cdk5 now boasts an extensive list of substrates, including N-methyl-D-aspartate (NMDA) receptor (Li et al., 2001), postsynaptic density,  $M_r$  95,000 (PSD-95) (Morabito et al., 2004), meiosis-specific kinase 1 (MEK1) (Sharma et al., 2002), c-Jun N-terminal kinase 3 (JNK3) (Li et al., 2002), P/Q type voltage-gated  $\text{Ca}^{2+}$  channel (Tomizawa et al., 2002), synapsin I (Matsubara et al., 1996), mammalian unc-18 (Munc18) (Fletcher et al., 1999; Shuang et al., 1998), amphiphysin I (Floyd et al., 2001; Nguyen and Bibb, 2003; Tan et al., 2003; Tomizawa et al., 2003), dynamin I (Nguyen and Bibb, 2003; Tan et al., 2003; Tomizawa et al., 2003), microtubule-associated protein 1B (MAP1B) (Paglini et al., 1998; Pigino et al., 1997),  $\beta$ -catenin (Kesavapany et al., 2001; Kwon et al., 2000), stathmin (Hayashi et al., 2006), focal adhesion kinase (FAK) (Xie et al., 2003), tyrosine hydroxylase (Kansy et al., 2004; Moy and Tsai, 2004), Pctaire1 (Cheng et al., 2002), mSds3 (mouse Sds3) (Li et al., 2004), p53 (Zhang et al., 2002), TrkB (Cheung et al., 2007), doublecortin (Graham et al., 2004; Tanaka et al., 2004), signal transducer and activator of transcription 3 (STAT3) (Fu et al., 2004), disabled 1 (Dab1) (Keshvara et al., 2002; Ohshima et al., 2007), NUDE-like (NUDEL) (Niethammer et al., 2000), collapsin response mediator protein-2 (CRMP-2) (Brown et al., 2004), and dopamine- and cAMP-regulated phosphoprotein,  $M_r$  32,000 (DARPP-32) (Bibb et al., 1999), an inhibitor-1 homologue. In the past decade,

Cdk5 has been implicated in many aspects of normal and abnormal neuronal function, including neurodevelopment, synaptic plasticity, and neurodegeneration.

In this report, we show that inhibitor-1 is actually phosphorylated at two sites by Cdk5 *in vitro* and *in vivo*. Following discovery of the second site by phosphopeptide and phosphoamino acid analyses, mass spectrometric identification of the novel site as Ser6 was confirmed by *in vitro* phosphorylation of site-directed mutants. Basal levels of phospho-Ser6 inhibitor-1 as detected by a phosphorylation-state specific antibody generated against the site allowed demonstration of its relevance to *in vivo* systems. Pharmacological manipulation of both striatal lysates and striatal slices suggested that basal levels of phosphorylation at Ser6 are controlled by the opposing actions of Cdk5, PP-2A, and PP-1, while biochemical analyses revealed a novel intramolecular regulatory function for Cdk5-dependent phosphorylation of inhibitor-1 that was recapitulated in two *in vivo* systems.

## **Experimental Procedures**

### *Chemicals and enzymes*

All chemicals were from Sigma, except where indicated. Trypsin, shrimp alkaline phosphatase, and endoproteinase Lys-C were from Promega. Phosphorylase *b* was purchased from Calzyme. Protease inhibitors, dithiothreitol

(DTT), isopropyl- $\beta$ -D-thiogalactopyranoside (IPTG), and adenosine triphosphate (ATP) were from Roche. [ $\gamma$ - $^{32}$ P]-ATP was from Perkin Elmer Life Sciences. Cyclosporin A, calyculin A, okadaic acid, and forskolin were from LC Laboratories, while U0126 and NMDA were from Tocris, and butyrolactone I was from Biomol. Roscovitine and indolinone A and B were generously provided by Laurent Meijer (Centre National de la Recherche Scientifique, Roscoff, France) and Frank Gillardon (Boehringer Ingelheim), respectively. The catalytic subunits of PKA and PP-1 were purified as previously described from bovine heart (Kaczmarek et al., 1980) by Atsuko Horiuchi (Rockefeller University) and rabbit skeletal muscle (Cohen et al., 1988) by Lim Tung (Weill Medical College of Cornell University), respectively. Cdk5 and p25-His<sub>6</sub> were co-expressed in insect Sf9 cultures using baculovirus vectors and affinity-purified by Janice W. Kansy (UT Southwestern Medical Center) and Kanehiro Hayashi (UT Southwestern Medical Center) (Saito et al., 2003). Cdk5/p35 was provided by Taro Saito (Tokyo Metropolitan University). Cdk1/cyclin B and mitogen-activated protein kinase (MAPK) were from New England Biolabs and Calbiochem, respectively. Cell culture reagents were from Invitrogen. Oligonucleotides were ordered from Integrated DNA Technologies, while phosphopeptides were synthesized at Rockefeller University.

### *Subcloning*

Inhibitor-1 was subcloned into pcDNA3.1 Flag (Invitrogen) from the pET-15b expression vector incorporating the cDNA for rat inhibitor-1-His<sub>6</sub> (Bibb et al., 2001b) using the HindIII and KpnI restriction sites and the following primers: 5'CGGCCGAAGCTTATG GAGCCCGACAACAGTCC<sup>3'</sup> and 5'CCCGGGGGTACCTCATTTATCGTCATCGTCTTTGTAGTCCATGACCAAGCTGGCTCCTTGGG<sup>3'</sup>. A C-terminal FLAG tag (underlined) was included into the primer design to avoid insertion of extraneous amino acids between the end of the protein and the FLAG tag.

### *Site-directed mutagenesis*

The pET-15b and pcDNA3.1 Flag vectors served as templates for site-directed mutagenesis using Stratagene's QuikChange kit. The manufacturer's recommendations for mutagenic primer design were followed, and mutations were confirmed by DNA sequencing using primer specific for the T7 promoter. Janice W. Kansy (UT Southwestern) created the Ser6Asp, Ser6Glu, and Ser6Ala/Ser67Ala pET-15b mutants. Primers used to introduce Ser6Asp, Ser6Glu, and Ser6Ala mutations were 5'CCATGGAGCCCGACAACxxxCCACGGAAGATCCAG<sup>3'</sup> and their reverse complements, where xxx represents GAT, GAA, and GCT, respectively. Primers used to introduce Ser67Asp, Ser67Glu, and Ser67Ala mutations were 5'GTCCACACTGTCAATGGATCCACGGCAACGGAAG<sup>3'</sup>,

5'CAAGTCCACACTGTCAATGGAGCCACGGCAACGGAAG<sup>3'</sup>, and 5'CCA  
CACTGTCAATGGCTCCACGGCAACGG<sup>3'</sup> and their reverse complements,  
respectively.

### *Purification of inhibitor-1*

Chemically competent BL21 (DE3) *E. coli* were transformed with pET-15b expression vectors containing wild-type or mutant inhibitor-1. Cultures were grown at 37°C in LB media until the OD<sub>600</sub> reached 0.6-0.8, at which time 0.1 mg/ml IPTG was added. Induction proceeded for two hours at 37°C, after which cells were harvested and washed with Tris-buffered saline (TBS). Pellets from 10,000 x g spins were stored at –80°C for subsequent lysis by French press in 50 mM NaH<sub>2</sub>PO<sub>4</sub> buffer, pH 8.0, containing 300 mM NaCl and protease inhibitors. Cleared lysates were incubated with a nickel-nitrilotriacetic acid-agarose resin (Qiagen) for one hour at 4°C, then washed 5 x 10 min in lysis buffer containing 10% glycerol. Bound protein was batch-eluted with wash buffer containing 0.5-1.0 M imidazole or eluted using a linear gradient of 0 to 1 M imidazole. Samples were dialyzed overnight in 10 mM 4-(2-hydroxyethyl)-1-piperazineethanesulfonic acid (HEPES), pH 7.4, with two changes of buffer. Proteins were stored at –80°C following analysis for purity by 15% sodium dodecyl sulfate polyacrylamide gel electrophoresis (SDS-PAGE) and Coomassie Brilliant Blue staining. Each time a fresh aliquot of protein sample buffer from

the freezer was used for SDS-PAGE, as recombinant rat inhibitor-1 is extremely sensitive to disulfide bond formation, in contrast to rabbit and human inhibitor-1, which completely lack cysteines (Sikes and Shenolikar, 2005). Sufficient DTT in the protein sample buffer was required to eliminate high molecular weight species (~40-52 kDa) found in preparations of recombinant rat inhibitor-1 (**Supplemental Figure 2.1**). The primary band ran at ~30 kDa; lower bands, likely corresponding to degradation products, were also observed.

#### *In vitro protein phosphorylation reactions*

Protein phosphorylation reactions were generally conducted at 30°C in a final volume of at least 20 µl containing 10 µM substrate, 200 µM ATP, and 0.2 mCi/ml [ $\gamma$ -<sup>32</sup>P]-ATP. PKA reactions were conducted in 50 mM HEPES, pH 7.4, 1 mM ethylene glycol-bis(2-aminoethyl ether)-N,N,N',N'-tetraacetic acid (EGTA), 10 mM magnesium acetate, and 0.1 mg/ml bovine serum albumin (BSA), while Cdk5 reactions were conducted in 30 mM 3-(N-morpholino)-propanesulfonic acid (MOPS), pH 7.2, and 5 mM MgCl<sub>2</sub>. A mixture of ATP and [ $\gamma$ -<sup>32</sup>P]-ATP was used to initiate the reactions. Reactions were stopped by the addition of an equal volume of 5x protein sample buffer (400 mM Tris, pH 6.8, 5% SDS, 35% glycerol, 128 mM DTT, and bromophenol blue). Time-course reactions were performed by removing aliquots from a master reaction at defined times. Dilutions of leftover reaction mixture (5 µl of 1:100 and/or 1:500) spotted



onto filter paper served as standards (counts/pmol phosphate) for stoichiometric calculations. Following separation of phosphorylated inhibitor-1 from unbound [ $\gamma$ - $^{32}$ P]-ATP by 15% SDS-PAGE, the dried gel and standards were analyzed by PhosphorImager technology, and bands were quantitated to determine the amount of phosphorylated product in each reaction. The stoichiometries of reactions lacking [ $\gamma$ - $^{32}$ P]-ATP were inferred from reactions containing [ $\gamma$ - $^{32}$ P]-ATP that were conducted in parallel.

In some studies, preparative phosphorylation of inhibitor-1 by a protein kinase was followed by repurification of phospho-inhibitor-1 prior to use in a subsequent assay. For these experiments, phospho-inhibitor-1 was repurified from *in vitro* protein phosphorylation reaction mixtures by precipitation with 15-20% trichloroacetic acid and 0.5 mg/ml BSA on ice for 1-3 hours. Precipitates were resuspended in 1 M Tris, pH 8.0 before overnight dialysis into 50 mM Tris, pH 7.4.

#### *In vitro protein dephosphorylation reactions*

Phosphatase assays employing tissue lysates were performed at 30°C for 15 min in a final volume of 30  $\mu$ l consisting of 10  $\mu$ l of substrate, 10  $\mu$ l of lysate, and 10  $\mu$ l of additive. [ $\gamma$ - $^{32}$ P]-Ser6/Ser67Asp and [ $\gamma$ - $^{32}$ P]-Ser6/Ser67Ala were generated by preparative phosphorylation of Ser67Asp and Ser67Ala inhibitor-1 with Cdk5 in the presence of [ $\gamma$ - $^{32}$ P]-ATP, respectively. Freshly-harvested

striatal/hippocampal tissue was lysed by Dounce homogenization in 50 mM Tris, pH 7.4, containing 150 mM NaCl and protease inhibitors, then cleared by centrifugation at 14,000 x g for 15 min at 4°C. In some reactions, 2 mM EGTA was included in the lysis buffer. Additives were used at a final concentration of 1  $\mu$ M microcystin, 5  $\mu$ M fostreicin, 0.1  $\mu$ g/ $\mu$ l neurabin, 1  $\mu$ M cyclosporin A, 5 mM/1 mM EGTA/ethylenediamine tetraacetic acid (EDTA), and 2 nM or 1  $\mu$ M okadaic acid. 15  $\mu$ g of cleared lysate was used for each reaction. Reactions were quenched and analyzed as with PP-1 inhibition assays described below.

Phosphorylase *a* served as the substrate for PP-1 inhibition assays. Phosphorylase *a* was generated by the preparative phosphorylation of phosphorylase *b* by phosphorylase kinase at 30°C for one hour in 100 mM Tris, pH 8.2, 100 mM  $\beta$ -glycerol phosphate, 0.1 mM CaCl<sub>2</sub>, 10 mM magnesium acetate, 200  $\mu$ M ATP, and 1.7 mCi/ml [ $\gamma$ -<sup>32</sup>P]-ATP. The reaction was stopped by the addition of an equal volume of 90% saturated ammonium sulfate. Following precipitation on ice for 20-60 min, the mixture was centrifuged at 14,000 x g for 15 min. The pellet was resuspended in wash buffer (50 mM Tris, pH 7.0, 0.1 mM EGTA, 0.1%  $\beta$ -mercaptoethanol) and dialyzed extensively overnight into 10 mM Tris, pH 7.5, 0.1 mM EGTA, and 10% glycerol. Alternatively, the reaction was stopped by desalting over a PD10 column (Amersham). Unincorporated [ $\gamma$ -<sup>32</sup>P]-ATP was then removed by ammonium sulfate precipitation and application to a

NICK column (Amersham). PP-1-mediated dephosphorylation reactions occurred at 30°C in a final volume of 30 µl containing 10 µM  $^{32}\text{P}$ -phosphorylase *a*, 50 mM Tris, pH 7.0, 0.01% Brij, 0.1%  $\beta$ -mercaptoethanol, 0.3 mg/ml BSA, 0.1 mM EGTA, and 5 mM caffeine. Reactions were stopped by the addition of 150 µl 20% trichloroacetic acid. Following incubation on ice for 15-30 min, mixtures were centrifuged at 14,000 x g for 10 min. 150 µl of the supernatant, as well as what remained in the centrifuged tube, was analyzed by Cerenkov counting. Percentage dephosphorylation was calculated as (counts in the supernatant – background) / (total counts in the supernatant and pellet). Background was calculated as (total counts in the supernatant and pellet) \* background percentage, where background percentage equaled (counts in the supernatant) / (total counts in the supernatant and pellet) in a reaction lacking PP-1 and inhibitor-1.

Calcineurin-mediated dephosphorylation assays were conducted similarly, except in 33 mM Tris, pH 7.0, 0.01% Brij, 0.1%  $\beta$ -mercaptoethanol, 0.3 mg/ml BSA, 100 µM  $\text{CaCl}_2$  and 1 µM calmodulin with 1 µM  $^{32}\text{P}$ -Thr35 inhibitor-1. Substrates for calcineurin assays were phosphorylated first by PKA, then by Cdk5.

*Phosphopeptide maps and phosphoamino acid analysis*

Phosphopeptide maps and phosphoamino acid analysis were conducted by James A. Bibb (UT Southwestern Medical Center) as previously described (Hemmings et al., 1984).

*Phosphorylation site identification by mass spectrometry*

<sup>32</sup>P-labeled phospho-Ser6/Ser67Ala inhibitor-1, resulting from phosphorylation by Cdk5 in the presence of [ $\gamma$ -<sup>32</sup>P]-ATP, was analyzed by SDS-PAGE and digested with Asp-N by James A. Bibb (UT Southwestern Medical Center). Joseph Fernandez (Rockefeller University) subjected some of the digest mixture to matrix-assisted laser desorption ionization time-of-flight mass spectrometry (MALDI-TOF MS) (Campbell and Morrice, 2002). The remainder was fractionated by reversed-phase high-performance liquid chromatography (HPLC) on a C<sub>18</sub> column (Vydac, 1.0 mm inner diameter  $\times$  150 mm), and collected fractions were screened for radioactivity (Bibb et al., 2001b). The fraction containing the radiolabel was analyzed by MALDI-TOF MS. A small aliquot of the fraction was also treated with shrimp alkaline phosphatase in 50 mM NH<sub>4</sub>HCO<sub>3</sub> at 37°C for 30 min before MALDI-TOF MS to confirm phosphorylation. The identity of the peptide was verified by Edman degradation.

### *Generation of phosphorylation state-specific antibodies*

Rabbit polyclonal phosphorylation state-specific antibodies for phospho-Ser6 inhibitor-1 were generated and affinity-purified, at least initially, by Janice W. Kansy (UT Southwestern Medical Center) as previously described (Czernik et al., 1997), using the synthetic phosphopeptide Met-Glu-Gln-Asp-Asn-phospho-Ser-Pro-Arg-Lys-Ile-Cys (Rockefeller University) as an immunogen. Antisera (1:200) were evaluated for specificity by immunoblot analysis of dephospho- and phospho-inhibitor-1 standards, as well as brain homogenates of wild-type and inhibitor-1 knockout mice (**Supplemental Figure 2.2**). Polyclonal antibodies were purified from high-titer antisera by column affinity chromatography to the peptide antigen, which was conjugated to AminoLink resin (Pierce). The column was washed with 50 mM Tris, pH 7.5, 1 M NaCl, 0.05% Tween-20, then with 50 mM sodium borate, pH 8.5, 500 mM NaCl, 0.05% Tween-20. Antibodies were eluted with 100 mM glycine, pH 2.5, quenched with 1.5 M Tris, pH 8.5, dialyzed into 10 mM MOPS, pH 7.5, 154 mM NaCl, stored at  $-20^{\circ}\text{C}$ , and checked for specificity.

### *Immunohistochemistry*

Mice were deeply anesthetized with halothane and subjected to intracardiac perfusion with 4% paraformaldehyde in phosphate-buffered saline (PBS). Brains were removed and fixed overnight before being cryoprotected in

30% sucrose-PBS. Coronal sections (8  $\mu\text{m}$ ) were cut using a cryostat (Leica Microsystems), placed on glass slides, and stored at 4°C. Sections containing the hippocampus were dried for 30 min and blocked with blocking buffer (5% BSA, 3% normal goat serum, and 0.1% Triton X-100) for 1 h at room temperature, then incubated with phospho-Ser6 inhibitor-1 antibody (1:100) overnight at 4°C. The next day slides were washed 3 x 10 min with blocking buffer before a 2-h incubation with Cy3-conjugated horse anti-rabbit secondary antibody (1:200, Jackson ImmunoResearch) in PBS. After one 10-min wash with blocking buffer, cells were stained with 4'-6-diamidino-2-phenylindole (DAPI, 1:10,000, Pierce) in PBS at room temperature for 10-15 min. Following 3 x 10 min washes with PBS, slides were successively dehydrated with 1-min incubations in 50%, 70%, 95%, and 100% ethanol, then cleared with 3 changes of Citrisolv (1, 5, and 10 min, Fisher Scientific). Slides were coverslipped with DPX mountant (Fluka) and examined with an Olympus DX51 epifluorescent light microscope.

#### *Preparation and incubation of acute slices*

Male C57BL/6 mice (6-12 weeks old) were sacrificed by live decapitation, two at a time. Brains were rapidly removed into partially frozen oxygenated Krebs buffer (124 mM NaCl, 4 mM KCl, 26 mM NaHCO<sub>3</sub>, 1.5 mM CaCl<sub>2</sub>, 1.25 mM KH<sub>2</sub>PO<sub>4</sub>, 1.5 mM MgSO<sub>4</sub>, and 10 mM D-glucose, pH 7.4), blocked slightly anterior to the cerebellum, and mounted onto a platform from which 400- $\mu\text{m}$

sections were prepared with a vibratome. Coronal dorsal striatal slices and paratransverse hippocampal slices were microdissected from these sections in cold oxygenated Krebs buffer using a Leica S4E dissecting light microscope. Each slice was transferred to a net-well (Costar) resting in one well of a 12-well plate containing 3 ml of Krebs buffer and allowed to recover at 30°C under constant oxygenation with 95% O<sub>2</sub>/5% CO<sub>2</sub> for 45-60 min, with one or two changes of buffer. Slices were subsequently treated with drugs as specified for each experiment, transferred to microfuge tubes, snap-frozen on dry ice, and stored at -80°C until further analysis. Where applicable, control slices were treated with dimethyl sulfoxide (DMSO), the solvent used to dissolve roscovitine, butyrolactone, U0126, indolinone A & B, okadaic acid, calyculin A, cyclosporin A, and forskolin.

#### *Transfection of PC12 cells*

PC12 rat pheochromocytoma cells were maintained in Dulbecco's modified Eagle's medium (DMEM) containing 5% fetal bovine serum (FBS) and 10% horse serum in 10-cm plates. Experiments were conducted in 24-well plates coated with poly-D-lysine. Cells were transfected using Lipofectamine 2000 (Invitrogen) according to the manufacturer's protocol. After 24 h, the culture medium was replaced with medium containing one-tenth the normal amount of serum. Transfected cells were cultured for an additional 16 h before being treated

with vehicle (DMSO) or forskolin (5  $\mu$ M, 10 min). After drug treatment, cells were washed twice with PBS and lysed directly in the plate with boiling 1% SDS containing 50 mM NaF. Lysates were boiled for 10 min and stored at  $-80^{\circ}\text{C}$  until further analysis.

#### *Immunoblot analysis of cell and tissue homogenates*

Striatal slices and gross dissections of brain regions were homogenized by sonication in boiling hot lysis buffer (1% SDS and 50 mM NaF), then immediately boiled for an additional 10 min. Samples for the peripheral distribution of inhibitor-1 had to be lysed in a different buffer (5 mM Tris, pH 8.4, 0.1 mM EGTA), boiled for 40 min, and centrifuged at 15,000  $\times$  g for 15 min to eliminate a cross-reactive band at the same molecular weight. An equal amount of total protein (80-100  $\mu$ g of brain homogenate, 25  $\mu$ g of cleared peripheral tissue homogenate, or 25  $\mu$ g of PC12 cell lysate) from each sample as determined by the bicinchoninic acid (BCA) protein assay (Pierce) was subjected to 15% SDS-PAGE and transferred to nitrocellulose membrane overnight. Membranes were blocked in 5% milk (or 5% BSA) + TBS-Tween (TBS-T) for one hour, then incubated with polyclonal antibodies for phospho-Ser6 inhibitor-1 (1:750) (see Results), phospho-Ser67 inhibitor-1 (1:4000) (Bibb et al., 2001b), total inhibitor-1 (1:2000) (Gustafson et al., 1991), or phospho-Thr34 DARPP-32/phospho-Thr35



inhibitor-1 (1:750) (Snyder et al., 1992) for one hour at room temperature or overnight at 4°C. Blots for phospho-Thr35 inhibitor-1 required overnight incubation for detection of a signal in brain lysate. After several brief rinses with deionized water, membranes were washed 3 x 10 min with TBS-T and incubated with horseradish peroxidase-conjugated goat anti-rabbit secondary antibody (Chemicon, 1:5000) for one hour at room temperature. Following more deionized water rinses and 3 x 10 min washes with TBS-T, membranes were developed with an enhanced chemiluminescence immunodetection system (Amersham Biosciences). All antibody incubations were in 5% milk + TBS-T, except that for phospho-Thr35 inhibitor-1, in which BSA replaced milk.

### *Nuclear magnetic resonance*

*E. coli* transformed with pET-15b containing inhibitor-1 were grown as described above, except in minimal media containing  $^{15}\text{NH}_4\text{Cl}$ . After nickel-affinity chromatography purification,  $^{15}\text{N}$ -labeled inhibitor-1 was dialyzed into 25 mM sodium phosphate, pH 6.5, for two-dimensional nuclear magnetic resonance (2D NMR) analysis. Heteronuclear single quantum correlation (HSQC) spectra were obtained and analyzed by Irina Dulubova (UT Southwestern Medical Center).

### *Data analysis*

Image J (NIH) was used to quantitate immunoblots. All results are stated as percentage decrease or fold increase of the mean  $\pm$  error. Error of the change was calculated from standard errors of the mean using error propagation formulas. Individual bands of representative blots were always taken from the same exposure of the same membrane, and all represented total bands were derived from the same sample on the same membrane as the corresponding phospho-band.

## **Results**

### *Discovery, identification, and confirmation of Ser6 as a novel Cdk5 site of inhibitor-1*

Inhibitor-1 was previously reported to be phosphorylated by Cdk5 at Ser67 (Bibb et al., 2001b). Phosphopeptide maps of wild-type and Ser67Ala inhibitor-1 phosphorylated by the proline-directed serine/threonine kinases Cdk1, MAPK, and Cdk5 were generated by James A. Bibb (UT Southwestern Medical Center) during the characterization of this phosphorylation site (**Figure 2.1A**). Surprisingly, unlike that for Cdk1 and MAPK, the phosphopeptide map for wild-type inhibitor-1 phosphorylated by Cdk5 revealed two major phosphopeptide species. Mutation of Ser67 to Ala eliminated one of these phosphopeptide species, suggesting the presence of an additional site of Cdk5-dependent

phosphorylation. Phosphoamino acid analysis of wild-type and Ser67Ala inhibitor-1 conducted by James A. Bibb (UT Southwestern Medical Center) revealed the novel site to be a serine (**Figure 2.1B**).

Ser67Ala inhibitor-1 preparatively phosphorylated by Cdk5 in the presence of [ $\gamma$ - $^{32}$ P]-ATP was next digested with Asp-N to facilitate identification of the novel site. MALDI-TOF mass spectrometry of the digest by Joseph Fernandez (Rockefeller University) revealed peaks at 1707.86 and 1613.20, representing the phosphorylated peptide  $^4$ DNSPRKIQFTVPLL<sup>17</sup> and its daughter ion, respectively (**Figure 2.2A**). The daughter ion, which resulted from a loss of H<sub>3</sub>PO<sub>4</sub>, formed a characteristic broad peak due to its inability to be focused on the MALDI-TOF detector (Campbell and Morrice, 2002). Since Ser6 is the only serine or threonine directly followed by a proline in this fragment, it was concluded to be the novel site of phosphorylation. As further confirmation, the proteolytic fragments were fractionated by capillary HPLC into a 96-well plate, and collected fractions were screened for radioactivity (**Figure 2.2B**, top panel). Counts were found primarily in a single fraction, which produced a predominant mass of 1708.26 by MALDI-TOF MS analysis (**Figure 2.2B**, middle panel). Upon treatment of a small portion of the fraction with alkaline phosphatase, a mass of 1708.26 – 80 Da ( $M_r$  PO<sub>3</sub>) = 1628.67 was observed (**Figure 2.2B**, bottom panel), confirming the peptide was phosphorylated. The identity of this peptide as  $^4$ DNSPRKIQFTVPLL<sup>17</sup> was verified by Edman degradation microsequencing.

These findings were supported by site-directed mutagenesis. Mutation of both Ser6 and Ser67 resulted in no detectable phosphorylation by Cdk5 (**Figure 2.3A**). Thus, Ser6 and Ser67 are the only sites of phosphorylation by Cdk5. Curiously, in *in vitro* phosphorylation reactions mutation of Ser6 to Ala decreased phosphorylation of inhibitor-1 by 44% after one hour, while mutation of Ser67 to Ala decreased phosphorylation by 85%, instead of the expected 66%. The incongruence of these numbers suggests that phosphorylation of Ser6 may have to follow that of Ser67. Indeed, phosphomimetic mutation of Ser67 to an aspartate more than doubled the ability of Cdk5 to phosphorylate Ser6, whereas phosphomimetic mutation of Ser6 did not affect the ability of Cdk5 to phosphorylate Ser67.

In a somewhat related experiment, the ability of various forms of inhibitor-1 to serve as a substrate for Cdk5/p35, rather than Cdk5/p25, was evaluated. Altered substrate specificity due to cofactor differences has previously been hypothesized, but not directly demonstrated. In time course reactions, the efficiency of phosphorylation of Ser67Ala inhibitor-1 compared to that of wild-type inhibitor-1 was similar for Cdk5/p35 and Cdk5/p25 (**Figure 2.3B**). The stoichiometry achieved by Cdk5/p35 was lower than that for Cdk5/p25, likely due to activity differences between different preparations of enzyme. There was no detectable phosphorylation of inhibitor-1 when both Ser6 and Ser67 were mutated to Ala.

*Demonstration of the in vivo phosphorylation of inhibitor-1 at Ser6*

To confirm the *in vivo* relevance of this novel phosphorylation event, a phosphorylation state-specific antibody to phospho-Ser6 inhibitor-1 was generated. Phospho-specificity of the purified antibody was demonstrated by immunoblot analysis of recombinant wild-type or Ser6Ala inhibitor-1 preparatively phosphorylated or mock phosphorylated by Cdk5 (**Figure 2.4A**). A strong signal was detected from wild-type inhibitor-1 incubated with Cdk5, but not wild-type inhibitor-1 incubated without Cdk5 or Ser6Ala inhibitor-1 incubated with Cdk5. In a tissue distribution analysis, basal levels of phospho-Ser6 inhibitor-1 were observed throughout the mouse brain in regions where total inhibitor-1 was detected, including the olfactory bulb, striatum, hippocampus, and cortex (**Figure 2.4B**). In peripheral tissues, phospho-Ser67 and total inhibitor-1 could be detected in kidney, fat, gastrocnemius, and abdominal skeletal muscle. However, phosphorylation of inhibitor-1 at Ser6 was not detected in peripheral tissues, with the exception of fat (**Figure 2.4C**). No signal was detected in the corresponding regions of inhibitor-1 knockout mice (Allen et al., 2000), confirming the specificity of the observed band in tissue homogenates. The developmental profile of phospho-Ser6 and phospho-Ser67 with respect to total inhibitor-1 in mouse striatum collected by Kanehiro Hayashi (UT Southwestern Medical Center) showed high levels of phosphorylation of both sites at embryonic day 18, which steadily decreased to stable levels by about four weeks of age

(**Figure 2.4D**). Immunohistochemical analysis using the phospho-Ser6 inhibitor-1 antibody revealed an apparently specific signal in the granule cell layer of the dentate gyrus and the surrounding cortex (**Supplemental Figure 2.3**). Preliminary estimates place the *in vivo* stoichiometry of phospho-Ser6 inhibitor-1 in the hippocampus at ~40% based on normalization to recombinant standards.

*In vivo phosphorylation of inhibitor-1 by Cdk5 at Ser6*

Acutely dissected striatal slices were treated with the commonly-used Cdk5 inhibitor roscovitine to determine whether Cdk5 is actually the kinase responsible for phosphorylating inhibitor-1 at Ser6 *in vivo*. Akinori Nishi (Kurume University School of Medicine) found that levels of phospho-Ser6 inhibitor-1 were reduced by roscovitine in a dose-dependent manner, with 50  $\mu$ M roscovitine causing a  $65 \pm 8\%$  reduction (**Figure 2.5A**). He also found that another Cdk5 inhibitor, butyrolactone I, also caused a decrease ( $37 \pm 7\%$ ), whereas the MAPK pathway inhibitor U0126 had no effect (**Figure 2.5B**).

As further evidence of the *in vivo* phosphorylation of inhibitor-1 by Cdk5 at Ser6, striatal slices were treated with the novel Cdk5 inhibitor indolinone A (Gillardon et al., 2005a; Gillardon et al., 2005b; Weishaupt et al., 2003). Indolinone A reduced levels of phospho-Ser6 inhibitor-1 in a dose-dependent manner, with 5  $\mu$ M indolinone A causing a  $36 \pm 17\%$  decrease (**Figure 2.5C**). In contrast, indolinone B, primarily an inhibitor of Cdk4 (Weishaupt et al., 2003),

had no effect (**Figure 2.5D**). Phospho-Ser67 inhibitor-1 levels were similarly reduced (**Supplemental Figure 2.4**). For unclear reasons, indolinone A had a much larger effect on the prototypical Cdk5-dependent site Thr75 of DARPP-32. At concentrations of 500 nM and 5  $\mu$ M, indolinone A reduced levels of phospho-Thr75 DARPP-32 by 48% and 74%, respectively (David R. Benavides, UT Southwestern Medical Center, personal communication).

Interestingly, pharmacological inhibition of Cdk5 in the hippocampus did not produce the same results. While treatment of acutely dissected hippocampal slices with roscovitine reduced levels of phospho-Ser67 inhibitor-1 by  $44 \pm 15\%$ , levels of phospho-Ser6 inhibitor-1 remained unaffected (**Figure 2.6**). As an aside, treatment with roscovitine increased levels of phospho-Thr35 inhibitor-1 by  $2.2 \pm 0.2$ -fold (**Supplemental Figure 2.5**), in keeping with the general observation that roscovitine elevates phosphorylation of many PKA-dependent sites (David R. Benavides and Kanehiro Hayashi, UT Southwestern Medical Center, personal communication).

One explanation for the lack of effect of roscovitine on phospho-Ser6 inhibitor-1 levels in the hippocampus is that perhaps the phosphorylation is stable, such that inhibition of Cdk5 activity for only one hour does not allow enough time for the site to turn over. Since turnover of Ser6 might be expected to occur after activation of inhibitor-1 by PKA, hippocampal slices were treated with the adenylyl cyclase activator forskolin. Levels of two PKA-dependent sites,

phospho-Thr34 DARPP-32 and phospho-Thr35 inhibitor-1, as well as the Cdk5-dependent sites of inhibitor-1, were monitored after varying durations of washout of the drug to identify conditions in which levels of phospho-Ser6 inhibitor-1 might be more amenable to regulation by inhibition of Cdk5 activity (**Supplemental Figure 2.6**). Unfortunately, washout of the effects of forskolin on phospho-Thr34 DARPP-32 and phospho-Thr35 inhibitor-1 did not occur in the time frame tested. Furthermore, levels of phospho-Ser6 inhibitor-1 were significantly reduced with time under both control and drug-treated conditions. Thus, it is difficult to attribute any changes in levels of phospho-Ser6 inhibitor-1 to the washout of forskolin. For unclear reasons, simply replacing the buffer in which the slice was incubating induced a decrease in phosphorylation at Ser6. In contrast, levels of phospho-Ser67 and total inhibitor-1 remained unchanged.

*In vivo dephosphorylation of inhibitor-1 by PP-2A, PP-1, and calcineurin at Ser6*

Phosphatase assays employing cell lysates were next employed to identify candidate phosphatases responsible for dephosphorylation of Ser6 (**Figure 2.7A**). [ $\gamma$ - $^{32}$ P]-Ser6/Ser67Asp, generated by preparative phosphorylation of Ser67Asp inhibitor-1 with Cdk5 in the presence of [ $\gamma$ - $^{32}$ P]-ATP, was used as a substrate for dephosphorylation by endogenous phosphatases found in acutely prepared striatal homogenates. In the presence of the  $\text{Ca}^{2+}$  chelator EGTA, there was measurable dephosphorylation of [ $\gamma$ - $^{32}$ P]-Ser6/Ser67Asp inhibitor-1 that was eliminated by



inclusion of microcystin, an inhibitor of both PP-2A and PP-1. Inclusion of fostreicin, primarily an inhibitor of PP-2A, and neurabin (McAvoy et al., 1999), a protein inhibitor of PP-1, caused  $66 \pm 6\%$  and  $37 \pm 4\%$  decreases in dephosphorylation, respectively. In contrast, the calcineurin inhibitor cyclosporin A had no effect. When the assay was repeated without EGTA in the lysis buffer, the rate of dephosphorylation increased by  $2.7 \pm 0.2$ -fold, suggesting that calcineurin was activated under this condition. This conclusion was supported by the fact that addition of cyclosporin A, a highly specific calcineurin inhibitor, resulted in a significant decrease in inhibitor-1 dephosphorylation ( $36 \pm 16\%$ ). Thus, PP-2A and PP-1 dephosphorylate Ser6 under basal conditions, and calcineurin can contribute to dephosphorylation under conditions of high  $\text{Ca}^{2+}$ .

Similar results were observed for the dephosphorylation of [ $\gamma$ - $^{32}\text{P}$ ]-Ser6/Ser67Ala by endogenous phosphatases found in hippocampal homogenates (**Figure 2.7B**). In these experiments, 1  $\mu\text{M}$  okadaic acid, used to inhibit PP-2A/PP-1, impaired dephosphorylation of Ser6. Although low nanomolar concentrations of okadaic acid effectively and selectively inhibit the catalytic subunit of PP-2A ( $\text{IC}_{50} = 1.6 \text{ nM}$ ) *in vitro* (Bialojan and Takai, 1988), 2 nM okadaic acid did not prevent dephosphorylation of Ser6 in these assays. One possibility is a relative impotency of okadaic acid towards PP-2A associated with regulatory factors found in the homogenate.

Akinori Nishi (Kurume University School of Medicine)

pharmacologically treated acutely dissected striatal slices with various phosphatase inhibitors to allow further exploration in a more intact system (**Figure 2.7C**). Calyculin A, an equally potent inhibitor of PP-1 and PP-2A, resulted in a  $1.4 \pm 0.2$ -fold increase in levels of phospho-Ser6 inhibitor-1. In striatal slices, 200 nM okadaic acid inhibits 80% of PP-2A activity and 5% of PP-1 activity, while 1  $\mu$ M okadaic acid inhibits 95% of PP-2A activity and 35% of PP-1 activity (Nishi et al., 1999). Both concentrations of okadaic acid raised levels of phospho-Ser6 inhibitor-1, 200 nM by  $1.42 \pm 0.2$ -fold and 1  $\mu$ M by  $2.1 \pm 0.2$ -fold. In contrast, the calcineurin inhibitor cyclosporin A was ineffective.

Striatal slices were next treated with NMDA to see if calcineurin could contribute to the dephosphorylation of Ser6 under conditions of increased intracellular  $\text{Ca}^{2+}$ . NMDA caused levels of phospho-Ser6 inhibitor-1 to decrease by  $80 \pm 12\%$ . Pairing the NMDA treatment with cyclosporin A resulted in a  $3.1 \pm 1.0$ -fold increase in the level of phosphorylation of Ser6 compared to NMDA treatment alone (**Figure 2.7D**). Thus, by two different systems, PP-2A and PP-1 were found to dephosphorylate Ser6 under basal conditions and calcineurin was found to act under conditions of elevated  $\text{Ca}^{2+}$ .

*Functional significance of Cdk5-dependent phosphorylation of inhibitor-1 in vitro*

Functional analyses of phosphorylation are greatly facilitated by the use of phosphomimetic mutants, since complete phosphorylation can be difficult to achieve *in vitro* (Bibb and da Cruz e Silva, 1997). Thus, we screened for potential functions using phosphomimetic mutants and confirmed positive results using preparatively phosphorylated material. Given the proximity of Ser6 to inhibitor-1's PP-1 binding motif <sup>8</sup>RKIQF<sup>12</sup>, studies to assess the effect of Cdk5-dependent phosphorylation of inhibitor-1 on PP-1 inhibition were conducted. Phosphomimetic mutation of one or both Cdk5 sites to Asp or Glu was equally ineffective in converting inhibitor-1 into an inhibitor of PP-1 in the standard assay involving dephosphorylation of phosphorylase *a* by PP-1 (Cohen et al., 1988) (**Figure 2.8A**). Likewise, phosphomimetic mutation of one or both Cdk5 sites in the context of prior preparative phosphorylation at Thr35 by PKA did not alter the ability of inhibitor-1 to inhibit PP-1. In accordance with previously published values, the IC<sub>50</sub> for all mutant forms of phospho-Thr35 inhibitor-1 was ~5 nM (Foulkes et al., 1983; Huang and Glinemann, 1976). Thus, phosphorylation at Ser6 functions neither in the direct inhibition of PP-1 nor the modulation of the activity of the activated protein.

A possible function for inhibitor-1 other than PP-1 inhibition is suggested by a study in which micromolar concentrations of peptides containing the PP-1 binding motif derived from DARPP-32 (similar to that for inhibitor-1) were able

to compete and interfere with phospho-Thr35 inhibitor-1 for *in vitro* inhibition of PP-1 (Kwon et al., 1997). Consequently, studies to evaluate whether PP-1 sequestration might be a function of inhibitor-1 altered by Cdk5-dependent phosphorylation were conducted. Phosphomimetic-Ser6/Ser67 did not alter the ability of dephospho-Thr35 inhibitor-1 to compete with phospho-Thr35 inhibitor-1 for PP-1 inhibition (**Figure 2.8B**). Addition of 10,000-fold excess of dephospho-Thr35 inhibitor-1 over phospho-Thr35 inhibitor-1 inhibited ~40% of the PP-1 inhibitory activity, whether or not Ser6 and/or Ser67 had been mutated to mimic phosphorylation.

Given the all-or-none importance of Thr35 to inhibitor-1 function, we next examined the effect of Cdk5-dependent phosphorylation of inhibitor-1 on the ability of PKA to phosphorylate inhibitor-1 at Thr35 and activate it. Phosphomimetic mutation of one or both Cdk5 sites did not alter the ability of PKA to phosphorylate inhibitor-1 at Thr35 in time-course reactions (**Figure 2.8C**). All reactions achieved the same stoichiometry. However, PKA reactions performed under linear conditions revealed that phosphomimetic mutation of both Cdk5 sites, but not one Cdk5 site, impaired phosphorylation and activation of the protein at Thr35 (**Figure 2.8D**).

The converse experiment involving dephosphorylation of Thr35 by calcineurin was also conducted. In the context of phosphomimetic mutation (data not shown) or prior phosphorylation at one or both Cdk5 sites (**Figure 2.8E**),

calcineurin was less efficient at dephosphorylating [ $\gamma$ - $^{32}$ P]-Thr35. Phosphorylation of Ser6 alone decreased initial rates of dephosphorylation of Thr35 by 26%; phosphorylation of both Ser6 and Ser67 led to a 61% decrease. Ser67Ala was used as another control, since isolation of the effects of Ser6 from Ser67 required Ser67 to be mutated to allow the preparative phosphorylation of Ser6 alone. Thus, the two Cdk5 sites appear to function in combination to intramolecularly inhibit the dephosphorylation and inactivation of inhibitor-1 at Thr35.

*Functional significance of Cdk5-dependent phosphorylation of inhibitor-1 in vivo*

To determine if this intramolecular inhibition of phosphorylation and dephosphorylation occurs *in vivo*, we subcloned inhibitor-1 into a mammalian expression vector and generated various forms in which one or both Cdk5 sites were mutated to either mimic or block phosphorylation. Since phospho-Ser6 inhibitor-1 exists almost exclusively in the brain, PC12 cells were chosen for transfection for their neuron-like phenotype and endogenous Cdk5 activity (Sharma et al., 1999). The ability of PKA to phosphorylate inhibitor-1 at Thr35 and of endogenous phosphatases to reverse PKA-dependent phosphorylation was examined. PC12 cells transfected with various forms of inhibitor-1 were treated with forskolin, an adenylyl cyclase activator (**Figure 2.9A**). Despite equal levels of inhibitor-1 expression, preventing endogenous Cdk5 from phosphorylating

inhibitor-1 by mutation of one or both of the Cdk5 sites to Ala decreased levels of phosphorylation at Thr35 by >75%, suggesting that the mutation(s) rendered inhibitor-1 more vulnerable to dephosphorylation. Conversely, phosphomimetic mutation of one or both Cdk5 sites resulted in a >45% increase in levels of phospho-Thr35 inhibitor-1 as compared to controls. Thus, intramolecular inhibition of dephosphorylation seems to predominate *in vivo*. Notably, for unclear reasons, levels of total inhibitor-1 were reduced independently of the Cdk5 sites upon treatment with forskolin (**Supplemental Figure 2.7**, top).

Phospho-Ser51 eukaryotic translation initiation factor 2 $\alpha$  (eIF2 $\alpha$ ) has previously been shown to be a PP-1/inhibitor-1 target in HEK293T cells (Weiser et al., 2004). However, despite a large increase in endogenous levels of phospho-Thr35 inhibitor-1 (data not shown), treatment of untransfected PC12 cells with forskolin *lowered* levels of phospho-Ser51 eIF2 $\alpha$  (**Supplemental Figure 2.7**, bottom). Transfection of the various forms of inhibitor-1 did not substantially alter basal levels of phospho-Ser51 eIF2 $\alpha$  (data not shown). Curiously, however, transfection of inhibitor-1 forms mutated to mimic phosphorylation at one or both Cdk5 sites impaired the ability of forskolin to reduce levels of phospho-Ser51 eIF2 $\alpha$  (**Supplemental Figure 2.7**, bottom), while transfection of wild-type inhibitor-1 or inhibitor-1 forms mutated to prevent phosphorylation at the Cdk5 sites did not substantially alter the effect of forskolin. These results suggest that PP-1 mediates the forskolin-induced reduction in levels of phospho-Ser51 eIF2 $\alpha$ .

and that a critical level of phospho-Thr35 inhibitor-1, indirectly provided by phosphomimetic mutation of the Cdk5 sites, is needed to prevent forskolin-induced dephosphorylation.

In a second more physiological approach, we used NMDA to manipulate levels of phospho-Ser6 and phospho-Ser67 inhibitor-1 in acutely dissected striatal slices and looked for a corresponding change in levels of phospho-Thr35 inhibitor-1 (**Figure 2.9B**). Treatment of all slices with the PKA pathway activator forskolin was necessary, as endogenous levels of phospho-Thr35 inhibitor-1 in striatum are virtually undetectable. Indeed, the decrease in levels of phospho-Ser6 ( $87 \pm 19\%$ ) and phospho-Ser67 ( $67 \pm 19\%$ ) inhibitor-1 caused by treatment with NMDA correlated with a decrease in levels of phospho-Thr35 inhibitor-1 ( $88 \pm 28\%$ ). The decreases in phospho-Thr35 and phospho-Ser6 inhibitor-1 were partially reversed with cyclosporin A, even though cyclosporin A alone had no effect. It is unclear whether the reversal in phospho-Thr35 levels is due to direct inhibition of dephosphorylation of Thr35 or indirect inhibition of dephosphorylation of Ser6. Regardless, together these data serve as the first demonstration of the direct modulation of inhibitor-1 function by Cdk5 in living cells.

*Structural effects of phosphomimetic mutation of inhibitor-1 at the Cdk5 sites*

Inhibitor-1 is a protein with little structure, consisting primarily of random coils and four short helical regions (Chyan et al., 2001). Recombinant wild-type and Ser6Asp/Ser67Glu inhibitor-1 enriched in  $^{15}\text{N}$  was purified from *E. coli*. 2D NMR conducted by Irina Dulubova (UT Southwestern Medical Center) revealed that phosphomimetic mutation results in no major structural alterations (**Figure 2.10**). A tight clustering of residues, characteristic of unfolded proteins, was observed in the  $^1\text{H}$ - $^{15}\text{N}$ -HSQC spectra. Chemical shift assignments ( $^1\text{H}$ ,  $^{15}\text{N}$ ) place Ser6, Ser67, and Thr35 at (8.2, 117.5), (8.37, 118.7), and (8.34, 117.2), respectively (Chyan et al., 2001). One of the minor differences in the spectra between wild-type and Ser6Asp/Ser67Glu inhibitor-1 occurs at (8.2, 117.5), likely due to the Ser6 mutation itself.

## Discussion

We report here the discovery, identification, and confirmation of a novel phosphorylation site on inhibitor-1. This phosphorylation event, as detected by a phosphorylation-state specific antibody, occurs *in vivo* and is mediated by Cdk5 in the striatum. Dependence upon Cdk5 was demonstrated through the use of the Cdk5 inhibitors roscovitine, butyrolactone I, and indolinone A. Though indolinone A ( $\text{IC}_{50} = 5 \text{ nM}$ ) (Weishaupt et al., 2003) is a much more potent



inhibitor of Cdk5 than roscovitine ( $IC_{50} = 0.2 \mu M$ ) (Meijer et al., 1997), it is a novel compound that has not been used extensively. Surprisingly, roscovitine did not cause levels of phospho-Ser6 inhibitor-1 to decrease in the hippocampus. This observation might indicate that Cdk5 is not the kinase responsible for phosphorylation of Ser6 in the hippocampus or that another kinase can compensate in the absence of Cdk5. Another explanation is that perhaps the phosphorylation of Ser6 is stable in the hippocampus, such that inhibition of Cdk5 activity for only one hour does not allow enough time for the site to turn over.

Higher expression of inhibitor-1 in the olfactory bulb, cortex, striatum, and hippocampus than in the brain stem and cerebellum agrees with results published at the protein (Lowenstein et al., 1995) and mRNA levels (Sakagami et al., 1994). That phosphorylation of inhibitor-1 at Ser6 seems to occur wherever inhibitor-1 is present in the brain suggests its importance to the function of the protein. Phosphorylation of Ser67 in the striatum is attributed to Cdk5, as Cdk1 is not active in postmitotic neurons and pharmacological inhibition of MAPK does not alter levels of phospho-Ser67 inhibitor-1 (Bibb et al., 2001b). While phosphorylation of Ser6 is relatively brain-specific, phosphorylation of Ser67 seems to be a general phenomenon occurring throughout the body.

Cdk5 activity is generally restricted to the brain (Lew et al., 1994; Tsai et al., 1994), so presumably other kinases such as Cdk1 and MAPK phosphorylate Ser67 in peripheral tissues. However, some evidence suggests the presence of

Cdk5 in low levels in peripheral tissues (Rosales and Lee, 2006), particularly the insulin-secreting  $\beta$  cells of the pancreas, where it regulates insulin release (Lilja et al., 2001; Wei et al., 2005a). Interestingly, PP-1 enhances the synthesis of insulin via the dephosphorylation of eukaryotic translation initiation factor  $2\alpha$  (eIF2 $\alpha$ ) (Vander Mierde et al., 2007), which has been shown to be regulated by inhibitor-1 in transfected HEK293T cells (Weiser et al., 2004). Furthermore, inhibitor-1 and its homologue DARPP-32 have recently been shown to localize to pancreatic  $\beta$  cells (Lilja et al., 2005). Thus, pancreatic  $\beta$  cells represent one non-neuronal tissue in which Cdk5-dependent phosphorylation of inhibitor-1 may be important.

It is unclear what protein kinase is responsible for the small amount of phospho-Ser6 inhibitor-1 detected in fat, as Ser6 was not shown to be a good substrate for Cdk1 or MAPK *in vitro*. Regardless, the major kinase responsible for phosphorylation of Ser6 in the striatum is Cdk5, because pharmacological inhibition of Cdk5 activity for one hour with roscovitine decreased phospho-Ser6 inhibitor-1 levels by ~65%.

Expression of total inhibitor-1 in kidney, fat, and skeletal muscle, but not in lung, agrees well with previous results obtained at the protein (MacDougall et al., 1989) and mRNA levels (Elbrecht et al., 1990). We could not detect inhibitor-1 in the liver, as rat and mouse liver possesses little or no inhibitor-1 protein (MacDougall et al., 1989) or mRNA (Elbrecht et al., 1990), in contrast to rabbit, guinea pig, porcine, and sheep liver. Although inhibitor-1 is widely

studied in relation to cardiac failure (El-Armouche et al., 2004; El-Armouche et al., 2003; Gupta et al., 2003; Gupta et al., 2005), we were also unable to detect a signal in heart. This likely relates to the very low abundance of inhibitor-1 in this tissue (Elbrecht et al., 1990; Gupta et al., 1996; Neumann et al., 1991).

That Cdk5-dependent phosphorylation of inhibitor-1 rendered it less susceptible to dephosphorylation at Thr35, rather than having a direct effect on its ability to inhibit PP-1, was somewhat surprising given the proximity of Ser6 to inhibitor-1's PP-1 binding motif (<sup>8</sup>RKIQF<sup>12</sup>). The consensus sequence of this degenerate motif is K/R/H/N/S V/I/L X F/W/Y (Bollen, 2001), and phosphorylation of serine(s) close to or within this motif has been shown to impair PP-1 binding to several partner proteins, including nuclear protein phosphatase-1 (NIPP-1) (Beullens et al., 1999), neurabin I (McAvoy et al., 1999), and muscle glycogen-binding subunit (G<sub>M</sub>) (Liu and Brautigan, 2000). One function of inhibitor-1 may be to facilitate interactions between PP-1 and various other proteins. While competition assays involving phospho-Thr35 inhibitor-1 did not reveal an effect of Ser6 on PP-1 binding, the potency with which phospho-Thr35 inhibitor-1 inhibits PP-1 leaves the distinct possibility that binding is somewhat altered and that phosphorylation of Ser6 might impair such interactions.

Ironically, PP-1—the phosphatase that inhibitor-1 is charged with inhibiting—can dephosphorylate inhibitor-1 at Ser6. This circuit may function as

a positive feedback loop in that activation of PKA will lead to phosphorylation of inhibitor-1 at Thr35 with consequent inhibition of PP-1 activity and maintenance of phosphorylation at Ser6. Phosphorylation at this and the other Cdk5 site, in turn, would render inhibitor-1 less susceptible to dephosphorylation at Thr35, perpetuating the PKA signal. Indeed, mutation of either or both Cdk5 sites to prevent phosphorylation resulted in lower levels of phospho-Thr35 inhibitor-1 induced by forskolin, presumably by making inhibitor-1 more vulnerable to dephosphorylation at Thr35. In contrast, phosphomimetic mutation of either or both Cdk5 sites resulted in greater forskolin-induced levels of phospho-Thr35 inhibitor-1. Thus, Cdk5 and PKA function synergistically in the case of inhibitor-1, in stark contrast to the inhibitor-1 homologue DARPP-32, in which Cdk5-dependent phosphorylation at Thr75 mediates conversion of the protein into a direct inhibitor of PKA (Bibb et al., 1999).

The opposing roles of inhibitor-1 and DARPP-32 in the regulation of PKA signaling pathways highlight the versatile repertoire of signaling cascades available to neurons through the use of different protein phosphatase regulators. Adding to this repertoire of regulatory molecules is the phenomenon of multi-site phosphorylation. Ser6 is the fourth phosphorylation site identified on inhibitor-1, following Thr35, Ser67, and Ser65. That phosphorylation of Ser67 protects PP-1 from reversing the protein kinase C (PKC)-dependent phosphorylation of Ser65 (Sahin et al., 2006) highlights the complex interplay that can occur among

multiple phosphorylation sites by different kinases on a single protein. Indeed, even with two phosphorylation sites on a single protein by a single kinase, there appears to be a precise sequence to the orchestration of phosphorylation events. Phosphomimetic data indicate that prior phosphorylation of Ser67 by Cdk5 facilitates phosphorylation of Ser6. Further adding to the complexity of multi-site phosphorylation is the fact that PP-1 does not exist in cells as a free catalytic subunit. Thus, the physiological impact of Cdk5-dependent phosphorylation of inhibitor-1 can only be understood in the context of multimeric PP-1 complexes.

The phosphorylation state of eIF2 $\alpha$ , and thus the initiation of protein translation, has been suggested to be regulated by the association of inhibitor-1 and PP-1 with growth arrest and DNA damage-inducible protein (GADD34) (Connor et al., 2001). As with HEK293T cells (Weiser et al., 2004), overexpression of inhibitor-1 in PC12 cells did not alter basal levels of phospho-Ser51 eIF2 $\alpha$ . However, in contrast to the increase in levels of phospho-Ser51 eIF2 $\alpha$  in HEK293T cells (Weiser et al., 2004), forskolin treatment of PC12 cells overexpressing wild-type inhibitor-1 resulted in a paradoxical decrease in levels of phospho-Ser51 eIF2 $\alpha$ , despite a large increase in levels of phospho-Thr35 inhibitor-1. That phosphomimetic mutation of the Cdk5 sites on inhibitor-1 impaired the reduction in phosphorylation of eIF2 $\alpha$  suggests the involvement of PP-1 and possibly a critical threshold of phospho-Thr35 inhibitor-1 necessary for regulation of eIF2 $\alpha$  phosphorylation. However, the exact role of Cdk5-dependent

phosphorylation of inhibitor-1 in the regulation of eIF2 $\alpha$  phosphorylation remains unclear without further study.

In another distinct interaction, PP-1 and glycogen synthase kinase 3 (GSK3) are thought to exist in a complex regulated by Cdk5 (Morfini et al., 2004). Inhibition of Cdk5 leads to the activation of PP-1 and consequent dephosphorylation and activation of GSK3, which in turn phosphorylates kinesin, a protein involved in the fast anterograde transport of membrane-bound organelles. Whether inhibitor-1 serves as the link between inhibition of Cdk5 and activation of PP-1 remains to be determined. Complicated cascades such as this Cdk5–PP-1–GSK3–kinesin one allow cells to fine-tune their responses to external stimuli that activate a whole host of intracellular signal transduction pathways.

Prominent among the external stimuli that control Cdk5 activity is glutamate acting via the ionotropic NMDA receptor. NMDA regulates Cdk5 activity (Kerokoski et al., 2004; Wei et al., 2005b), and levels of phospho-Ser67 inhibitor-1 decrease upon treatment of acutely dissected striatal slices with NMDA (Bibb et al., 2001b). We show here that phospho-Ser6 is similarly affected, but to a greater extent than phospho-Ser67 inhibitor-1. Together, Ser6 and Ser67 represent an opportunity for NMDA receptor signaling to converge upon PKA signaling pathways originating from G<sub>s</sub>-coupled receptors such as the D<sub>1</sub> dopamine receptor, A<sub>2A</sub> adenosine receptor, or  $\beta$ -adrenergic receptor. The indirect modulation of inhibitor-1 activity by Cdk5 may provide an important

point for the amplification of PKA signaling resulting from activation of these receptors. We have shown that inhibitor-1 serves as a critical junction between kinase and phosphatase signaling pathways, linking PP-1 to not only PKA and calcineurin, but also Cdk5.

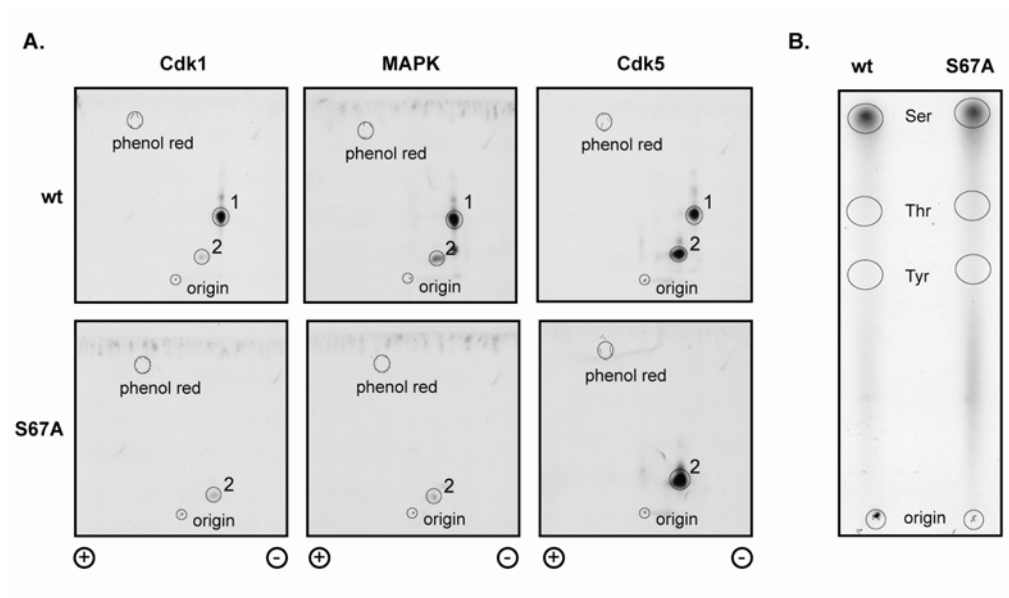


**Figure 2.1. Discovery of a novel Cdk5 site on inhibitor-1.** **A**, Phosphopeptide maps of tryptic digests of wild-type (wt) and S67A I-1 phosphorylated by Cdk1/cyclin B, MAPK, or Cdk5/p25 *in vitro*. **B**, Phosphoamino acid analysis of acid-hydrolyzed tryptic digests of wt and S67A I-1 phosphorylated by Cdk5/p25 *in vitro*.



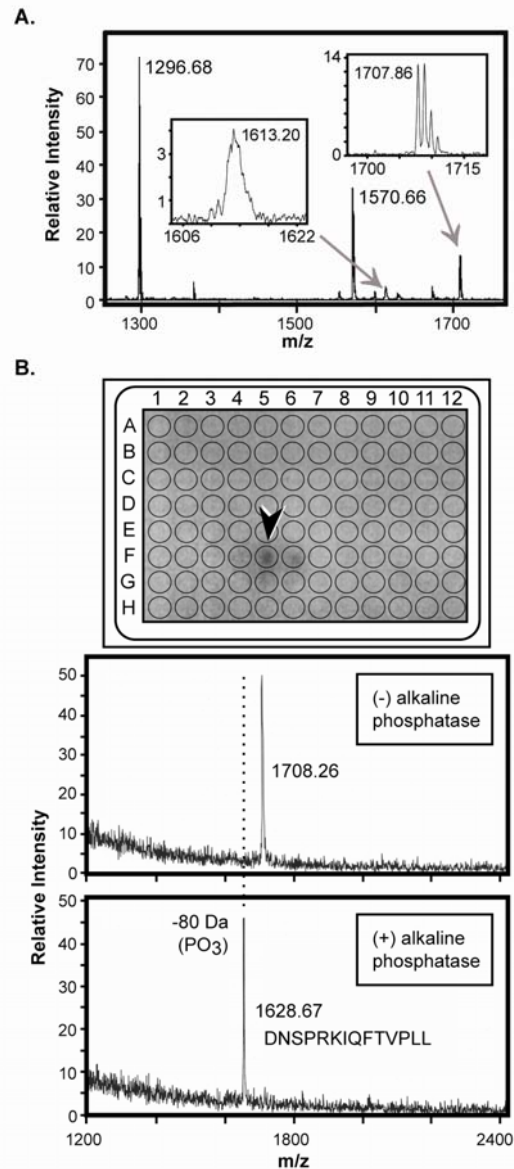


**Figure 2.2. Identification of Ser6 as the novel Cdk5 site of inhibitor-1.**

**A,** MALDI-TOF MS of an Asp-N digest of S67A I-1 phosphorylated by Cdk5/p25. Insets show enlargements of the peaks for the phosphorylated peptide  $^4$ DNSPRKIQFTVPLL<sup>17</sup> and its daughter ion. Masses (Da) of peptides are indicated. **B,** Autoradiogram of the 96-well plate into which fractions were robotically collected after capillary HPLC purification of the Asp-N digest (top) and MALDI-TOF MS of the radiolabeled fraction before and after alkaline phosphatase treatment (bottom).

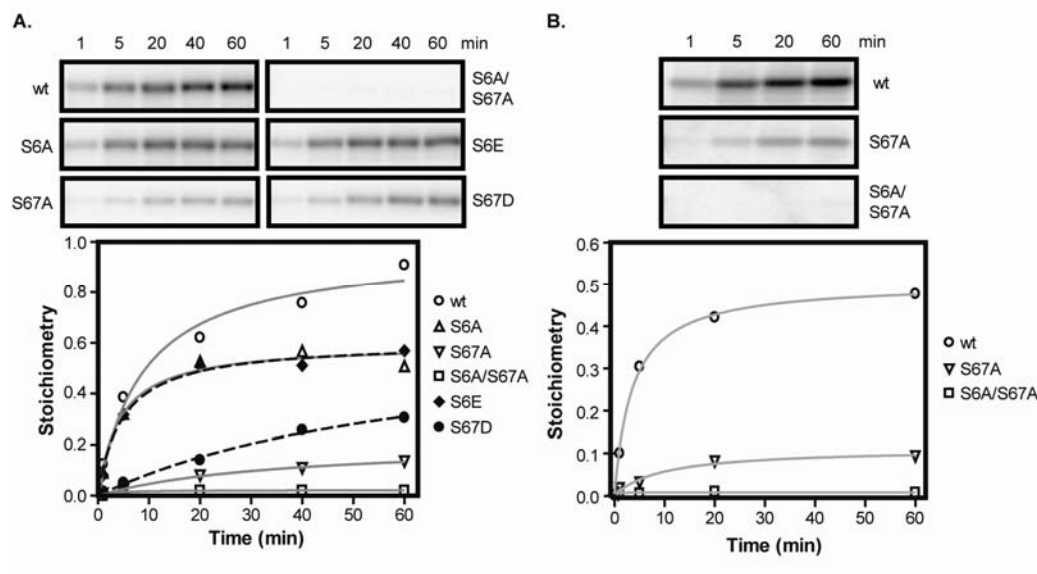


**Figure 2.3. Confirmation of Ser6 as the novel Cdk5 site of inhibitor-1.**

**A.** Phosphorimages (top) and quantitation (bottom) of *in vitro* phosphorylation of wt, S6A, S67A, S6A/S67A, S6E, and S67D I-1 by Cdk5/p25 in a time-course experiment. **B.** Phosphorimages (top) and quantitation (bottom) of *in vitro* phosphorylation of wt, S67A, and S6A/S67A I-1 by Cdk5/p35 in a time-course experiment.

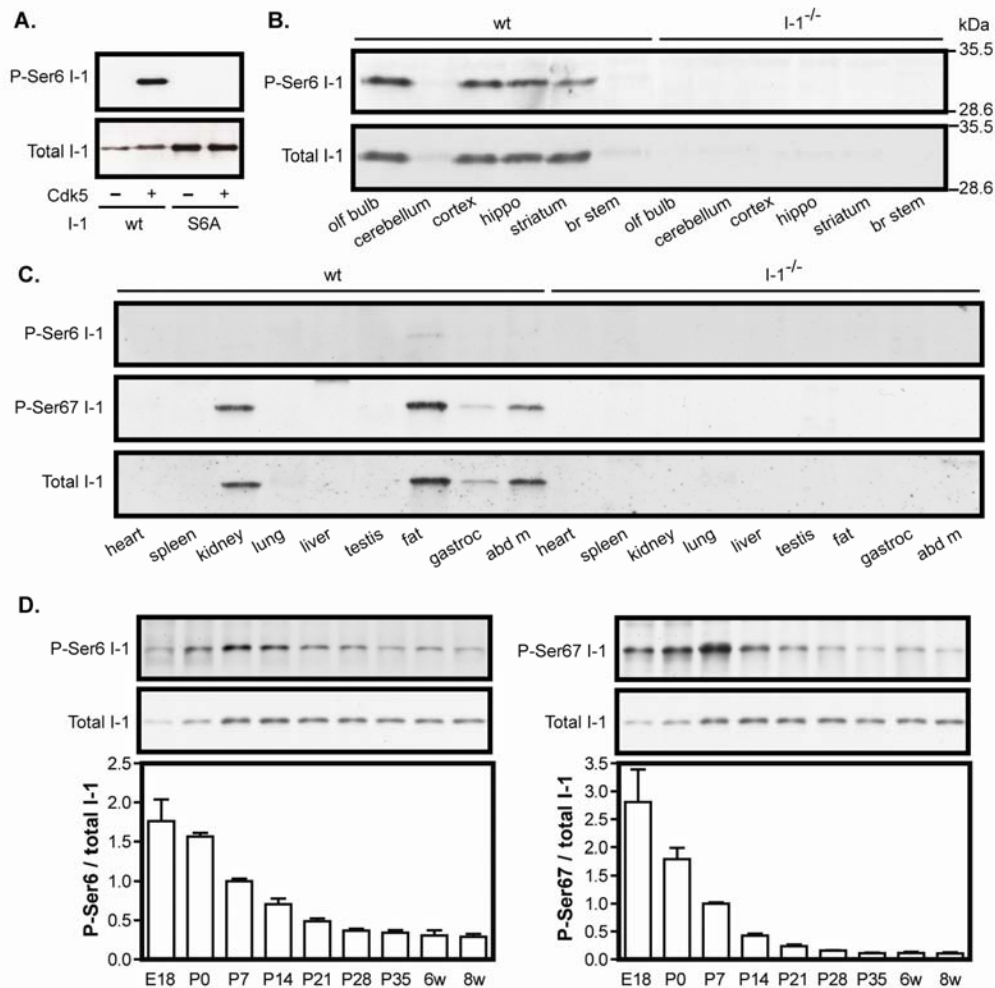


**Figure 2.4. Demonstration of the *in vivo* phosphorylation of inhibitor-1 at Ser6.** **A**, Immunoblots of wt and S6A I-1 phosphorylated or mock phosphorylated by Cdk5 using antibodies against phospho-Ser6 and total I-1. Immunoblots showing the **B**, distribution of phospho-Ser6 and total I-1 throughout the brains of wt and I-1<sup>-/-</sup> mice; olf bulb, olfactory bulb; cortex, frontal cortex; hippo, hippocampus; br stem, brain stem. **C**, distribution of phospho-Ser6, phospho-Ser67, and total I-1 throughout the bodies of wt and I-1<sup>-/-</sup> mice; gastroc, gastrocnemius; abd m, abdominal muscle. **D**, developmental time course with quantitation of phospho-Ser6 (left) and phospho-Ser67 (right) relative to total I-1 in mouse striatum, n = 2-4.

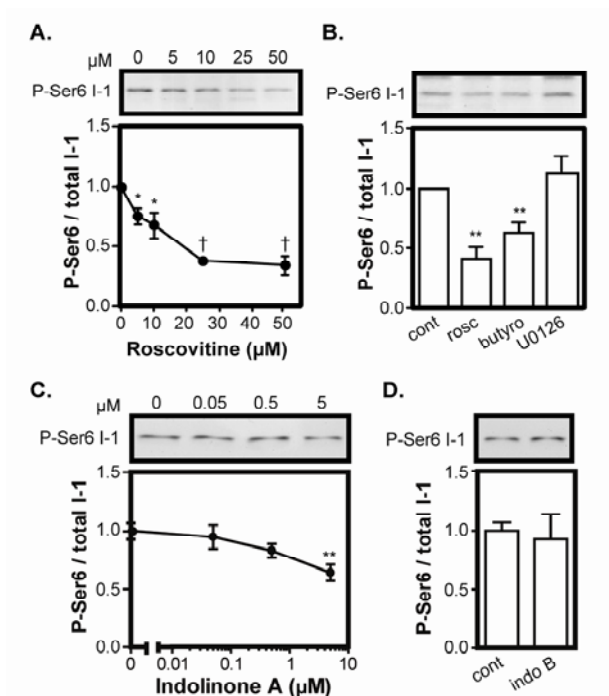


**Figure 2.5. *In vivo* phosphorylation of inhibitor-1 by Cdk5 at Ser6.**

**A-D**, Quantitative immunoblot analysis of acute striatal slices incubated with **A**, different concentrations of the Cdk5 inhibitor roscovitine (60 min),  $n = 4$ . **B**, the Cdk5 inhibitors roscovitine (rosc, 50  $\mu$ M) and butyrolactone I (butyro, 20  $\mu$ M) or the MAPK pathway inhibitor U0126 (40  $\mu$ M) for 60 min,  $n = 3$ . **C**, different concentrations of the novel Cdk5 inhibitor indolinone A (60 min). \*\*,  $p < 0.01$ , Kruskal-Wallis with Dunn's multiple comparison test,  $n = 4-5$ . **D**, the Cdk4 inhibitor indolinone B (indo B, 5  $\mu$ M, 1 h),  $n = 3-4$ . **A-B**, \*,  $p < 0.05$ , \*\*,  $p < 0.01$ , †,  $p < 0.001$ , one-way analysis of variance (ANOVA) with Newman-Keuls multiple comparison test.

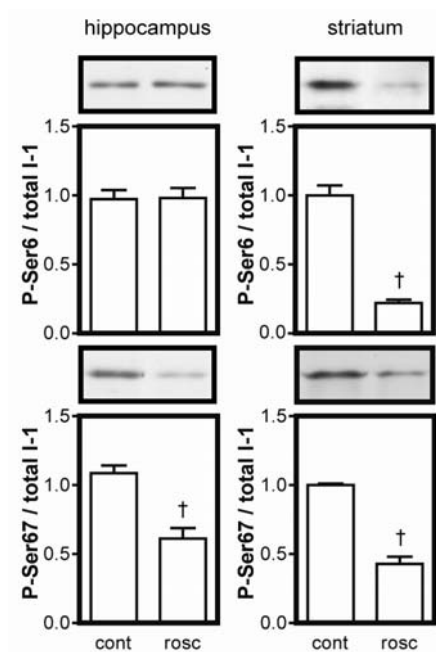


**Figure 2.6. Comparison of Cdk5-dependent phosphorylation of inhibitor-1 at Ser6 and Ser67 in the hippocampus and the striatum.** Quantitative immunoblot analysis of acute hippocampal (left) or striatal (right) slices incubated with or without 50  $\mu$ M roscovitine (60 min),  $n = 5-7$ . <sup>†</sup>,  $p < 0.001$ , student's unpaired  $t$  test.

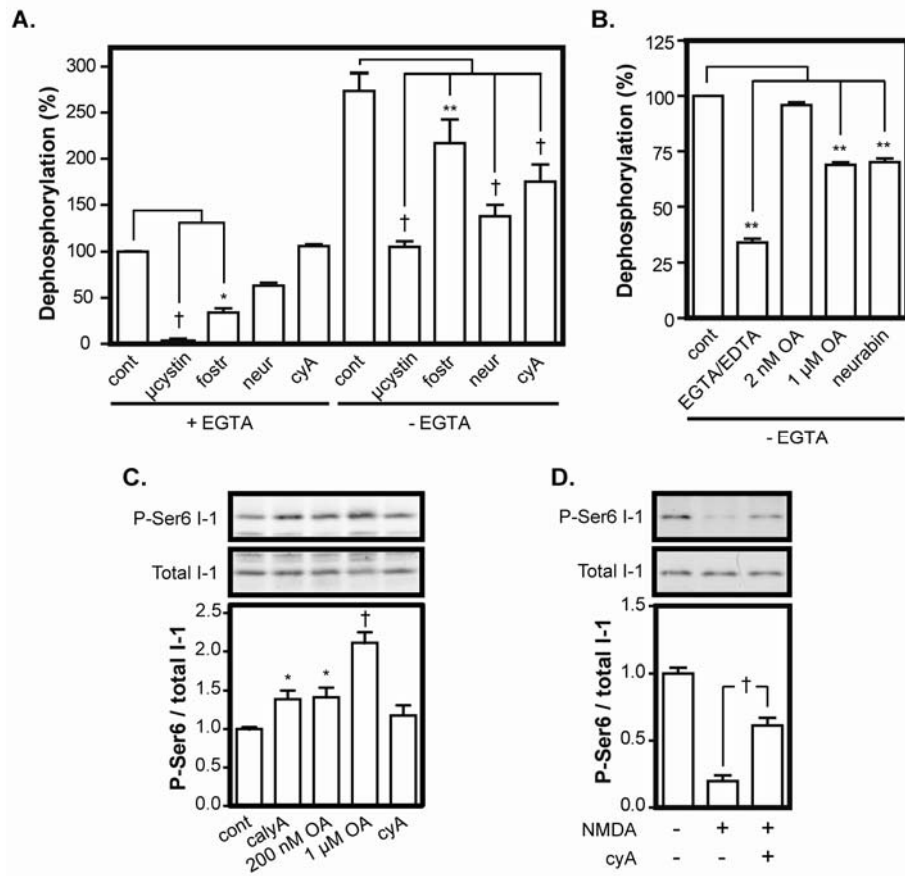


**Figure 2.7. *In vivo* dephosphorylation of inhibitor-1 by PP-2A, PP-1, and calcineurin at Ser6.** **A-B,** Phosphatase reconstitution assays in which the dephosphorylation of **A**,  $^{32}$ P-Ser6/Ser67Asp I-1 or **B**,  $^{32}$ P-Ser6/Ser67Ala I-1 was measured 15 min after the addition of  $\sim 15$   $\mu$ g [**A**, striatal or **B**, hippocampal] lysate with or without various phosphatase inhibitors [microcystin ( $\mu$ cystin, 1  $\mu$ M), fostreicin (fostr, 5  $\mu$ M), neurabin (0.1  $\mu$ g/ $\mu$ l), cyclosporin A (cyA, 1  $\mu$ M), EGTA/EDTA (5 mM/1 mM), okadaic acid (OA, 2 nM or 1  $\mu$ M)] in the presence (+) or absence of (–) EGTA (2 mM),  $n = 3-4$ . **C**, Quantitative immunoblot analysis of acute striatal slices incubated in the absence or presence of various phosphatase inhibitors [calyculin A (calyA, 200 nM), okadaic acid (OA, 200 nM or 1  $\mu$ M), cyclosporin A (cyA, 10  $\mu$ M)] for 60 min,  $n = 4$ . **D**, Quantitative immunoblot analysis of acute striatal slices treated with cyclosporin A (cyA, 10  $\mu$ M, 60 min) and/or NMDA (50  $\mu$ M, 5 min),  $n = 5-7$ . **A-D**, \*,  $p < 0.05$ , \*\*,  $p < 0.01$ , †,  $p < 0.001$ , one-way ANOVA with Newman-Keuls multiple comparison test.

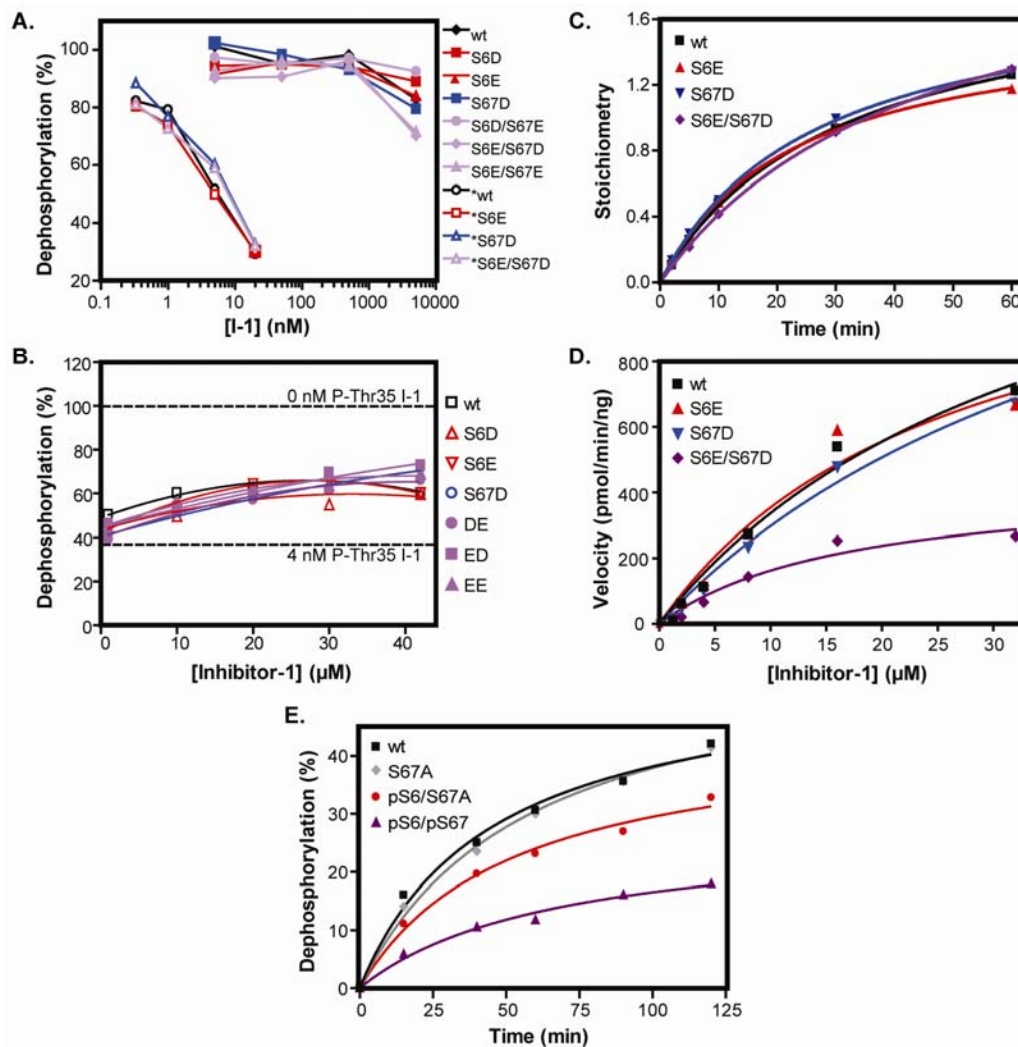


**Figure 2.8. Functional significance of Cdk5-dependent phosphorylation of inhibitor-1 *in vitro*.** **A**, *In vitro* phosphatase assays involving dephosphorylation of the substrate phosphorylase *a* by PP-1 in the presence of wt I-1 or various forms of I-1 mutated to mimic phosphorylation at one or both Cdk5 sites. (\*) indicates prior phosphorylation by PKA. **B**, Competition of wt or various forms of I-1 mutated to mimic phosphorylation at one or both Cdk5 sites with 4 nM phospho-Thr35 I-1 for PP-1 inhibition. **C**, Time course of *in vitro* phosphorylation of wt or various mutant forms of I-1 by PKA. **D**, Kinetic analysis of *in vitro* phosphorylation of wt or various mutant forms of I-1 by PKA. **E**, Time course of *in vitro* calcineurin-mediated dephosphorylation of different forms of <sup>32</sup>P-Thr35 I-1 previously phosphorylated or mock phosphorylated by Cdk5.

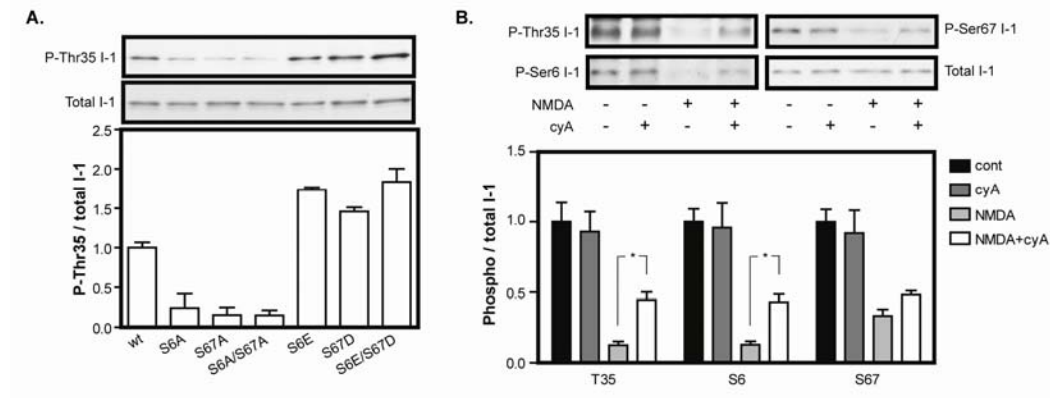


**Figure 2.9. Functional significance of Cdk5-dependent phosphorylation of inhibitor-1 *in vivo*.** **A**, Quantitative immunoblot analysis of PC12 cells treated with 5  $\mu$ M forskolin (10 min) 40 h after transfection with wt I-1 or various forms of I-1 mutated to either prevent or mimic phosphorylation at one or both Cdk5 sites,  $n = 2$ . **B**, Quantitative immunoblot analysis of acute striatal slices treated with forskolin (10  $\mu$ M, 10 min) in the absence or presence of NMDA (50  $\mu$ M, 5 min) and cyclosporin A (cyA, 10  $\mu$ M, 60 min). \*,  $p < 0.05$ , one-way ANOVA with Newman Keuls multiple comparison test,  $n = 3-6$ .



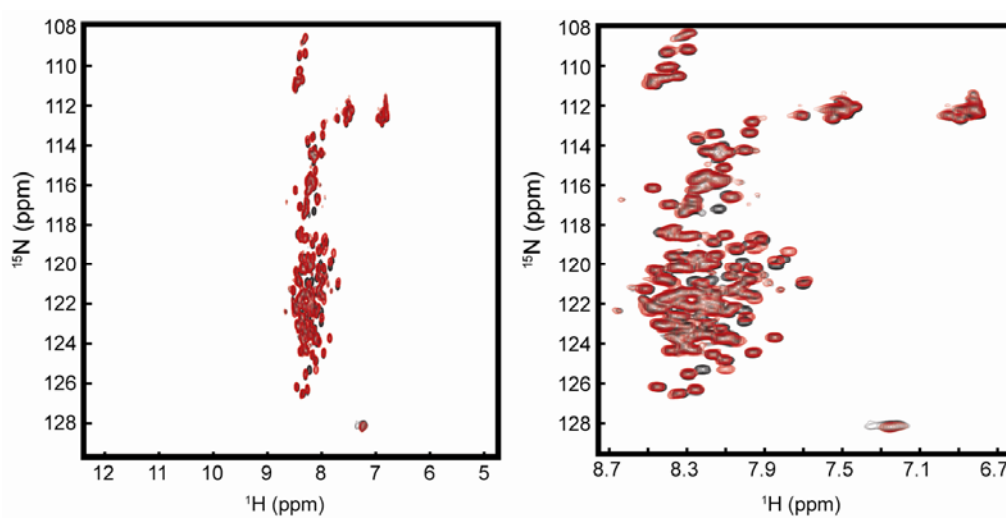
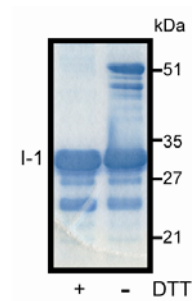
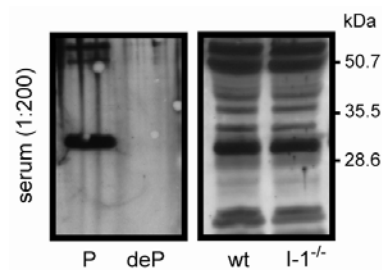


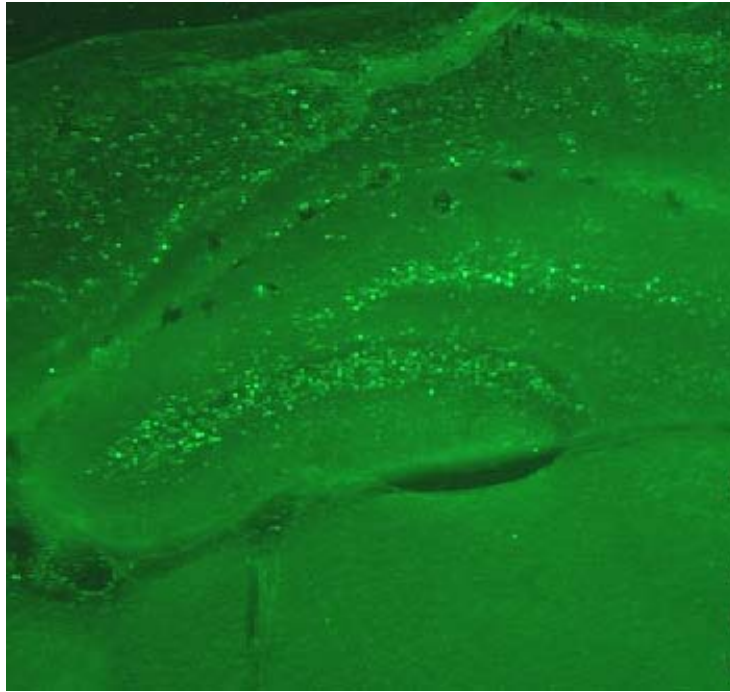
**Figure 2.10. Analysis of the structural effects of phosphomimetic mutation of inhibitor-1 by 2D NMR.** Overlay of HSQC spectra for wt (black) and S6E/S67D (red) I-1. The entire spectrum (left) and an enlargement (right) are shown.



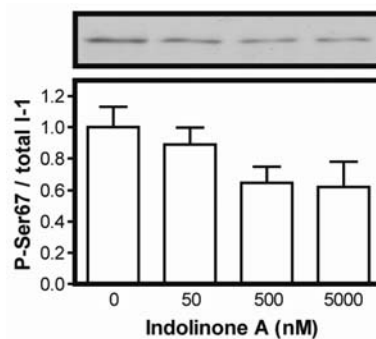
**Supplemental Figure 2.1. Disulfide-bond reduction of recombinant rat inhibitor-1.** Coomassie stain of a 15% SDS-PAGE analysis of wt recombinant rat I-1 (10  $\mu$ g) prepared in protein sample buffer with (+) or without (-) 26 mM DTT.



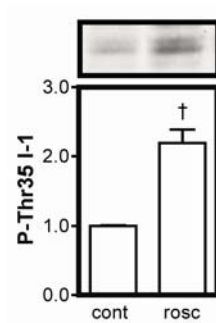
**Supplemental Figure 2.2. Specificity of antisera against phospho-Ser6 inhibitor-1.** Immunoblot analysis of phospho-Ser6 (P) and dephospho-Ser6 (deP) I-1 standards (50 ng), as well as brain homogenates of wt and I-1<sup>-/-</sup> mice, using antisera against phospho-Ser6 I-1 (1:200). Detection of the multiple cross-reactive bands in brain homogenate was eliminated upon purification of the antisera.



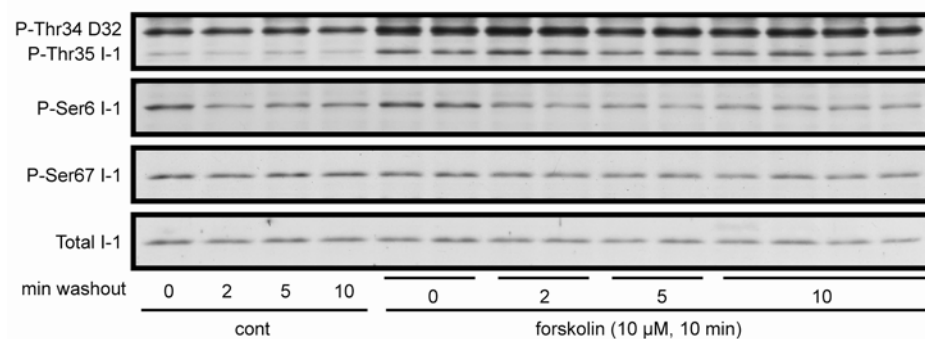
**Supplemental Figure 2.3. Immunostain for phospho-Ser6 inhibitor-1.** Cells in the granule cell layer of the dentate gyrus and the surrounding cortex can be visualized.



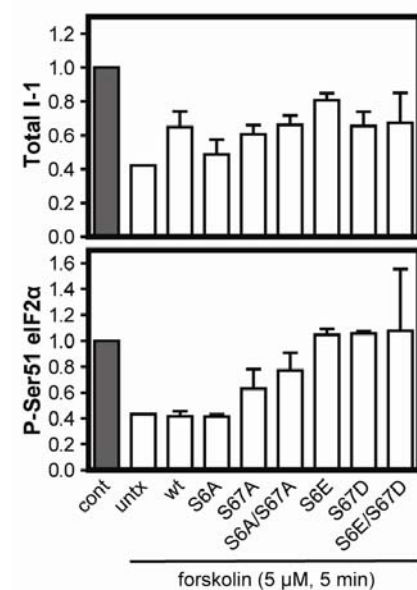
**Supplemental Figure 2.4. Reduction in levels of phospho-Ser67 inhibitor-1 by indolinone A.** Quantitative immunoblot analysis of acute striatal slices treated with different doses of indolinone A (60 min), n = 4-5.



**Supplemental Figure 2.5. Enhancement of phosphorylation of PKA-dependent site of inhibitor-1 by roscovitine.** Quantitative immunoblot analysis of acute hippocampal slices treated with 50  $\mu$ M roscovitine (60 min),  $n = 4-5$ . <sup>†</sup>,  $p < 0.001$ , student's unpaired  $t$  test.



**Supplemental Figure 2.6. Effects of washout of forskolin on PKA-dependent sites of DARPP-32 and inhibitor-1 and Cdk5-dependent sites of inhibitor-1.** Immunoblot analysis of acute hippocampal slices treated with 10  $\mu$ M forskolin or vehicle for 10 min before washout for the indicated times. Similar results were seen in another independent experiment.



**Supplemental Figure 2.7. Forskolin-induced changes in levels of total inhibitor-1 and phospho-Ser51 eIF2 $\alpha$  in PC12 cells.** Quantitative immunoblot analysis of PC12 cells treated with 5  $\mu$ M forskolin (10 min) 40 h after (mock) transfection with various forms of I-1. Levels of total I-1 and phospho-eIF2 $\alpha$  are expressed relative to levels in cells transfected with the same form of I-1 but treated with vehicle instead of forskolin,  $n = 3$  for total I-1 and  $n = 2$  for phospho-eIF2 $\alpha$ , except untransfected (untx) where  $n = 1$ .



## CHAPTER THREE

### DIFFERENTIAL REGULATION OF THE CDK5-DEPENDENT PHOSPHORYLATION SITES OF INHIBITOR-1 AND DARPP-32 BY DEPOLARIZATION

#### Summary

While cyclin-dependent kinase 5 (Cdk5) is of growing importance to neuronal signaling, its regulation remains relatively unexplored. Examination of the mechanism by which NMDA induces decreases in the phosphorylation of protein phosphatase inhibitor-1 at Ser6 and Ser67 and dopamine- and cAMP-regulated phosphoprotein  $M_r$  32,000 (DARPP-32) at Thr75 revealed that generalized depolarization, rather than specific activation of NMDA receptors, was sufficient to induce decreases in these Cdk5 sites. Although no evidence for the involvement of the Cdk5 cofactors p35 or p39, or for L- and T-type voltage-gated  $\text{Ca}^{2+}$  channels, was found, evaluation of the role of phosphatases and extracellular cations revealed differential regulation of the three sites. NMDA-induced decreases in the phosphorylation of Thr75 of DARPP-32 required protein phosphatase 1/2A (PP-1/2A) activity and extracellular  $\text{Ca}^{2+}$ . In contrast, the effects on Ser6 and Ser67 of inhibitor-1 were not cation-specific; either  $\text{Na}^+$  or  $\text{Ca}^{2+}$  sufficed. Furthermore, while the decrease in phosphorylation of Ser6 was partially dependent on protein phosphatase 2B (PP-2B), that of Ser67 was

independent of the major protein serine/threonine phosphatases, likely indicating the presence of a pathway by which NMDA inhibits Cdk5 activity. Thus, in the striatum the regulation of phosphorylation of Cdk5-dependent sites by NMDA occurs through multiple distinct pathways.

## **Introduction**

In spite of its name, Cdk5, a proline-directed serine/threonine kinase (Lew et al., 1992), is not cyclin-dependent. Its activity is instead dependent on the relatively neuron-specific cofactor p35 (Lew et al., 1994; Tsai et al., 1994), or its homologue p39 (Tang and Wang, 1996; Tang et al., 1995), thereby largely restricting its activity to postmitotic neurons. Cdk5 now possesses an extensive list of substrates, among them two protein kinase A (PKA)-dependent inhibitors of PP-1, DARPP-32 (D32) (Bibb et al., 1999) and protein phosphatase inhibitor-1 (inhibitor-1, I-1) (Bibb et al., 2001b and Chapter 2). Cdk5-dependent phosphorylation of DARPP-32 at Thr75 converts it into an inhibitor of PKA (Bibb et al., 1999). In direct contrast, Cdk5-dependent phosphorylation of inhibitor-1 at Ser6 and Ser67 impairs dephosphorylation and inactivation of the protein, allowing perpetuation of the PKA signal (Chapter 2).

In striatal slices, levels of phosphorylation of Thr75 of DARPP-32 and Ser6 and Ser67 of inhibitor-1 are reduced upon treatment with NMDA (Bibb et

al., 2001b; Nishi et al., 2002 and Chapter 2), suggesting potential NMDA-dependent regulation of Cdk5 activity. Interestingly, counter-regulation of the NMDA receptor by Cdk5 has been observed. Phosphorylation of the NR2A subunit of the NMDA receptor by Cdk5 has been suggested to increase NMDA receptor activity required for the induction of long-term potentiation in the Schaffer collateral pathway (Li et al., 2001). Moreover, Cdk5 is thought to regulate NMDA receptor constituency by modulating the stability of the NR2B subunit (Hawasli et al., manuscript submitted).

Interactions between NMDA receptors and dopamine receptors modulate psychostimulant action in the striatum, a critical aspect of the function of Cdk5-dependent phosphorylation of DARPP-32 (Bibb et al., 2001a). D<sub>2</sub> dopamine receptors directly associate with NR2B subunits of the NMDA receptor, preventing phosphorylation of the subunit and activation of the NMDA receptor by Ca<sup>2+</sup>/calmodulin-dependent kinase II (CaMKII) (Liu et al., 2006). D<sub>1</sub> dopamine receptors not only physically associate with NMDA receptors, but also potentiate NMDA receptor function via second messenger action (Cepeda and Levine, 2006).

Mechanisms for the regulation of Cdk5 activity by NMDA have been varied. Ionotropic glutamate receptors, including NMDA receptors, mediate cleavage of p35 to p25 (Kerokoski et al., 2004) by the Ca<sup>2+</sup> activated protease calpain (Kusakawa et al., 2000; Lee et al., 2000; Nath et al., 2000). Cleavage of

p35 releases it from the membrane, allowing Cdk5 to aberrantly phosphorylate substrates implicated in a wide range of neuropathologies (Nath et al., 2000; Nguyen et al., 2001; Patrick et al., 1999; Wang et al., 2003). Ionotropic glutamate receptor-mediated regulation of Cdk5 activity independent of p25 generation has also been observed (Wei et al., 2005b). Treatment of cortical cultures with NMDA or kainate induces autophosphorylation of p35, which targets it for degradation by the proteasome, ultimately leading to a reduction in Cdk5 activity.

Like other cyclin-dependent kinases, Cdk5 appears to be regulated by the availability of its cofactors (Hisanaga and Saito, 2003). The transcriptional upregulation of p35 by Egr1 results in Cdk5 activation, which is required for nerve growth factor (NGF)-induced differentiation of PC12 pheochromocytoma cells (Harada et al., 2001). In contrast, Cdk5-dependent autophosphorylation of p35 results in its ubiquitin-dependent proteasomal degradation with consequent Cdk5 inhibition (Kerokoski et al., 2002; Patrick et al., 1998; Saito et al., 1998; Saito et al., 2003; Wei et al., 2005b). Autophosphorylation of p35 also protects it from calpain-dependent conversion to p25 (Kamei et al., 2007). Supporting this conclusion is the observation that p35 from adult brains is both less phosphorylated at Thr138 and more susceptible to calpain-dependent cleavage than that from fetal brains (Kamei et al., 2007). Much less is known about p39, but it too seems to be converted to p29 by calpain (Patzke and Tsai, 2002). Recently, phosphorylation of p35 was shown to affect Cdk5 activity by regulating

association of the Cdk5/p35 complex with membranes (Sato et al., manuscript submitted; Zhu et al., 2005).

Distinctly different from the downregulation of Cdk5 activity by ionotropic glutamate receptors is the transient upregulation of Cdk5 activity by Group I metabotropic glutamate receptors, a process dependent on activation of casein kinase 1 (CK1) (Liu et al., 2001). How CK1 mediates activation of Cdk5 remains unclear; the ability of CK1 to directly phosphorylate and activate the catalytic subunit of Cdk5 is a matter of some debate (Liu et al., 2001; Sharma et al., 1999). Direct phosphorylation and activation of the catalytic subunit of Cdk5 at Tyr15 by protein tyrosine kinases is another means of activation of Cdk5 (Fu et al., 2007; Sasaki et al., 2002; Zukerberg et al., 2000), as is the phosphatidylinositol-linked D<sub>1</sub> dopamine receptor (Zhen et al., 2004). Pharmacological inhibition of protein kinase C (PKC) activity with calphostin C prevented D<sub>1</sub> receptor-mediated activation of Cdk5, suggesting a novel PKC-dependent pathway for the positive regulation of Cdk5 activity (Zhen et al., 2004). However, activation of PKC in striatal slices with phorbol-12,13-dibutyrate (PDBu) caused time- and dose-dependent decreases in levels of phospho-Ser67 inhibitor-1 and phospho-Thr75 DARPP-32, and levels of these two phospho-sites were elevated in brain tissue from PKC- $\alpha$  knockout mice, suggesting negative regulation of Cdk5 activity by PKC (Bogachan Sahin, UT Southwestern Medical Center, personal communication). Thus, the complex

pathways regulating Cdk5 activity are only beginning to be understood. In this study, we examined the mechanism by which NMDA induces decreases in the phosphorylation of three Cdk5-dependent sites on inhibitor-1 and DARPP-32.

## **Experimental Procedures**

### *Drugs*

NMDA,  $\alpha$ -amino-3-hydroxy-5-methyl-4-isoxazolepropionic acid (AMPA), kainate, DL-2-amino-5-phosphonopentanoic acid (DL-AP5), and 6,7-dinitroquinoxaline-2,3-dione (DNQX) were from Tocris. Okadaic acid and calyculin A were from Alexis, cyclosporin A from LC Laboratories, and 1,2-bis(2-aminophenoxy)ethane-*N,N,N',N'*-tetraacetic acid-acetomethylester (BAPTA-AM) from Calbiochem. Cocaine hydrochloride, SKF81297, quinpirole, KCl, MgCl<sub>2</sub>, MK801, NiCl<sub>2</sub>, and ethylene glycol-bis(2-aminoethyl ether)-*N,N,N',N'*-tetraacetic acid (EGTA) were purchased from Sigma.

### *Preparation and incubation of acute striatal slices*

Slice pharmacology was conducted as described in Chapter 2. Where applicable, control slices were treated with dimethyl sulfoxide (DMSO), the solvent used to dissolve okadaic acid, calyculin A, cyclosporin A, and BAPTA-AM.

### *Immunoblots and data analysis*

Lysis and immunoblot analysis of striatal slices were performed as described in Chapter 2. The following additional antibodies were used: phospho-Thr75 DARPP-32 (1:2000) (Bibb et al., 1999), total DARPP-32 (1:8000) (Hemmings and Greengard, 1986), p35 (1:1000, Santa Cruz, C-19), and p39 (1:1000) (Fu et al., 2002). All but one antibody (total DARPP-32) were polyclonal. Horseradish peroxidase-conjugated anti-mouse secondary antibody (Chemicon) was used to detect the total DARPP-32 signal. Antibody incubations were in 5% milk + Tris-buffered saline-Tween (TBS-T), except that for p39, in which bovine serum albumin (BSA) replaced milk. Data analysis was conducted as in Chapter 2. Results are stated as mean  $\pm$  standard error of the mean. Changes are stated as percentage decrease or fold increase of the mean  $\pm$  error.

## **Results**

### *Dose-dependent reduction of three Cdk5-dependent phosphorylation sites by NMDA, independent of changes in levels of p35 and p25*

Inhibitor-1 is phosphorylated by Cdk5 at two sites, Ser6 and Ser67 (Bibb et al., 2001b). The inhibitor-1 homologue DARPP-32 serves as a substrate for Cdk5 at Thr75 (Bibb et al., 1999). We discovered robust regulation of these phosphorylation sites *in vivo*; treatment of acutely dissected striatal slices with NMDA reduced phosphorylation at all three sites (**Figure 3.1A**). Levels of

phospho-Ser6 and phospho-Ser67 inhibitor-1 and phospho-Thr75 DARPP-32 were  $12 \pm 1\%$ ,  $45 \pm 4\%$ , and  $32 \pm 5\%$  of control levels, respectively, after treatment with 50  $\mu\text{M}$  NMDA for 5 min. Neither doubling the dose of NMDA from 50 to 100  $\mu\text{M}$  nor increasing the exposure time from 5 min to 20 min resulted in a substantially larger effect. In spite of previous findings reporting ionotropic glutamate receptor-induced downregulation of Cdk5 activity via the degradation of p35 (Wei et al., 2005b), we observed no corresponding changes in levels of p35 in our preparation. Minimal amounts of p25 were detected in control slices, and application of NMDA did not induce further generation of p25 until a dose of 100  $\mu\text{M}$  was reached, even though 25  $\mu\text{M}$  NMDA was enough to induce reductions in all three Cdk5-dependent sites (**Figure 3.1B**). Interestingly, levels of phospho-Ser6 inhibitor-1 consistently decreased more than those of phospho-Ser67 inhibitor-1, with 25  $\mu\text{M}$  NMDA reducing levels to  $23 \pm 7\%$  and  $39 \pm 3\%$  of control, respectively. Thus, NMDA can markedly reduce phosphorylation of Ser6, Ser67, and Thr75 in a dose-dependent manner without affecting levels of p35 or p25.

#### *Evaluation of the role of Cdk5-activating cofactors*

In contrast to the apparent lack of effect of low doses of NMDA on p35 and p25, we detected a shift in the electrophoretic mobility of p39 in slices treated



with NMDA (**Figure 3.2A**). NMDA treatment caused the p39 doublet to collapse into a single band with the same mobility as the lower band of the doublet. Notably, in some gels, we were able to detect a very slight downward shift in the mobility of p35 upon NMDA treatment (**Figure 3.2B**), but this effect was inconsistent, being highly dependent on stochastic gel conditions, and we did not pursue it further. Small mobility shifts are frequently caused by changes in the state of phosphorylation of a protein. While phosphorylation of p39 has not previously been reported, phosphorylation of p35 has been linked to changes in Cdk5 activity (Sato et al., manuscript submitted). Since the threshold for the p39 mobility shift was 25  $\mu$ M, the same as the threshold for NMDA-induced reduction in levels of phosphorylation of inhibitor-1 and DARPP-32, we suspected that NMDA might be reducing levels of phosphorylation at Ser6, Ser67, and Thr75 by inhibiting Cdk5 activity via a dephosphorylation of p39. To determine if the effect of NMDA on the phosphorylation state of inhibitor-1 and DARPP-32 was cofactor-specific, we treated acutely dissected striatal slices from p35 (Chae et al., 1997) and p39 (Ko et al., 2001) knockout mice with NMDA. Neither constitutive loss of p35 nor p39 influenced the ability of NMDA to reduce levels of phosphorylation of inhibitor-1 or DARPP-32 (**Figure 3.2C**), suggesting either compensation by the remaining cofactor in the knockout mice or simply the lack of a causal relationship. Paradoxically, basal levels of phospho-Ser67 inhibitor-1

are higher in the hippocampus of 18-21 day old p35 knockout mice than in control mice (**Supplemental Figure 3.1**).

#### *Evaluation of the role of protein phosphatases*

Decreases in the level of phosphorylation of a protein can be due to either a reduction in kinase activity or an enhancement of phosphatase activity. Ser6 of inhibitor-1 is a rather promiscuous site for phosphatases, serving as a substrate for PP-1 and PP-2A basally, and additionally for PP-2B (calcineurin, or  $\text{Ca}^{2+}$ /calmodulin-dependent protein phosphatase) with increased intracellular  $\text{Ca}^{2+}$  (Chapter 2). PP-2A and PP-2B both contribute to the dephosphorylation of Ser67 of inhibitor-1 (Bibb et al., 2001b), while PP-2A, and to a lesser extent, PP-1 and protein phosphatase 2C (PP-2C) contribute to that of Thr75 of DARPP-32 (Nishi et al., 2000). To examine the possibility that NMDA reduces levels of phosphorylation of these three Cdk5 sites by activating a phosphatase, we treated striatal slices with various phosphatase inhibitors alone and in combination with NMDA.

Treatment with the PP-1/PP-2A inhibitors okadaic acid and calyculin A raised basal levels of phosphorylation at Ser6 (**Figure 3.3A**). NMDA eliminated the okadaic acid- and calyculin A-induced increases and further reduced levels of phospho-Ser6 inhibitor-1 to  $20 \pm 2\%$  and  $54 \pm 15\%$  of control levels, respectively. In contrast, these phosphatase inhibitors did not change levels of phospho-Ser67

inhibitor-1, either basally or in combination with treatment with NMDA. Importantly, NMDA was unable to attenuate okadaic acid- and calyculin A-induced increases in basal levels of phospho-Thr75 DARPP-32, indicating a role for PP-1/PP-2A in mediating the effects of NMDA on DARPP-32. Thus, the regulation of Cdk5 sites by NMDA receptors occurs by at least two distinct mechanisms. An enhancement of PP-1/PP-2A activity is responsible for NMDA-induced reductions in the phosphorylation of DARPP-32. An alternate pathway, independent of PP-1/PP-2A, allows NMDA to reduce levels of phospho-Ser6 and phospho-Ser67 inhibitor-1 in the face of treatment with okadaic acid and calyculin A.

In contrast to the PP-1/PP-2A inhibitors, the PP-2B inhibitor cyclosporin A did not alter basal levels of phosphorylation of Ser6 (**Figure 3.3B**). It did, however, partially reverse the ability of NMDA to reduce levels of phospho-Ser6 inhibitor-1 (from  $20 \pm 4\%$  to  $61 \pm 6\%$  of control), but not that of phospho-Ser67 inhibitor-1 or phospho-Thr75 DARPP-32. Thus, while phosphatases are somewhat or majorly responsible for the reduction in levels of phospho-Ser6 inhibitor-1 and phospho-Thr75 DARPP-32, there remains a mechanism by which NMDA reduces the phosphorylation of Ser67 independent of the major serine/threonine phosphatases, possibly via a reduction in Cdk5 activity.

Interestingly, cyclosporin A also attenuated the NMDA-induced p39 mobility shift (**Figure 3.3B**), indicating that the shift represents a dephosphorylation. However, since this treatment did not block NMDA-induced decreases in the phosphorylation of Ser67 or Thr75, we concluded that the p39 shift probably represents an epiphenomenon that is not causally related to the reductions in phosphorylation.

#### *Evaluation of potential modulation by dopamine*

We treated striatal slices with dopamine receptor agonists to determine whether dopamine plays a modulatory role in the effect of NMDA on Cdk5-dependent phosphorylation of inhibitor-1 and DARPP-32. The D<sub>1</sub> receptor agonist SKF81297 did not affect the ability of 100  $\mu$ M (**Figure 3.4A**) or 50  $\mu$ M (**Figure 3.4B**) NMDA to lower levels of phospho-inhibitor-1 and -DARPP-32. The D<sub>2</sub> receptor agonist quinpirole was similarly ineffective (**Figure 3.4B**).

Chronic treatment of the intact animal oftentimes produces results different from acute treatment of slice preparations. As such, wild-type mice were dosed daily for 10 days with saline or cocaine (20 mg/kg, i.p.). Acute striatal slices prepared from animals treated with cocaine one day after the last injection responded to NMDA in a dose-dependent manner indistinguishable from those treated with saline (**Figure 3.4C**). In striatal slabs provided by David R. Benavides (UT Southwestern Medical Center), basal levels of phospho-Ser6 and

phospho-Ser67 inhibitor-1 were not altered by 5- and 10-day regimens of cocaine (20 mg/kg, i.p.) (**Supplemental Figure 3.2**).

#### *Evaluation of the roles of calpain and PKC*

Toxicity-induced calpain-dependent cleavage of p35 to p25 has long been thought to regulate Cdk5 activity, and emerging evidence suggests that PKC also regulates Cdk5 activity. Acutely dissected striatal slices were treated with NMDA in the absence or presence of the PKC inhibitor Ro-32-0432 and the calpain inhibitor calpeptin to assess the contribution of these two proteins to the effect of NMDA. Neither inhibitor was effective at blocking the effect of NMDA on phospho-Ser6 and phospho-Ser67 inhibitor-1 (**Supplemental Figure 3.3**).

#### *Similar effects on the three Cdk5-dependent sites by other ionotropic glutamate receptor agonists and by direct depolarization*

The ability of other ionotropic glutamate receptor agonists to reduce phosphorylation of inhibitor-1 and DARPP-32 at the Cdk5 sites was next assessed. When applied at a concentration of 25  $\mu$ M for 5 min, both AMPA and kainate reduced levels of phospho-Ser6 inhibitor-1 ( $22 \pm 8\%$  and  $28 \pm 14\%$  of control, respectively), phospho-Ser67 inhibitor-1 ( $66 \pm 1\%$  and  $60 \pm 3\%$  of control), and phospho-Thr75 DARPP-32 ( $51 \pm 1\%$  and  $48 \pm 13\%$  of control)

(**Figure 3.5A**). Doubling the concentration of AMPA or kainate did not further reduce phosphorylation at any of the sites.

Since application of ionotropic glutamate receptor agonists can have numerous consequences, one of which is generalized depolarization, the effect of direct depolarization using KCl was tested. KCl dose-dependently reduced levels of phosphorylation at Ser6, Ser67, and Thr75, with a dose of 45 mM reducing levels to  $29 \pm 10\%$ ,  $34 \pm 6\%$ , and  $31 \pm 6\%$  of control, respectively (**Figure 3.5B**). The minimal effective dose for all three sites was 20 mM. Increasing the dose beyond 45 mM to 100 mM further reduced levels of phospho-Thr75 DARPP-32 to  $14 \pm 3\%$  of control, but not phospho-Ser6 or phospho-Ser67 inhibitor-1. These findings indicate that simple depolarization is sufficient for the reduction in phosphorylation of these Cdk5 sites.

Seizures in the intact animal represent a massive discharge of neurotransmitter and the depolarization of a large number of neurons, which might be expected to lower levels of phosphorylation of inhibitor-1 at the Cdk5 sites. However, levels of phospho-Ser6 inhibitor-1 were unchanged in the hippocampus of mice sacrificed 20 min after the initiation of seizures induced by kainate or pilocarpine (membrane provided by Ammar H. Hawasli, UT Southwestern Medical Center) (**Supplemental Figure 3.4**).

*Evaluation of the role of NMDA receptors*

Relief of the  $Mg^{2+}$  block by depolarization is a prerequisite for NMDA receptor activity. Furthermore, NR2B subunits of the NMDA receptor physically associate with Cdk5 (Hawasli et al., manuscript submitted). To determine if the reductions in phosphorylation caused by AMPA and KCl resulted from secondary activation of the NMDA receptor, we employed the activity-dependent and activity-independent NMDA receptor antagonists MK801 and AP5. Neither MK801 (Tomohisa Hosokawa, Tokyo Metropolitan University, **Figure 3.6A**) nor AP5 (**Figure 3.6B**) blocked the AMPA-induced decrease in phosphorylation of Ser6, Ser67, and Thr75. MK801 (**Supplemental Figure 3.5**) and AP5 (**Figure 3.6B**) were similarly ineffective at blocking the effect of KCl. AP5 was, however, able to block the effect of NMDA, returning phospho-Ser6 and phospho-Ser67 inhibitor-1 and phospho-Thr75 DARPP-32 to  $79 \pm 5\%$ ,  $86 \pm 11\%$ , and  $106 \pm 3\%$  of control levels, respectively (**Figure 3.6C**). Thus, while the effects of NMDA were specifically mediated by NMDA receptors, the effects of AMPA and KCl did not result from secondary activation of NMDA receptors. Furthermore, the effect of KCl did not result from activation of AMPA receptors, as it was not affected by the inclusion of the AMPA receptor antagonist DNQX (**Supplemental Figure 3.5**).

### *Evaluation of the role of voltage-gated $\text{Ca}^{2+}$ channels*

Depolarization results in the activation of voltage-gated  $\text{Ca}^{2+}$  channels, which may set off a whole host of intracellular signaling cascades. As an initial screen for the involvement of these channels, the ability of NMDA to reduce phosphorylation of inhibitor-1 and DARPP-32 in the presence of 1 mM  $\text{Ni}^{2+}$  was assessed (**Figure 3.7A**). At this concentration,  $\text{Ni}^{2+}$  acts as a non-specific  $\text{Ca}^{2+}$  channel blocker. Application of 1 mM  $\text{Ni}^{2+}$  ablated the effect of NMDA on phospho-Ser6 and phospho-Ser67 inhibitor-1 and phospho-Thr75 DARPP-32, returning levels to  $94 \pm 12\%$ ,  $88 \pm 12\%$ , and  $115 \pm 7\%$  of control, respectively. However, neither nimodipine, a T-type voltage-gated  $\text{Ca}^{2+}$  channel antagonist, nor 100  $\mu\text{M}$   $\text{Ni}^{2+}$ , a specific T-type voltage-gated  $\text{Ca}^{2+}$  channel antagonist at this concentration, had any effect on the ability of NMDA to reduce phosphorylation of inhibitor-1 or DARPP-32 (**Figure 3.7B**). These results suggest either the involvement of another type of  $\text{Ca}^{2+}$  channel or a non-selective action of 1 mM  $\text{Ni}^{2+}$ .

### *Evaluation of the role of cations*

Depolarization generally results from the influx of cations into the cytoplasm. The possible contribution of  $\text{Ca}^{2+}$  was evaluated first. Neither chelation of intracellular  $\text{Ca}^{2+}$  with 20  $\mu\text{M}$  BAPTA-AM (**Figure 3.8A**) nor with 1 mM BAPTA-AM (**Figure 3.8B**) blocked the effect of NMDA. While BAPTA-



AM might be expected to block all  $\text{Ca}^{2+}$ -dependent signaling events, complete chelation of intracellular  $\text{Ca}^{2+}$  with extracellularly-applied BAPTA-AM may not be possible in slice preparations.

Thus, we assessed the contribution of extracellular  $\text{Ca}^{2+}$  by removing  $\text{Ca}^{2+}$  from the buffer during the period of NMDA treatment and replacing it with  $\text{Mg}^{2+}$  in order to preserve divalency and avoid surface charge issues. The effect of NMDA on the phosphorylation of inhibitor-1 was marginally affected under these conditions, possibly due to enhanced  $\text{Mg}^{2+}$ -dependent block of the NMDA receptor (**Figure 3.9A**). In contrast, the effect of NMDA on the phosphorylation of DARPP-32 was greatly affected, changing from  $22.5 \pm 0.8\%$  of control levels in normal buffer to  $70.5 \pm 3.1\%$  of control levels in minimal  $\text{Ca}^{2+}$  buffer. Incomplete reversal of the effect of NMDA on DARPP-32 may have resulted from residual  $\text{Ca}^{2+}$  in the extracellular matrix. In a more stringent  $\text{Ca}^{2+}$ -free treatment paradigm, inclusion of the  $\text{Ca}^{2+}$  chelator EGTA in minimal  $\text{Ca}^{2+}$  buffer produced similar results for inhibitor-1 (**Figure 3.9B**). Surprisingly, however, this treatment did not reverse the effect of NMDA on the phosphorylation of DARPP-32, unlike the minimal  $\text{Ca}^{2+}$  treatment. One explanation is enhanced release of  $\text{Ca}^{2+}$  from intracellular stores caused by increased influx of  $\text{Na}^+$  through voltage-gated  $\text{Ca}^{2+}$  channels normally guarded by bound  $\text{Ca}^{2+}$  (Bernath, 1992).

To assess the contribution of  $\text{Na}^+$ , Tomohisa Hosokawa (Tokyo Metropolitan University) replaced  $\text{Na}^+$  in the extracellular buffer with the

impermeant ion choline during the period of NMDA treatment. Even in the absence of extracellular  $\text{Na}^+$ , NMDA was able to reduce phosphorylation of all three Cdk5 sites (**Figure 3.9B**). Thus, specific removal of either  $\text{Ca}^{2+}$  or  $\text{Na}^+$  was ineffective in reversing the effect of NMDA on inhibitor-1.

However, concurrent removal of both ions completely ablated the effect of NMDA (**Figure 3.9C**). Slices were prepared and recovered in choline media containing normal amounts of  $\text{Ca}^{2+}$  then pre-treated for 20 min with media containing EGTA before the addition of NMDA, AMPA, or KCl. In contrast to previous experiments in which EGTA was applied only during the period of NMDA treatment, pre-treatment with  $\text{Ca}^{2+}$ - and  $\text{Na}^+$ -free media containing EGTA caused a large increase in basal levels of phospho-Ser6 inhibitor-1 ( $2.4 \pm 0.6$ -fold), which was not significantly reversed by NMDA or AMPA. KCl caused a small reversal. Levels of phospho-Ser67 inhibitor-1 were unaltered by pre-treatment with EGTA alone or in combination with any of the depolarizing agents, while levels of phospho-Thr75 DARPP-32 were lowered to  $48 \pm 5\%$  of control by EGTA, with no further reduction upon addition of any of the depolarizing agents. Considered as a whole, these data suggest that simple depolarization, in a non-cation-specific manner, regulates Cdk5-dependent phosphorylation of inhibitor-1. In contrast, the regulation of phospho-Thr75 DARPP-32 by depolarization is  $\text{Ca}^{2+}$ -specific.

## Discussion

The regulation of any phosphorylation site depends on the balance of activity between the kinase(s) and the phosphatase(s) acting on the site. In this study, we explored the mechanism by which NMDA causes a decrease in phosphorylation of two inhibitors of PP-1 at three Cdk5-dependent phosphorylation sites, Ser6 and Ser67 of inhibitor-1 and Thr75 of DARPP-32. NMDA-induced reductions in these phosphorylation sites has been reported previously (Bibb et al., 2001b; Nishi et al., 2002; Wei et al., 2005b and Chapter 2).

Studies by Wei et al. support the notion that NMDA and kainate globally induce reduction of phosphorylation at Cdk5 sites in primary cortical neurons and in hippocampal slices by causing the degradation of p35 and the downregulation of Cdk5 activity (Wei et al., 2005b). In contrast, studies by Nishi et al. found that levels of Cdk5 activity in striatal slices were unchanged by treatment with NMDA, AMPA, or KCl (Nishi et al., 2002). These traditional Cdk5 activity assays were conducted as immunoprecipitation (IP)-kinase assays in which Cdk5 immunoprecipitated from a detergent-solubilized lysate was allowed to phosphorylate histone H1 in the presence of [ $\gamma$ -<sup>32</sup>P]-ATP. Given the recent finding that detergent-induced membrane dissociation leads to the activation of latent Cdk5/p35 complexes (Zhu et al., 2005), the results of these types of Cdk5 assays should be interpreted carefully.

Regardless, the use of phosphatase inhibitors allowed Nishi *et al.* to attribute reductions in levels of phospho-Thr75 DARPP-32 caused by NMDA, AMPA, and KCl to a  $\text{Ca}^{2+}$ -dependent enhancement of PP-2A activity. Supporting this conclusion was the finding that NMDA decreased levels of phospho-Thr75 DARPP-32 to the same extent regardless of the absence or presence of the Cdk5 inhibitor butyrolactone. The apparently contradictory results of Wei *et al.* and Nishi *et al.* might be due to differences in the preparation used (cultured cortical and acute hippocampal vs. acute striatal) and/or the duration of NMDA treatment. The time course of the effect of NMDA on Cdk5 activity in primary cortical neurons conducted by Wei *et al.* reveals transient stimulation of Cdk5 activity at 1 min, a return to control levels at 5 min, and a down-regulation thereafter, with levels reaching a nadir at the longest time point, 60 min. Since Nishi *et al.* examined only the 5 min time point, they would not have observed a subsequent decrease in Cdk5 activity. Thus, our studies and those by Nishi *et al.*, both conducted at 5 min of treatment, relate to a shorter NMDA exposure than the studies by Wei *et al.*

We found that 5 min of treatment of striatal slices with NMDA, AMPA, kainate, or KCl all reduced phosphorylation of the Cdk5 sites on inhibitor-1 and DARPP-32. While levels of p35 and p25 were unaffected by 5 min of 50  $\mu\text{M}$  NMDA, p39 exhibited an electrophoretic mobility shift consistent with dephosphorylation. The threshold for this p39 shift was the same as the threshold

for decreased phosphorylation of inhibitor-1 and DARPP-32, but we concluded that the events were probably not causally related, since cyclosporin A was able to dissociate them.

NMDA receptors were involved in the regulation of phosphorylation by NMDA, but not by AMPA or KCl. Even though 1 mM  $\text{Ni}^{2+}$  blocked the effect of NMDA on the three Cdk5 sites, L- and T-type voltage-gated  $\text{Ca}^{2+}$  channels were found to be uninvolved. While 1 mM  $\text{Ni}^{2+}$  is generally regarded as a non-specific  $\text{Ca}^{2+}$  channel blocker, it can have a number of other actions. At a concentration of 1 mM,  $\text{Ni}^{2+}$  alters the properties of numerous channels, including but not limited to NMDA receptors (Gavazzo et al., 2006), epithelial  $\text{Na}^+$  channels (Sheng et al., 2002), cardiac (Perchenet and Clement-Chomienne, 2001) and smooth muscle (Stockand et al., 1993)  $\text{K}^+$  channels, and acid-sensing ion channels (Staruschenko et al., 2006). Furthermore, increasing the concentration of extracellular divalent cations by addition of  $\text{Ni}^{2+}$  reduces the negative potential at the surface of the cell, thereby effectively increasing the transmembrane potential (Piccolino and Pignatelli, 1996). Stronger depolarizations would then be required to activate voltage-dependent channels. In addition, the direct binding of  $\text{Ni}^{2+}$  to acidic ligands such as glutamate and kainate has been suggested to compete with free ligands for binding to AMPA receptors (Dorofeeva et al., 2005). Thus, blockade of the NMDA effect by 1 mM  $\text{Ni}^{2+}$  could have resulted from a number of factors.

Assessment of the dependence of the NMDA effect on phosphatases and extracellular  $\text{Na}^+$  and  $\text{Ca}^{2+}$  revealed differential regulation of the three Cdk5 sites. Entirely consistent with Nishi *et al.*, we observed  $\text{Ca}^{2+}$ - and PP-1/PP-2A-dependent regulation of phospho-Thr75 DARPP-32 by NMDA. In contrast, regulation of the Cdk5 sites on inhibitor-1 was not cation-specific. Individual removal of extracellular  $\text{Na}^+$  or  $\text{Ca}^{2+}$  had minimal effects on the ability of NMDA to decrease levels of phospho-Ser6 and phospho-Ser67 inhibitor-1; however, simultaneous removal of both cations completely blocked the effect of NMDA. Moreover, NMDA-induced decreases in the phosphorylation of Ser6 were partially PP-2B-dependent, but those for Ser67 were not PP-1-, PP-2A, or PP-2B-dependent. Thus, NMDA appears to regulate the phosphorylation of Cdk5-dependent sites via pathways involving both enhanced phosphatase activity and reduced kinase activity. In conclusion, by altering levels of phosphorylation at the Cdk5-dependent sites of inhibitor-1 and DARPP-32, depolarization can positively regulate striatal PP-1 and PKA activity. The multiple distinct mechanisms by which depolarization regulates the phosphorylation of inhibitor-1 and DARPP-32 highlight the complexity of the cascades that can originate from a single signal.

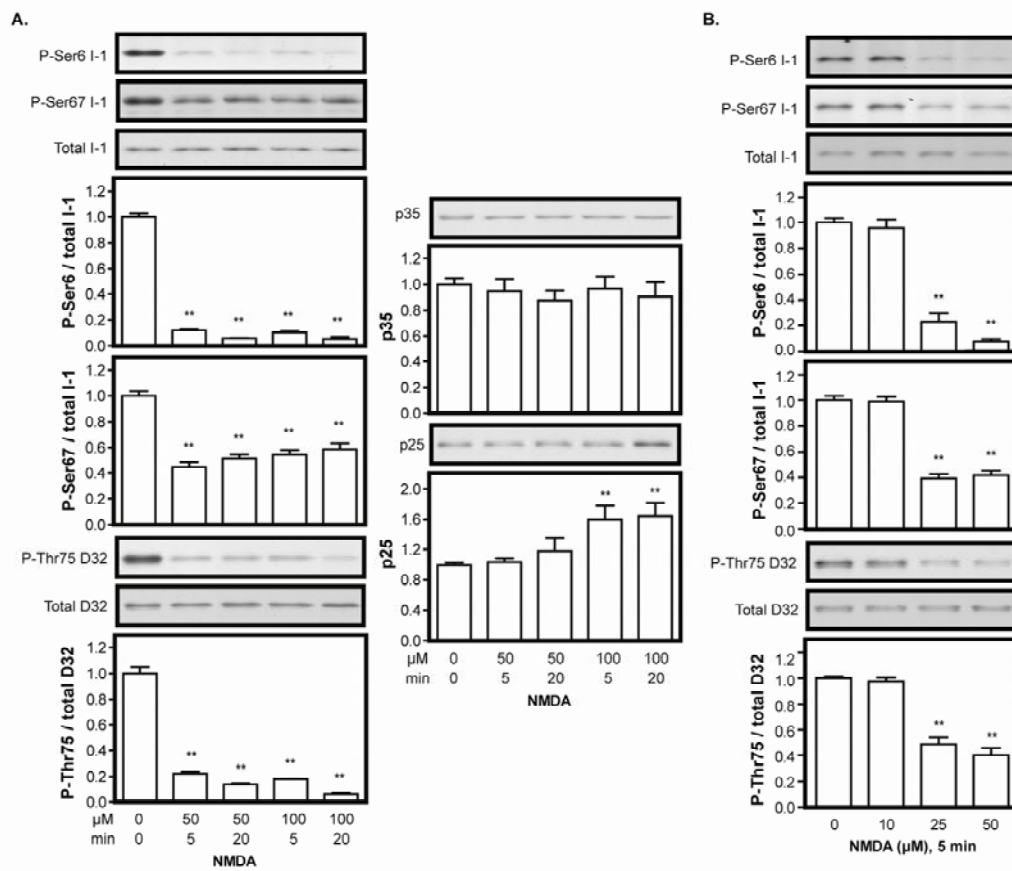


**Figure 3.1. Reduction in phosphorylation of three Cdk5 sites by NMDA.** Quantitative immunoblot analysis of acute striatal slices incubated with NMDA for **A**, the doses and times indicated,  $n = 3-6$  or **B**, the doses indicated for 5 min,  $n = 4-12$ . \*\*,  $p < 0.01$  vs. control, one-way analysis of variance (ANOVA) with Dunnett's multiple comparison test.

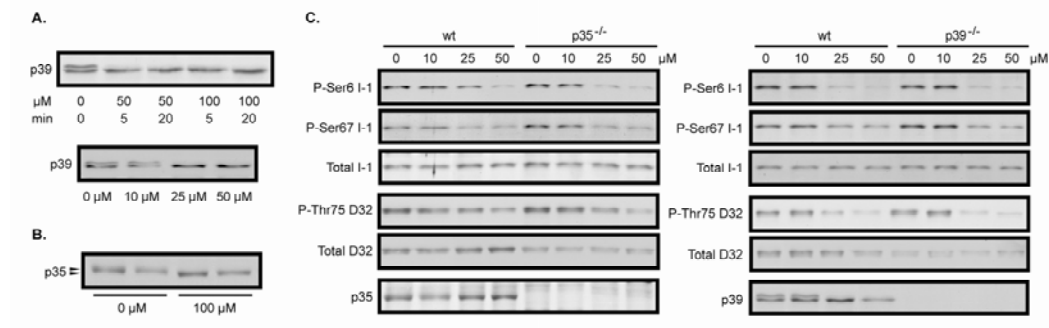


**Figure 3.2. Evaluation of the role of Cdk5-activating cofactors.**

**A-B,** Immunoblots of acute striatal slices treated with NMDA for the doses and times indicated (**A**, top,  $n = 2-3$ ) or for the doses indicated for 5 min (**A**, bottom,  $n = 4$ ; **B**). **C,** Immunoblots of acute striatal slices from wild-type and p35<sup>-/-</sup> (left) or p39<sup>-/-</sup> (right) mice treated with NMDA at the indicated doses for 5 min,  $n = 2$ .



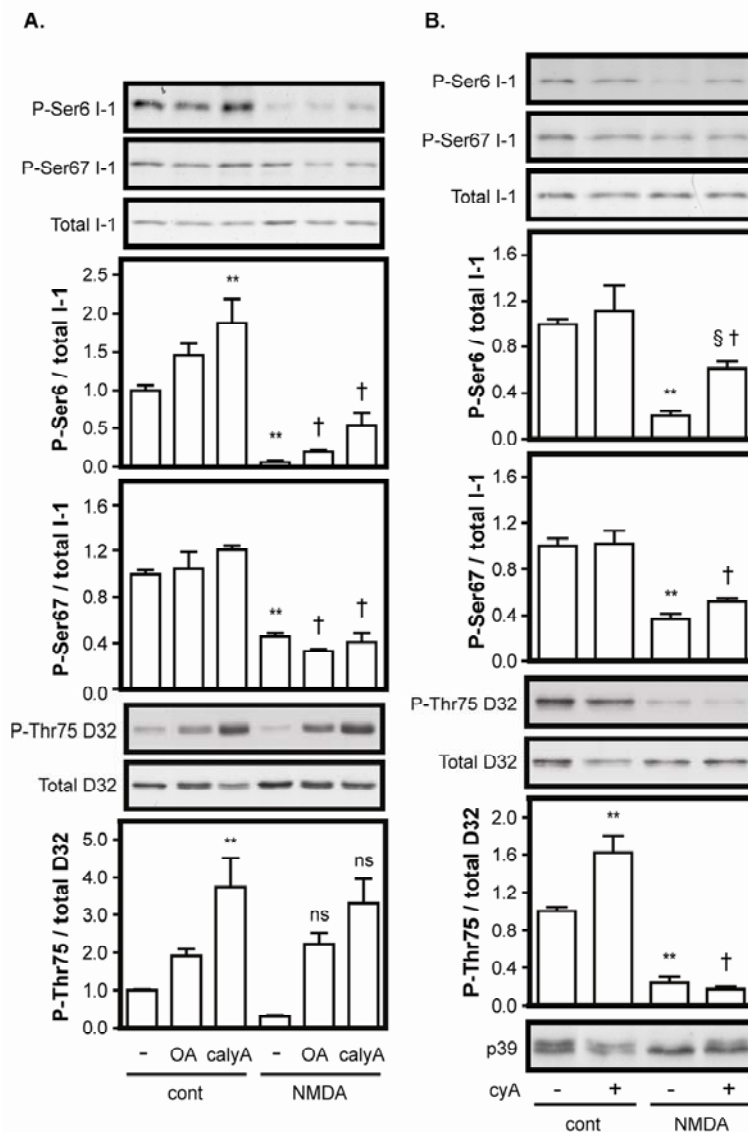


**Figure 3.3. Evaluation of the role of protein phosphatases.** Quantitative immunoblot analysis of acute striatal slices incubated in the absence or presence of 50  $\mu$ M NMDA for 5 min with or without 60 min pre-incubation with **A**, okadaic acid (OA, 1  $\mu$ M) or calyculin A (calyA, 1  $\mu$ M),  $n = 3-5$  or **B**, cyclosporin A (cyA, 10  $\mu$ M),  $n = 2-7$ . \*\*,  $p < 0.01$  vs. control; §,  $p < 0.001$  vs. NMDA alone; †,  $p < 0.01$  and ns, not significant vs. corresponding treatment without NMDA; one-way ANOVA with Bonferroni's multiple comparison test.

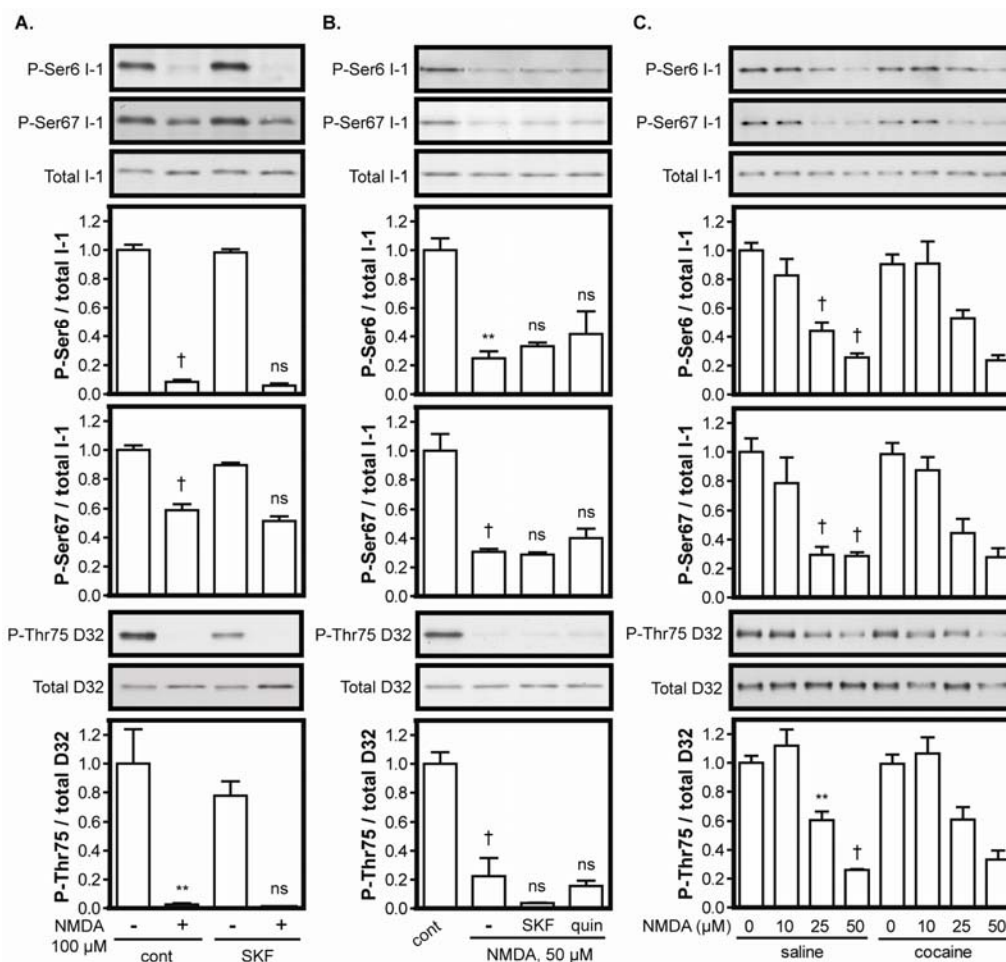


**Figure 3.4. Evaluation of potential modulation by dopamine.** Quantitative immunoblot analysis of acute striatal slices incubated in the absence or presence of NMDA (50 or 100  $\mu$ M) for 5 min with or without co-incubation with **A**, SKF81297 (1  $\mu$ M),  $n = 3$  or **B**, SKF81297 (1  $\mu$ M) or quinpirole (1  $\mu$ M),  $n = 3$ . **C**, Acute striatal slices prepared from mice dosed daily with saline or cocaine (20 mg/kg, i.p.) for 10 days were incubated with the indicated doses of NMDA for 5 min one day after the last injection and subjected to quantitative immunoblot analysis,  $n = 4-7$  slices from 3 mice/group. \*\*,  $p < 0.01$  and †,  $p < 0.001$  vs. control; ns, not significant vs. NMDA alone; one-way ANOVA with Bonferroni's multiple comparison test.

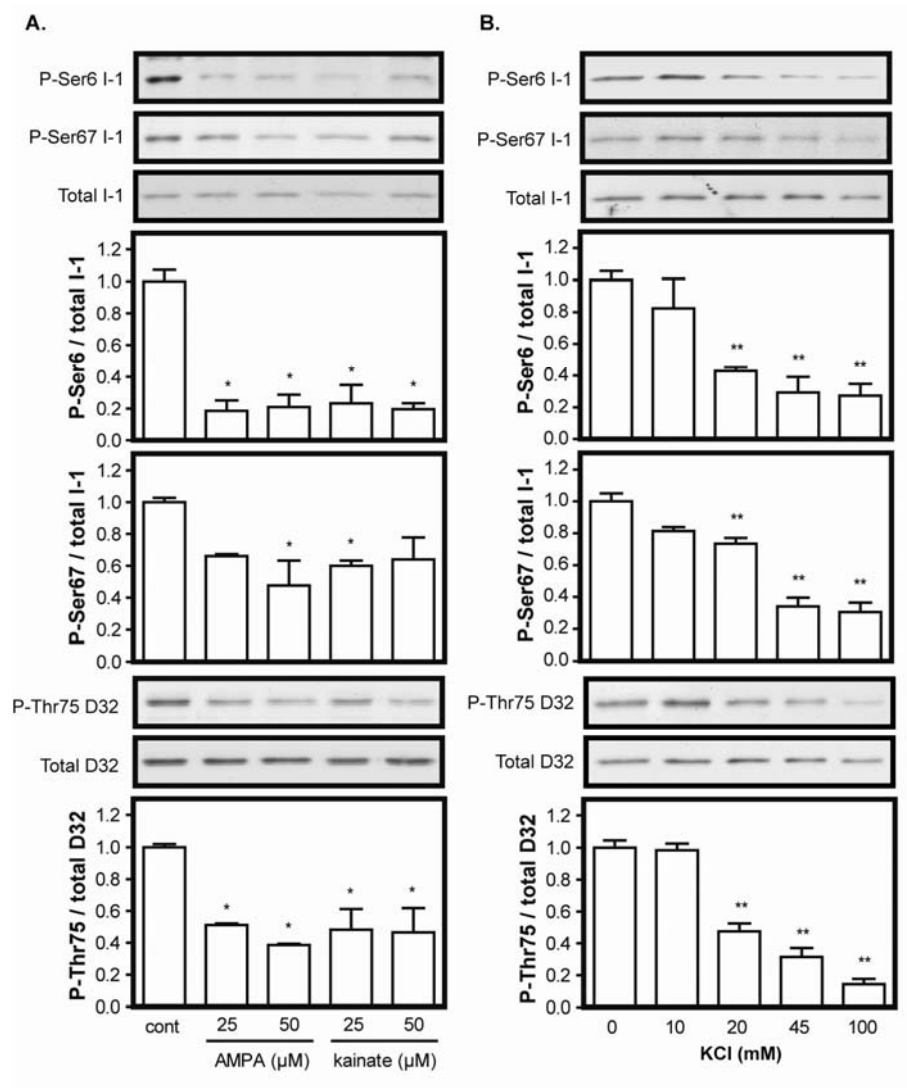


**Figure 3.5. Similar reductions in phosphorylation of three Cdk5 sites by AMPA, kainate, and KCl.** Quantitative immunoblot analysis of acute striatal slices incubated with **A**, AMPA or kainate at the doses indicated for 5 min,  $n = 2-3$  or **B**, KCl at the doses indicated for 5 min,  $n = 3-5$ . \*,  $p < 0.05$  and \*\*,  $p < 0.01$  vs. control, one-way ANOVA with Dunnett's multiple comparison test.

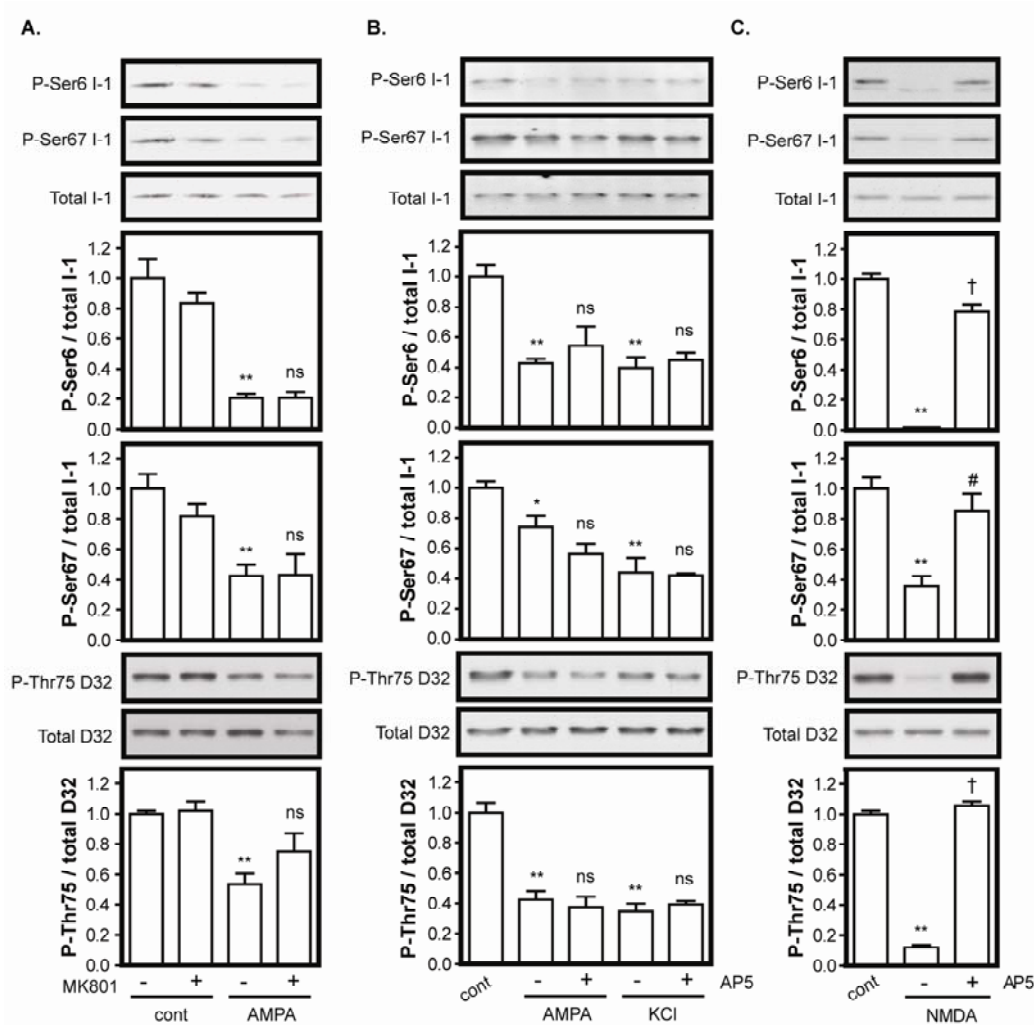


**Figure 3.6. Evaluation of the role of NMDA receptors.** Quantitative immunoblot analysis of acute striatal slices incubated in the absence or presence of NMDA (50  $\mu$ M), AMPA (50  $\mu$ M), or KCl (45 mM) for 5 min with or without 7 min pre-incubation with **A**, MK801,  $n = 5-6$ , **B**, AP5,  $n = 5-6$ , or **C**, AP5,  $n = 3$ . \*,  $p < 0.05$  and \*\*,  $p < 0.01$  vs. control; #,  $p < 0.05$ , †,  $p < 0.001$  and ns, not significant vs. corresponding treatment without NMDA receptor antagonist; one-way ANOVA with Bonferroni's multiple comparison test.

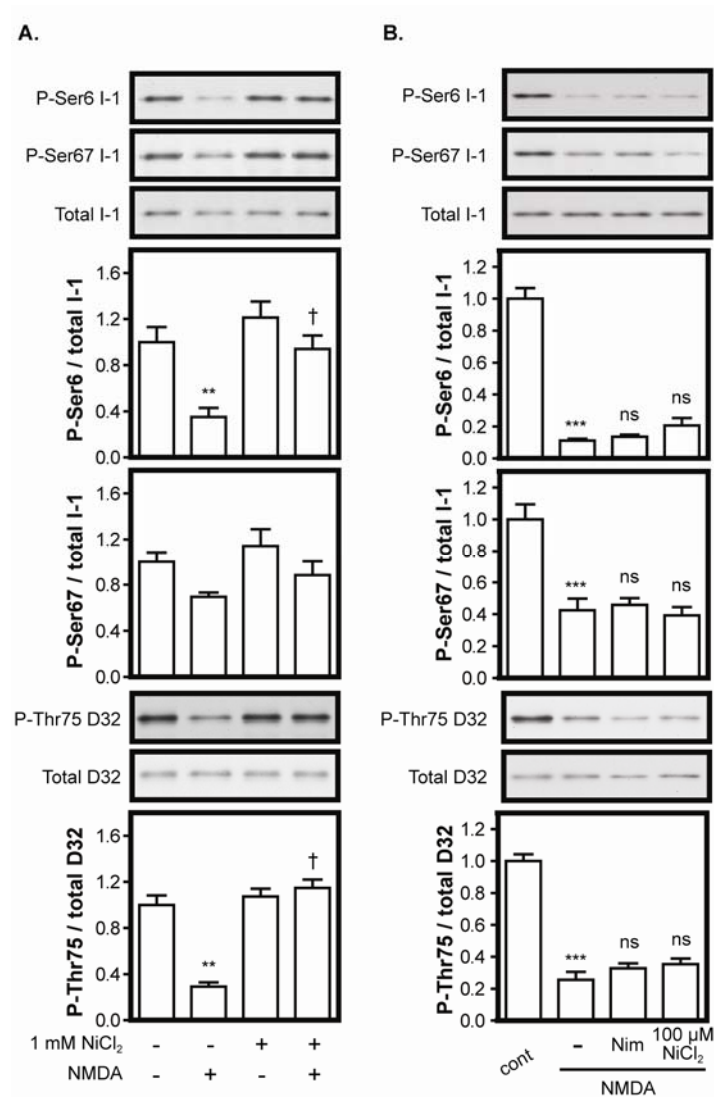


**Figure 3.7. Evaluation of the role of voltage-gated Ca<sup>2+</sup> channels.** Quantitative immunoblot analysis of acute striatal slices incubated in the absence or presence of 50  $\mu$ M NMDA for 5 min with or without **A**, 5 min pre-incubation with 1 mM NiCl<sub>2</sub>,  $n = 4-6$  or **B**, 20 min pre-incubation with 15  $\mu$ M nimodipine (Nim) or 5 min pre-incubation with 100  $\mu$ M NiCl<sub>2</sub>,  $n = 5-6$ . \*\*,  $p < 0.01$  and \*\*\*,  $p < 0.001$  vs. control; †,  $p < 0.01$  and ns, not significant vs. NMDA alone; one-way ANOVA with Bonferroni's multiple comparison test.

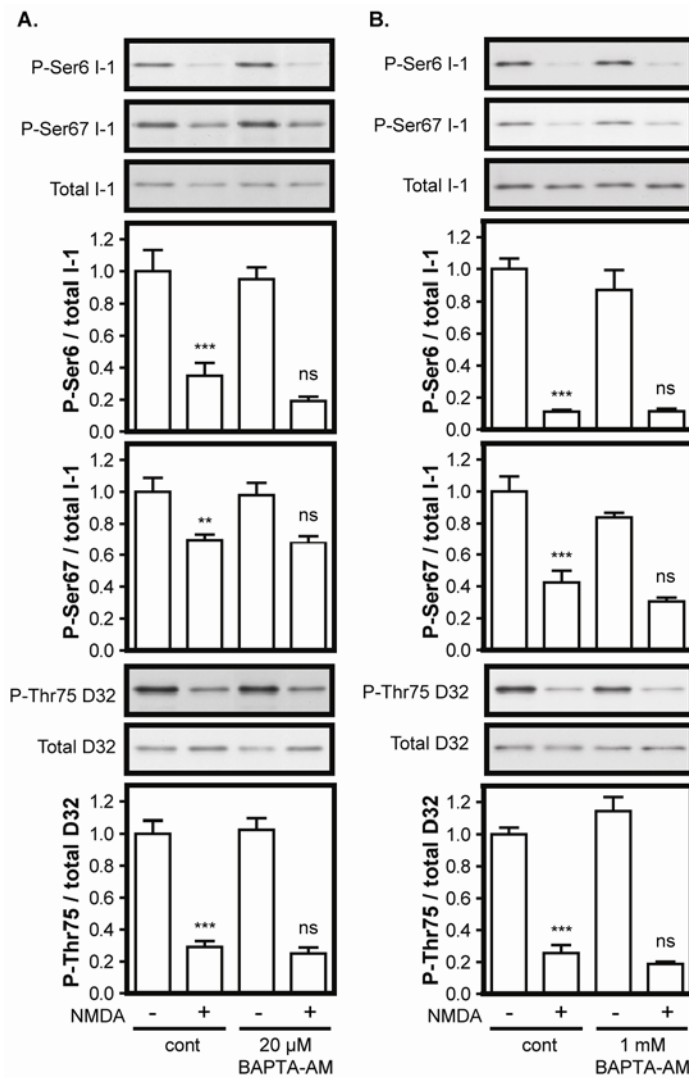


**Figure 3.8. Evaluation of the role of intracellular  $\text{Ca}^{2+}$ .** Quantitative immunoblot analysis of acute striatal slices incubated in the absence or presence of 50  $\mu$ M NMDA for 5 min with or without 20 min pre-incubation with **A**, 20  $\mu$ M BAPTA-AM,  $n = 4-6$  or **B**, 1 mM BAPTA-AM,  $n = 4-6$ . \*\*,  $p < 0.01$  and \*\*\*,  $p < 0.001$  vs. control; ns, not significant vs. NMDA alone; one-way ANOVA with Bonferroni's multiple comparison test.

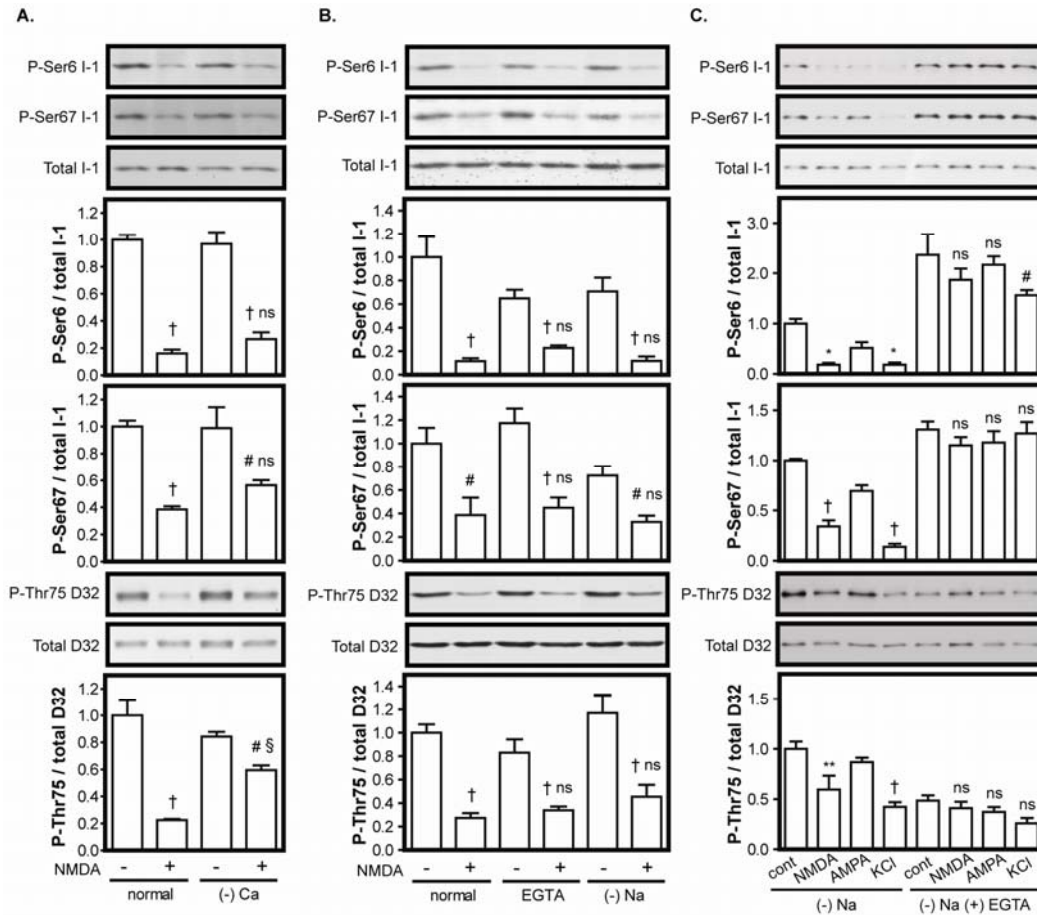
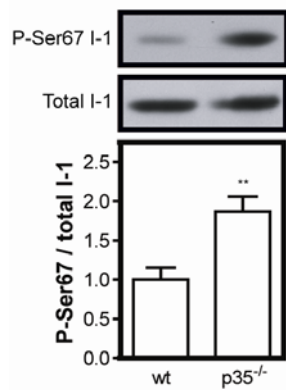
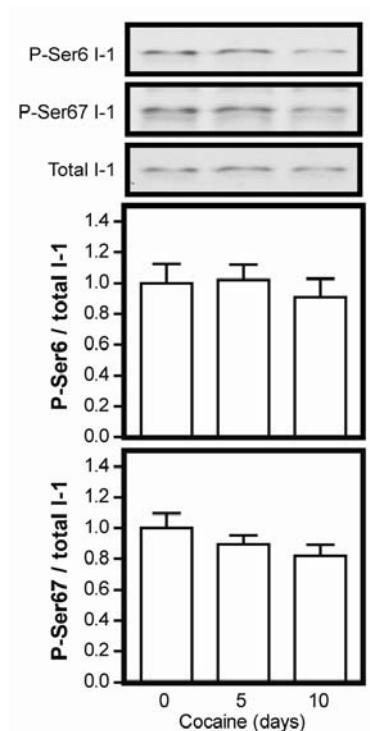


**Figure 3.9. Evaluation of the role of extracellular cations.** Quantitative immunoblot analysis of acute striatal slices incubated in the absence or presence of NMDA (50  $\mu$ M) for 5 min in normal buffer or in buffer in which **A**,  $\text{Ca}^{2+}$  is replaced by  $\text{Mg}^{2+}$  [(-) Ca],  $n = 4$  or **B**, extracellular  $\text{Ca}^{2+}$  is chelated with 1 mM EGTA (and  $\text{Ca}^{2+}$  is replaced by  $\text{Mg}^{2+}$ ) or  $\text{Na}^{+}$  is replaced by choline [(-) Na],  $n = 3-6$ . #,  $p < 0.05$  and †,  $p < 0.01$  vs. corresponding buffer without NMDA; §,  $p < 0.01$  and ns, not significant vs. normal buffer with NMDA; one-way ANOVA with Bonferroni's multiple comparison test. **C**, Quantitative immunoblot analysis of acute striatal slices recovered in choline buffer and treated with NMDA (50  $\mu$ M), AMPA (50  $\mu$ M), or KCl (45 mM) for 5 min in choline buffer [(-)Na] or in choline buffer lacking  $\text{Ca}^{2+}$  and containing 10 mM EGTA [(-)Na(+)EGTA]. \*,  $p < 0.05$ , \*\*,  $p < 0.01$ , †,  $p < 0.001$ , and ns, not significant vs. corresponding buffer without depolarizing agent; one-way ANOVA with Bonferroni's multiple comparison test.

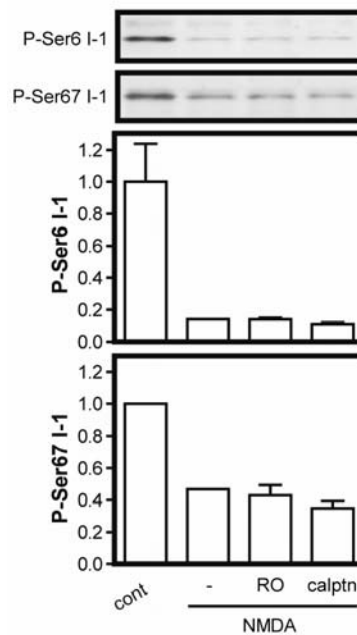


**Supplemental Figure 3.1. Levels of phospho-Ser67 inhibitor-1 in the hippocampus of juvenile wild-type and p35 knockout mice.** Quantitative immunoblot analysis of grossly dissected hippocampus from 18-21 day old wild-type (wt) and p35<sup>-/-</sup> mice, n = 5-6. \*\*,  $p < 0.01$ , student's unpaired  $t$  test.

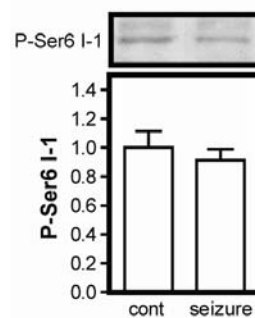




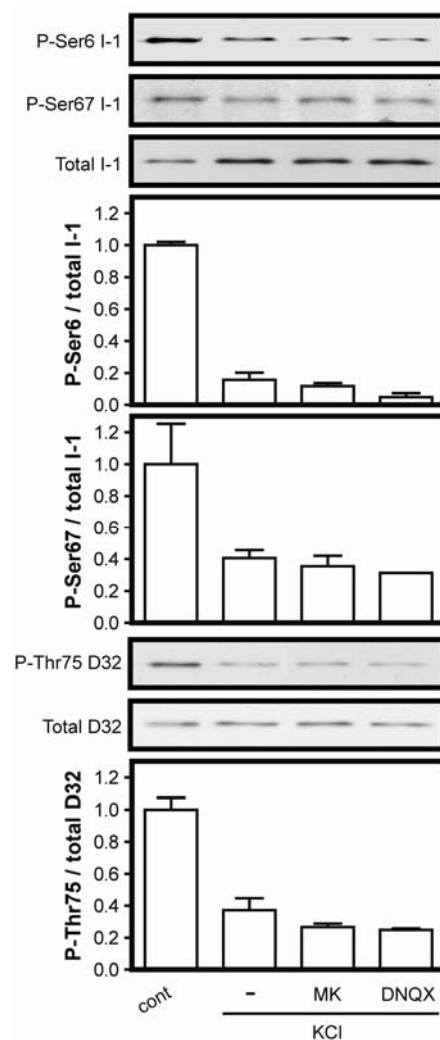
**Supplemental Figure 3.2. Levels of phospho-Ser6 and phospho-Ser67 inhibitor-1 in the striatum after chronic cocaine.** Quantitative immunoblot analysis of microdissected striatal matrix-slabs from mice treated with daily injections of saline or cocaine (20 mg/kg, i.p.) for a total of 10 days,  $n = 7-8$ .



**Supplemental Figure 3.3. Evaluation of the roles of PKC and calpain.** Quantitative immunoblot analysis of acute striatal slices incubated in the absence or presence of 50  $\mu$ M NMDA for 5 min with or without 60 min pre-incubation with 5  $\mu$ M Ro-32-0432 (RO) or 20  $\mu$ M calpeptin (calptn),  $n = 1-2$ .



**Supplemental Figure 3.4. Levels of phospho-Ser6 inhibitor-1 in the hippocampus after seizures.** Quantitative immunoblot analysis of grossly dissected hippocampus from control mice or mice with kainate- or pilocarpine-induced seizures, n = 6-7.



**Supplemental Figure 3.5. Evaluation of the roles of NMDA and AMPA receptors in the effect of KCl.** Quantitative immunoblot analysis of acute striatal slices incubated in the absence or presence of KCl (45 mM) for 5 min with or without 7 min pre-incubation with MK801 or DNQX, n = 2-3.

## **CHAPTER FOUR**

### **LOSS OF PROTEIN PHOSPHATASE INHIBITOR-1 ALTERS LEARNING AND RUNNING-INDUCED NEUROGENESIS**

#### **Summary**

Protein phosphatase inhibitor-1, the first identified endogenous inhibitor of protein phosphatase 1 (PP-1), has been widely implicated in many biochemical models of synaptic plasticity. Despite the critical position that inhibitor-1 occupies in these models, the behavioral and biochemical effects of loss of inhibitor-1 have not been extensively studied. Inhibitor-1 is particularly abundant within granule neurons of the hippocampal dentate gyrus. Considering the possible relationship between neurogenesis and learning in this region, we examined the role of inhibitor-1 in neurogenesis induced by voluntary wheel running. Levels of inhibitor-1 increased dramatically after just six days of running. Furthermore, loss of inhibitor-1 significantly increased running-induced neurogenesis in the subgranular zone, but had no effect on the running behavior of the mice. Together these data indicate that inhibitor-1 may function in a homeostatic anti-neurogenic mechanism. Further behavioral characterization has revealed that although inhibitor-1 knockout mice display a deficit in habituation to a novel environment, they are normal with regard to fear conditioning and novelty learning. These findings suggest that the role of inhibitor-1 in the

mnemonic functions of the hippocampus has been overemphasized and that inhibitor-1 may be more important in the modulation of dopamine-dependent behaviors.

## **Introduction**

Protein phosphatase inhibitor-1, or simply inhibitor-1, was identified from rabbit skeletal muscle in 1976 as a conditional inhibitor of PP-1. Only when phosphorylated by cAMP-dependent protein kinase (PKA) at Thr35 does inhibitor-1 become a potent and selective inhibitor of PP-1 (Endo et al., 1996; Foulkes et al., 1983; Huang and Glinzmann, 1976). Thus, inhibitor-1 serves as one mechanism whereby PKA can amplify cAMP signals by preventing the dephosphorylation of sites shared with PP-1. Dephosphorylation of Thr35 by calcineurin (PP-2B, or  $\text{Ca}^{2+}$ /calmodulin-dependent protein phosphatase) (Ingebritsen and Cohen, 1983) inactivates inhibitor-1, preventing it from further inhibiting PP-1. As a substrate whose function relies on the balance of activity between PKA and calcineurin, both of which are known to be important to the long-term modification of synaptic strength, inhibitor-1 became incorporated into well-accepted biochemical models of Schaffer collateral plasticity as a critical switch between potentiation and depression (Lisman, 1989; Winder and Sweatt, 2001). Long-term potentiation (LTP) and long-term depression (LTD), two processes that might be expected to result from opposite regulation of the same

proteins, are induced by different stimulation protocols, but both depend on the activation of N-methyl-D-aspartate (NMDA) receptors and the elevation of intracellular  $\text{Ca}^{2+}$  levels. Calcineurin and PKA, by way of calcium/calmodulin-dependent adenylyl cyclase, are both responsive to increases in intracellular  $\text{Ca}^{2+}$  levels but to different degrees. Convergent signaling by these two proteins onto inhibitor-1, a regulator of PP-1, provides a mechanism by which the magnitude of the rise in intracellular  $\text{Ca}^{2+}$ , dictated by the frequency and duration of stimulation, can translate into the converse regulation of the same set of proteins by PP-1. Included in the list of PP-1 substrates important to plasticity are  $\text{Ca}^{2+}$ /calmodulin-dependent protein kinase II (CaMKII) (Strack et al., 1997), NMDA (Blank et al., 1997; Snyder et al., 1998) and  $\alpha$ -amino-3-hydroxy-5-methyl-4-isoxazolepropionic acid (AMPA) (Yan et al., 1999) receptors, and cAMP response element-binding protein (CREB) (Bito et al., 1996; Hagiwara et al., 1992).

Despite the prominent position inhibitor-1 has occupied as a regulator of PP-1 in biochemical models of Schaffer collateral plasticity, inhibitor-1 knockout mice display normal LTP and LTD in this pathway (Allen et al., 2000). Instead, they show impaired LTP at lateral, but not medial, perforant path-dentate granule cell synapses. Perhaps this is not surprising given the distinct expression profile of inhibitor-1 in the hippocampus. Virtually all the inhibitor-1 expressed in hippocampus is localized to the dentate gyrus, although some studies report

moderate amounts in the CA1 region (Allen et al., 2000; Barbas et al., 1993; Gustafson et al., 1991; Lowenstein et al., 1995; Sakagami et al., 1994). Behaviorally, inhibitor-1 knockout mice show no deficit in spatial learning as assessed by the Morris water maze (Allen et al., 2000). However, they do show an impairment in reward-related learning as suggested by a deficiency in conditioned place preference to a low dose (5 mg/kg) of cocaine (Zachariou et al., 2002).

While sustained changes in the strength of existing synapses has long been regarded as the basis for learning, the formation of new synapses by newly born neurons has recently come into consideration (Leuner et al., 2006). Neurons born in the subgranular zone migrate a short distance into the granule cell layer of the dentate gyrus and send axonal projections along mossy fiber pathways to synapse on CA3 pyramidal neurons (Hastings and Gould, 1999; Markakis and Gage, 1999; Stanfield and Trice, 1988; Zhao et al., 2006). Deficits in learning observed upon selective depletion of these neurons using antimetabolic agents or irradiation have provided direct evidence that the circuits formed by these new neurons are involved in learning and memory (Raber et al., 2004; Rola et al., 2004; Shors et al., 2001; Shors et al., 2002). Indirect evidence of the functionality of these newly formed circuits has come in the form of studies demonstrating a positive correlation between neurogenesis and learning. For instance, environmental enrichment and voluntary wheel running have been shown to improve both



neurogenesis and performance on hippocampal-dependent learning tasks (Shors et al., 2001; Snyder et al., 2005; van Praag et al., 1999). Given the relationship between learning and neurogenesis, the abundance of inhibitor-1 in the dentate gyrus, and the position inhibitor-1 occupies in biochemical models of long-term plasticity, we conducted a more thorough behavioral and biochemical analysis of learning and memory in inhibitor-1 knockout mice with emphasis on dentate-associated behaviors.

## **Experimental Procedures**

### *Subjects*

Mice were group-housed in a temperature-controlled colony room (25°C) on a 12 h light/dark cycle with ad libitum access to food and water. Age-matched adult male wild-type and inhibitor-1 knockout mice (Allen et al., 2000) (8-20 weeks of age for voluntary wheel running, 12-13 weeks for neurogenesis, and 6-12 weeks for all else) on a C57/Bl6 background were used for behavioral analyses. Tissue for immunoblot analysis of PP-1/I-1 targets was obtained from a separate group of naïve age- and sex-matched wild-type and inhibitor-1 knockout mice (6-17 months of age, male and female). Most of the mice (>75%) were littermates derived from crossing individuals heterozygous for the inhibitor-1 gene, although some were not, being derived from a knockout x knockout and a wild-type x wild-type breeding strategy. All experiments conformed to National

Institutes of Health *Guide for the Care and Use of Laboratory Animals* (1996). Less stressful behaviors were tested first. The order of tests was as follows: open field habituation, novelty task, locomotor activity, fear conditioning. A separate cohort of mice was tested only for running wheel behavior then sacrificed for analysis of neurogenesis. Mice were moved within the animal facility to the testing room and allowed to habituate to the new location for at least 30 min prior to behavioral testing. C57/Bl6 mice (Charles River) were used in the determination of subregional distribution and for the analysis of inhibitor-1 levels after voluntary wheel running.

#### *Contextual fear conditioning*

Mice were placed in a plexiglass shock box with clear front and rear walls (MedAssociates) for 5 min. Two-second, 0.5 mA foot shocks were delivered at 2, 3, and 4 min for trials involving three pairings and at 2 min for those with one pairing. Freezing behavior, defined as a lack of motion except for respiration, was monitored at 5-sec intervals by an observer blind to the genotype. The boxes were cleaned with 70% ethanol, and bedding below the shock grid was changed after each mouse. Baseline freezing was considered to be freezing during the first two minutes of the training session before the delivery of any foot shock. Twenty-four, forty-eight, and seventy-two hours after training, contextual

learning and extinction were assessed by monitoring freezing behavior upon re-exposure to the training context for 5 min.

### *Immunoblots*

Slice pharmacology was conducted as in previous chapters. Control slices were treated with DMSO, the solvent used to dissolve forskolin. Lysis and immunoblot analysis of gross hippocampal dissections and striatal slices were performed as described in Chapter 2. The following additional antibodies were used:  $\beta$ -actin (1:500,000, Abcam), phospho-Ser133 CREB (1:1000, Cell Signaling), phospho-Ser845 GluR1 (1:1200, Upstate), phospho-Thr286 CaMKII $\alpha$  (Santa Cruz), and phospho-Ser51 eukaryotic translation initiation factor 2 $\alpha$  (eIF2 $\alpha$ , 1:1000, Biosource). Of these, two ( $\beta$ -actin and phospho-Ser133 CREB) were monoclonal.

### *Voluntary wheel running*

Mice were singly-housed in cages with either a freely-moving wheel or a locked wheel connected to an electronic counter. Computer-generated white noise was used to drown out ambient noise over the course of the experiment.

*Neurogenesis*

After one month of voluntary wheel running, mice were sacrificed by Diane C. Lagace (UT Southwestern Medical Center) via rapid decapitation 2 h following intraperitoneal injection of the thymidine analog 5-bromo-2-deoxyuridine (BrdU; 150mg/kg). Brains were cut along the mid-sagittal fissure, and half was preserved for protein analysis. The remaining half-brain was immersion-fixed in 4% paraformaldehyde for three days and cryopreserved in 30% sucrose. Thirty-micron sections were collected through the hippocampus by Stephanie J. Fischer (UT Southwestern Medical Center) on a freezing microtome and placed in 0.1%  $\text{NaN}_3$ -phosphate-buffered saline (PBS) until processed for immunohistochemistry. Every ninth section was mounted on a slide and allowed to dry overnight. Immunohistochemistry for BrdU-immunoreactive (BrdU+) cells was performed as previously described (Lagace et al., 2007). Briefly, sections were incubated overnight in a rat monoclonal anti-BrdU antibody (Accurate, Westbury, NY, Cat # OBT0030, 1:400) to label cells in S-phase of the cell cycle, and staining was visualized via fluorescent secondary antibody. 4'-6-diamidino-2-phenylindole (DAPI, 1:5000 in PBS) was used as a counterstain, and blood vessel background was eliminated by a 20-min incubation in cupric sulfate solution (5 mM  $\text{CuSO}_4$ , 50 mM ammonium acetate in PBS) (Schnell et al., 1999). Cells counts were performed as previously described (Harburg et al., 2007), where BrdU+ cells were counted in four subregions of the dentate gyrus

(subgranular zone, molecular layer, outer granule cell layer, and hilus). The habenula was also examined as a non-neurogenic region to confirm BrdU uptake (data not shown). Actual counts were multiplied by 18 to derive the number of BrdU+ cells in each region of both hemispheres.

#### *Open field habituation*

Mice were habituated for 5 min each day for 4 days in an empty white open field box (44 cm x 44 cm). Locomotor activity, as well as time spent in each region of the box, was followed with a video-tracking system (Ethovision, Noldus Information Technology, Wageningen, Netherlands). The center region encompassed a 14 cm x 14 cm square in the middle of the box, whereas the peripheral region included all areas within 5 cm of the edge. The non-periphery was defined as all areas not included in the periphery.

#### *Novel location and object recognition*

Twenty-four hours after the 4 days of open field habituation, the mice underwent five 6-min training sessions (Sessions 1-5) in which they were exposed to three identical 50-ml conical tubes filled with water. One conical was placed in each of three corners approximately 7 cm from each wall, and one visual cue (vertical stripes, interlocking circles, or stars) was mounted on each of three walls to orient the mice. The fourth wall was blank. For the novel location test session

(Session 6), Conical A was moved to the empty corner. For the novel object test session (Session 7), Conical A remained in its new position and Conical B was replaced with a 125-ml glass bottle. Conical C remained constant throughout all the sessions. All boxes and objects were cleaned with 50% ethanol in between every session, and each session lasted 6 min. Intersession intervals were 6 min, except that between Sessions 2 & 3 and Sessions 5 & 6, which were both 45 min. Mice were videotaped under dim lighting for subsequent hand-scoring by an observer blind to the genotype. Interactions were scored by the number of nose-pokes involving direct contact with each object during the 6-min session, and prolonged nose-pokes ( $> 1$  s) were counted according to the number of seconds of interaction. Interactions involving other parts of the body (e.g. rear or tail) were not counted. Occasionally, the mice climbed on top of the objects; in these instances, the interaction was only counted once no matter how long the mice rested atop the objects. Interaction ratios were calculated as the ratio of the percentage of nose-pokes directed at Objects A or B to that directed at Object C. An interaction ratio of greater than 1.0 indicates that the animal spent more time interacting with Object A or B than with Object C.

#### *Locomotor activity*

Mice were placed in a fresh home cage with minimal bedding for 2 hr each day for 3 days. Horizontal activity was monitored using photobeams linked

to computer data acquisition software (San Diego Instruments).

### *Data analysis*

Data analysis was conducted as in Chapter 2. Results are stated as mean  $\pm$  standard error of the mean.

## **Results**

### *Contextual fear conditioning*

Inhibitor-1 knockout mice perform normally in the Morris water maze (Allen et al., 2000). We tested another hippocampal-dependent learning task, contextual fear conditioning. The acquisition and extinction of this associative task were tested 24, 48, and 72 h after a training protocol involving three foot shocks. Re-exposure of the mice to the training context after 24 h induced robust freezing behavior compared to baseline in both controls ( $62.4 \pm 6.4\%$  vs.  $12.1 \pm 4.5\%$ ) and knockouts ( $64.2 \pm 5.5\%$  vs.  $16.4 \pm 3.1\%$ ) (**Figure 4.1A**). Subsequent exposure of the animals to the context without any further foot shocks reduced the amount of freezing in both groups ( $46.7 \pm 5.9\%$  for controls and  $47.1 \pm 7.2\%$  for knockouts) on the following day. No further decrease was observed the third day, and no differences between the groups emerged. To exclude the possibility that no differences were detected due to a ceiling effect, we tested another cohort of

mice using a milder training protocol involving only one foot shock. Significant freezing and extinction were observed; however, there were no differences between controls and knockouts (**Figure 4.1B**).

#### *Voluntary wheel running and neurogenesis*

The relative importance of the dentate gyrus, CA3, and CA1 subregions to particular hippocampal-dependent learning tasks varies (Lee et al., 2005). As such, we conducted a subregional analysis of inhibitor-1 protein expression in the hippocampal formation. Immunoblots of the microdissected subregions revealed a striking abundance of inhibitor-1 in the dentate gyrus as compared to the CA1, with ~90% of inhibitor-1 expression in the hippocampal formation belonging to the dentate gyrus (**Figure 4.2A**). Neurogenesis in the adult mammalian nervous system occurs primarily in the subventricular zone and in the subgranular zone of the dentate gyrus. Given the specific localization of inhibitor-1 to one of two neurogenic regions in the adult brain and the supposed relationship between neurogenesis and learning, we examined the role of inhibitor-1 in neurogenesis induced by voluntary wheel running. Remarkably, just six days of running increased protein levels of inhibitor-1 in the hippocampus by  $1.64 \pm 0.33$ -fold (**Figure 4.2B**). Supporting this is the observation that, according to microarray analysis, one month of voluntary wheel running increased inhibitor-1 mRNA levels in the nucleus accumbens by ~1.6-fold (Colleen A. McClung, UT



Southwestern Medical Center, personal communication,  $n = 3$  arrays/group with each array consisting of RNA derived from bilateral tissue punches of 4 mice).

Loss of inhibitor-1 had no effect on the acquisition or expression of running behavior by the mice over the course of one month. Running by both groups occurred during the dark cycle and increased steadily during the first week, reaching a peak of  $\sim 75$  rpm at the end of the week (**Figure 4.2C**, top panel). By the third week, both groups peaked at  $\sim 85$  rpm each day (**Figure 4.2C**, bottom panel). In contrast to the lack of effect on running behavior, Stephanie J. Fischer (UT Southwestern Medical Center) found that loss of inhibitor-1 increased running-induced neurogenesis by  $1.28 \pm 0.15$ -fold specifically in the subgranular zone (**Figure 4.2D**). No changes were observed in the molecular layer, outer granule layer, or hilus.

#### *Novel location and object recognition*

The dentate gyrus is thought to be responsible for the orthogonalization of sensory inputs (Kesner et al., 2004). Novel location recognition, in contrast to novel object recognition, has been reported to be a particularly dentate-dependent task (Lee et al., 2005). As such, we tested the ability of inhibitor-1 knockout mice to recognize familiar objects moved to an unfamiliar location and unfamiliar objects placed in a familiar location. Mice were habituated to an empty box for 5 min each day for 4 days before being familiarized with three identical inverted,

water-filled 50-ml conical tubes arranged in specific corners relative to distinct cues on the wall of the box (**Figure 4.3A**). Forty-five minutes after five such training sessions lasting 6 min each, the mice were tested for spatial novelty recognition, then object novelty recognition. For the spatial novelty test, Conical A was moved to the previously unoccupied corner. For the object novelty test, Conical A remained in its new location, and Conical B was replaced with a 125-ml glass bottle. Conical C remained constant throughout, serving as a control. The aforementioned training paradigm was effective, as the interaction ratio of Conical A to Conical C significantly increased for both wild-type ( $1.41 \pm 0.14$  vs.  $0.82 \pm 0.10$ ) and knockout ( $1.41 \pm 0.11$  vs.  $0.78 \pm 0.08$ ) mice during the spatial novelty test compared to the last training session (**Figure 4.3B**). However, there were no differences between wild-types and knockouts. Likewise, the interaction ratio of Object B to Conical C robustly increased for both wild-type ( $2.40 \pm 0.19$  vs.  $0.82 \pm 0.10$ ) and knockout ( $2.52 \pm 0.16$  vs.  $0.88 \pm 0.13$ ) mice during the object novelty test compared to the last training session, but there were no differences between the two groups (**Figure 4.3C**).

### *Habituation*

Many different types of learning exist, and they are subserved by distinct pathways. Habituation to a novel environment is one of the most basic nonassociative learning tasks. Rodents submitted to an open field for the first

time display more exploratory activity than in subsequent exposures. To determine if inhibitor-1 functions in this type of learning, we assessed open field habituation in inhibitor-1 knockouts. Although locomotor activity during the first session was not different between the groups, knockouts consistently exhibited more locomotion than wild-types during subsequent sessions, suggesting a mild habituation defect in inhibitor-1 knockouts (**Figure 4.4A**). Time spent in the periphery of the box, a measure of anxiety, was not different between the groups (**Supplemental Figure 4.1**). In another context, that of a locomotor box, inhibitor-1 knockouts displayed a similar habituation defect. Locomotor activity during the first ten minutes in the box was comparable between the groups during the first session, but subsequent sessions revealed greater activity in the knockouts (**Figure 4.4B**). Total locomotor activity over two hours was indistinguishable between wild-type and knockout mice, suggesting a specific habituation defect rather than generalized hyperactivity in the knockouts (**Figure 4.4C**). Thus, by two different paradigms, inhibitor-1 knockout mice were observed to have a deficit in habituation.

#### *Biochemical targets of PP-1 and inhibitor-1*

In an effort to identify possible downstream targets of PP-1 and inhibitor-1 responsible for the habituation defect observed in inhibitor-1 knockout mice, we compared levels of phosphoproteins known to be PP-1 substrates in hippocampi

from wild-type and inhibitor-1 knockout mice. Despite being PP-1 substrates strongly implicated in long-term synaptic plasticity, phospho-Ser133 CREB (Bito et al., 1996; Hagiwara et al., 1992), phospho-Ser845 GluR1 (AMPA receptor subunit) (Yan et al., 1999), and phospho-Thr286 CaMKII (Strack et al., 1997) levels were not different between the two groups (**Figure 4.5A**). Phospho-Ser51 eIF2 $\alpha$  has previously been shown to be a PP-1/inhibitor-1 target in cultured mammalian cells (Weiser et al., 2004); levels of this phospho-site were marginally but not significantly lower in knockout mice (95% confidence interval, 0.78 to 1.07). Finally, even though the mitogen-activated protein kinase (MAPK) pathway has been suggested to act downstream of PP-1 in the regulation of human prolactin gene expression in a pituitary cell line (Manfroid et al., 2001), levels of phospho-Thr202/Tyr204 MAPK were unchanged in the hippocampus of inhibitor-1 knockout mice (data not shown).

Since inhibitor-1 only functions as an inhibitor of PP-1 when it is activated by PKA, we also assessed the state of phosphorylation of various PP-1 targets in inhibitor-1 knockout mice after pharmacological activation of PKA. Levels of phospho-Ser845 GluR1 and phospho-Ser51 eIF2 $\alpha$  were similar between wild-type and inhibitor-1 knockout mice in acutely dissected striatal slices even after treatment with the D<sub>1</sub> dopamine receptor agonist SKF81297 or the adenylyl cyclase activator forskolin (**Figure 4.5B**).

## Discussion

Despite a plethora of studies purportedly linking inhibitor-1 to hippocampal learning and memory, there is little evidence directly implicating inhibitor-1. Most studies have employed exogenous inhibitor-1 to effect a change in plasticity or learning (Blitzer et al., 1998; Brown et al., 2000; Genoux et al., 2002; Morishita et al., 2001; Mulkey et al., 1994), thereby truly implicating PP-1 and not inhibitor-1. Furthermore, the few studies that have specifically examined the function of endogenous inhibitor-1 have been conducted in the CA1 region of the hippocampus (Blitzer et al., 1998; Brown et al., 2000), which possesses negligible amounts of inhibitor-1 compared to the dentate gyrus. That inhibitor-1 function in the hippocampus is mostly limited to the dentate is supported by the finding that inhibitor-1 knockout mice display deficits in LTP in the lateral perforant pathway, but not the Schaffer collateral pathway (Allen et al., 2000). Behaviorally, endogenous inhibitor-1 was found to be important for conditioned place preference to cocaine (Zachariou et al., 2002), but not for water maze learning (Allen et al., 2000).

Dopaminergic projections from the ventral tegmental area to the nucleus accumbens and the frontal cortex have historically been the focus of studies examining the neuroadaptations responsible for drug addiction. The conditioned place preference phenotype observed in inhibitor-1 knockout mice may result from loss of normal expression of inhibitor-1 in these areas (Gustafson et al.,

1991; Lowenstein et al., 1995; Sakagami et al., 1994). However, neuroadaptations in limbic structures, including the hippocampus, are being increasingly implicated. The hippocampus has been shown to increase dopamine levels in the nucleus accumbens and influence dopaminergic behaviors such as locomotion (Mitchell et al., 2000; Mogenson and Nielsen, 1984). In particular, dentate granule cells, as specifically targeted by colchicine lesioning, have been shown to regulate the control of locomotor activity by the nucleus accumbens (Emerich and Walsh, 1990). Thus, it is possible that inhibitor-1 knockout mice display a deficit in conditioned place preference due to a defect in dentate granule cell function.

Habituation to a novel environment is a related task also involving modulation of the meso-accumbens dopamine system by the hippocampus (Hooks and Kalivas, 1995; Leussis and Bolivar, 2006). Inhibitor-1 knockout mice displayed habituation deficits in both an open field context and a locomotor box context. These deficits could have resulted from disruption of the dopaminergic circuitry itself or the modulation of that circuitry by the hippocampus. That mice lacking inhibitor-1 exhibit normal water maze learning and contextual fear conditioning but abnormal conditioned place preference and habituation to a novel environment suggests that if inhibitor-1 function is important in the hippocampus, it may be specific to the modulation of dopamine-dependent learning behaviors.

Of notable importance to theories underlying hippocampus-dependent learning is the possible contribution of newly born neurons in the dentate gyrus (Bayer et al., 1973). Here we report that mice lacking inhibitor-1 showed increased running-induced neurogenesis in the subgranular zone. Furthermore, exposure to a running wheel increased the amount of inhibitor-1 found in the hippocampus. In contrast, chronic, but not acute, exposure to drugs of abuse, including opiates, psychostimulants, nicotine, and ethanol, has been shown to inhibit neurogenesis (Eisch and Harburg, 2006). Together with the deficit in conditioned place preference observed in inhibitor-1 knockout mice (Zachariou et al., 2002), these data indicate that inhibitor-1 may function in a homeostatic anti-neurogenic mechanism targeted by drugs of abuse. It will be interesting to see whether conditioned place preference and habituation to a novel environment are behavioral correlates of neurogenesis in the subgranular zone. Interestingly, one study has already found that reactivity to novelty in rats is inversely correlated with neurogenesis (Lemaire et al., 1999).

Similar to the behavioral characterization, the biochemical characterization of mice lacking inhibitor-1 has been limited. Despite an enormous list of PP-1 substrates important for learning that inhibitor-1 could potentially impact, there has not been a direct demonstration of regulation of these substrates by inhibitor-1. The catalytic subunit of PP-1 can bind to any of nearly sixty actual and putative regulatory molecules (Cohen, 2002), only one of which

is inhibitor-1. We compared the phosphorylation state of four PP-1 substrates important for learning in the hippocampus of wild-type and inhibitor-1 knockout mice. Levels of phospho-Ser133 CREB (Bito et al., 1996; Hagiwara et al., 1992), phospho-Ser845 GluR1 (Yan et al., 1999), and phospho-Thr286 CaMKII (Strack et al., 1997) were equal between the groups, indicating either a lack of regulation by inhibitor-1 or compensation by another PP-1 regulator. Ser51 of eIF2 $\alpha$  has previously been shown to be a direct target of PP-1 susceptible to regulation by overexpressed inhibitor-1 in cultured mammalian cells (Weiser et al., 2004); however, this site of phosphorylation was not significantly reduced in inhibitor-1 knockout mice.

The regulation of inhibitor-1 function by PKA on the one hand and calcineurin on the other hand provides a fertile integration point for signal transduction cascades and a theoretical basis for how one signal (i.e. NMDA) can lead to the induction of seemingly opposite processes (i.e. LTP and LTD). Inhibitor-1 is also regulated by cyclin-dependent kinase 5 (Cdk5) at Ser6 and Ser67 (Bibb et al., 2001b) and by protein kinase C (PKC) at Ser65 (Sahin et al., 2006). Thus, despite the lack of direct evidence that inhibitor-1 modulates key aspects of learning in the hippocampus via PP-1 regulation, inhibitor-1 integrates multiple signaling cascades that underlie various neurotransmitter receptors. Our studies indicate that inhibitor-1 may function in an anti-neurogenic mechanism



and be more important in the direct or indirect modulation of dopamine-dependent behaviors than in the mnemonic functions of the hippocampus.

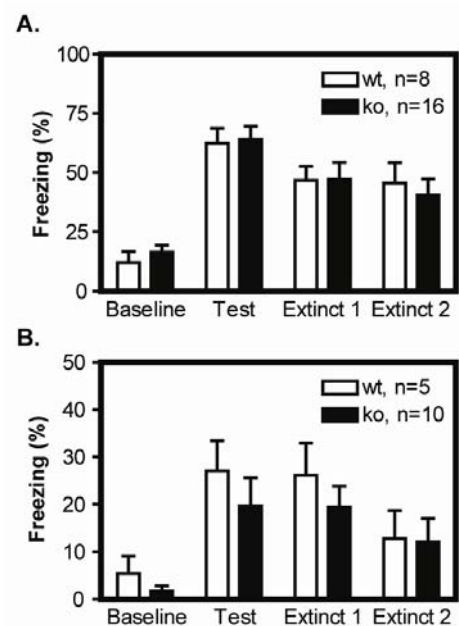


**Figure 4.1. Fear conditioning.** Freezing behavior of wild-type (wt) and inhibitor-1 knockout (ko) mice under baseline conditions and 24 h (Test), 48 h (Extinct 1), or 72 h (Extinct 2) after association of the context with **A**, three foot shocks or **B**, one foot shock.  $p < 0.0001$  effect of session, repeated measures two-way analysis of variance (ANOVA),  $p < 0.001$  Bonferonni's post-test comparing Baseline to Test for both wt and ko.

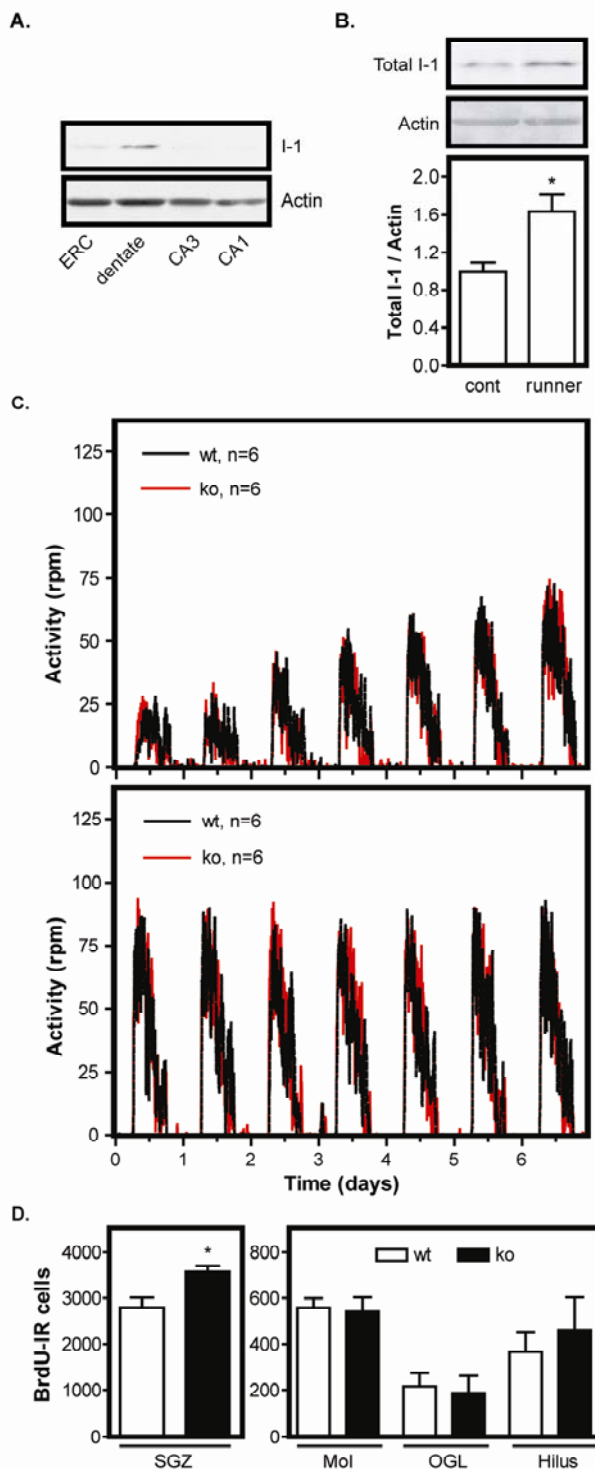


**Figure 4.2. Voluntary wheel running and neurogenesis.**

**A,** Immunoblots showing distribution of inhibitor-1 in the entorhinal cortex (ERC) and subregions of the hippocampal formation (dentate, CA3, CA1) compared to actin. **B,** Quantitative immunoblot analysis of hippocampal homogenates for inhibitor-1 and actin from C57/Bl6 mice exposed to a locked wheel (cont) or a freely-moving wheel (runner) for 6 days,  $n = 5$ . **C,** Running behavior of wt and inhibitor-1 ko mice during the first (top panel) and third (bottom panel) week of exposure to the wheels. **D,** BrdU-positive cells from wt and inhibitor-1 ko mice in the subgranular zone (SGZ, left) or other areas of the dentate (right), including the molecular layer (Mol), outer granule layer (OGL), and hilus, after 4 weeks of voluntary wheel running,  $n = 3$ . \*,  $p < 0.05$ , student's unpaired  $t$  test.

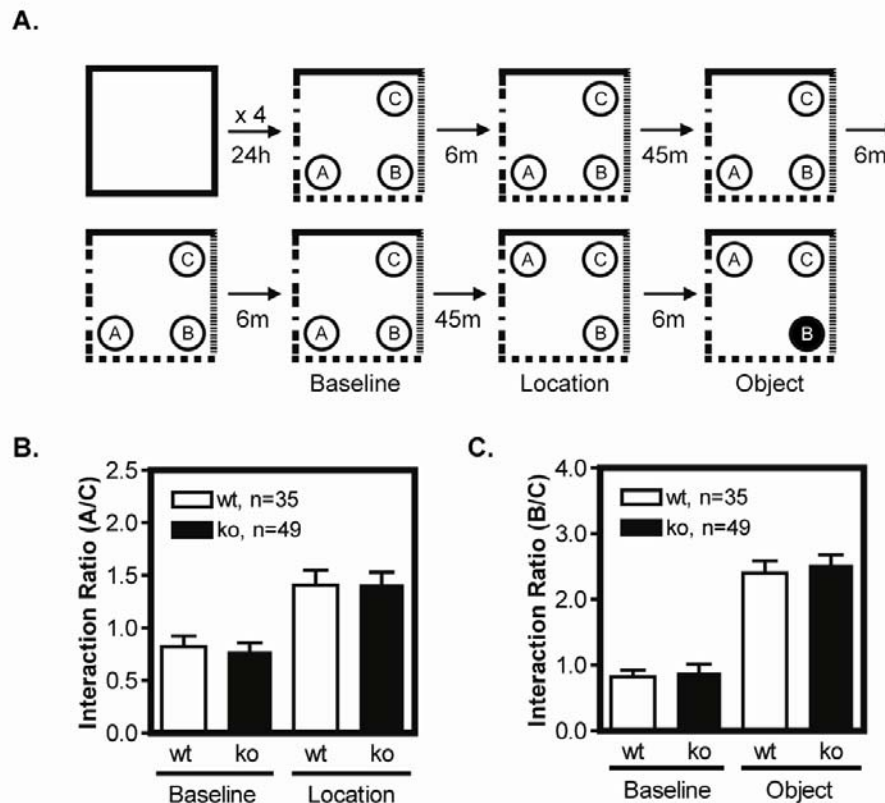


**Figure 4.3. Novel location and object recognition.** **A**, Schematic depicting experimental design. Objects are indicated by letters, and dashed lines represent the presence of a unique cue on the wall of the box. **B-C**, For wt and inhibitor-1 ko mice, the ratio of interaction directed at Conical A or Object B compared to Conical C during the Baseline, Novel Location, or Novel Object sessions.  $p < 0.0001$  effect of session, repeated measures two-way ANOVA for both Novel Location and Novel Object compared to Baseline.

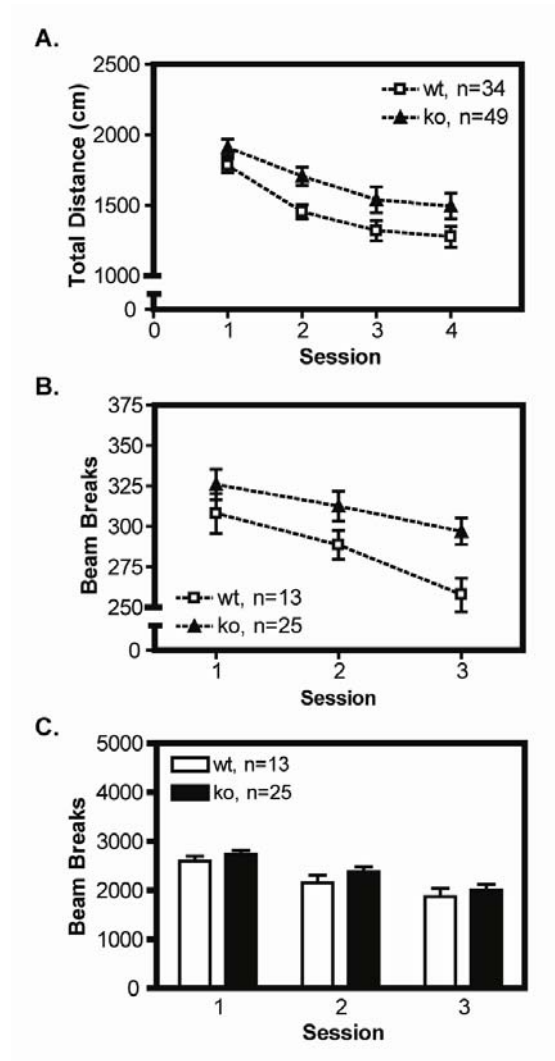


**Figure 4.4. Habituation.** Locomotor activity of wt and inhibitor-1 ko mice during **A**, daily open field sessions lasting 5 min each,  $p = 0.0001$  effect of session,  $p = 0.02$  effect of genotype, repeated measures two-way ANOVA, **B**, the first 10 min of daily locomotor box sessions,  $p < 0.0001$  effect of session,  $p = 0.02$  effect of genotype, repeated measures two-way ANOVA, or **C**, the entire 2 h of daily locomotor box sessions.

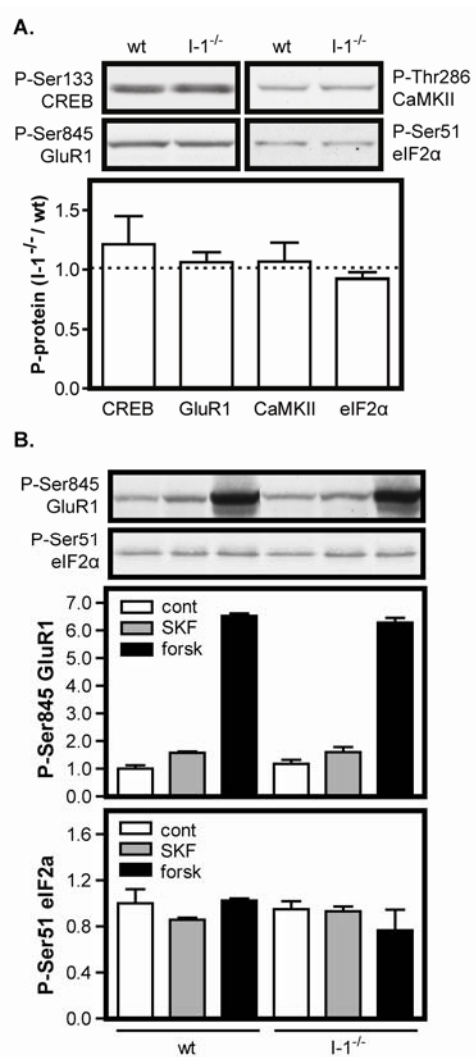
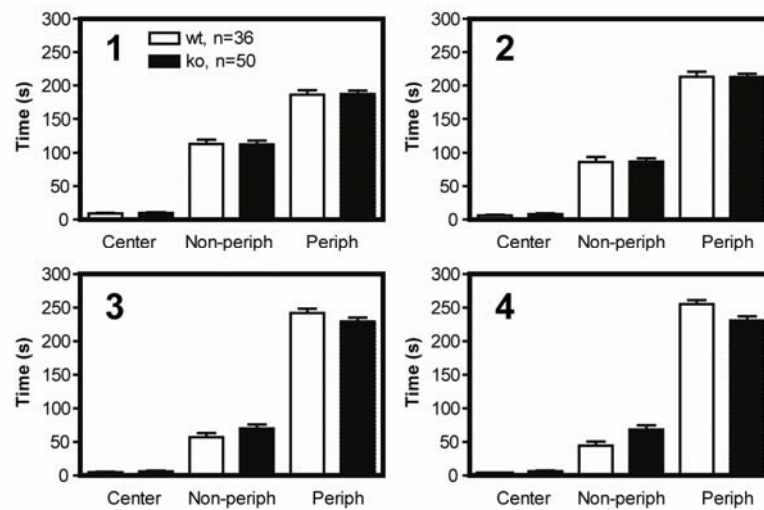


**Figure 4.5. Biochemical targets of PP-1 and inhibitor-1.** Quantitative immunoblot analysis of **A**, four phosphoproteins, including CREB, GluR1, CaMKII, and eIF2α, expressed as a ratio of levels found in the hippocampus of inhibitor-1 ko mice to that of age- and sex-matched wt mice,  $n = 5-6$  or **B**, acutely dissected striatal slices from wt or inhibitor-1 ko mice treated with vehicle (cont), SKF81297 (SKF, 1 μM, 5 min), or forskolin (forsk, 10 μM, 10 min),  $n = 2-3$ .



**Supplemental Figure 4.1. Open field behavior.** Time wt and inhibitor-1 ko mice spent in the center, non-periphery (non-periph), and periphery (periph) of the open field box during each of four daily 5-min sessions (numbered).

## **CHAPTER FIVE**

### **ELECTROPHYSIOLOGICAL CHARACTERIZATION OF MICE LACKING INHIBITOR-1 AND CDK5**

#### **Summary**

A number of passive and active electrical properties of dentate granule cells (GCs) from wild-type and protein phosphatase inhibitor-1 knockout mice were evaluated, including input resistance, action potential half-width and maximum derivative, train frequency breakpoint, subthreshold membrane potential oscillations, and voltage-dependent amplification of responses to simulated synaptic input. In spite of a limiting number of animals, a significant impairment in the ability of inhibitor-1 knockout cells to respond to high-frequency trains of stimuli was detected. In a related study aimed at identifying possible functions of cyclin-dependent kinase 5 (Cdk5)-dependent phosphorylation of inhibitor-1, pharmacological inhibition of Cdk5 was found to increase granule cell excitability, as measured by an increase in firing frequency and a decrease in action potential threshold. Finally, in a separate study aimed at providing a synaptic basis for the enhanced learning and memory observed in conditional Cdk5 knockout mice, synaptically evoked responses in CA1 pyramidal neurons from these mice were dissected. Whole-cell analysis revealed normal  $\alpha$ -amino-3-hydroxy-5-methyl-4-isoxazolepropionic acid (AMPA)



receptor-mediated and enhanced N-methyl-D-aspartate (NMDA) receptor-mediated currents. Through the use of the NR2B subunit-selective inhibitor ifenprodil, conditional Cdk5 knockout mice were demonstrated to specifically have enhanced NR2B-mediated NMDA receptor currents.

## **Introduction**

Protein phosphatase 1 (PP-1) dephosphorylates a number of substrates that might impinge on the electrical properties of neurons (Herzig and Neumann, 2000). The availability and open probability of L-type  $\text{Ca}^{2+}$  channels in rabbit cardiac tissue is increased by phosphorylation (Ono and Fozzard, 1993). Non-L-type neuronal  $\text{Ca}^{2+}$  channels are similarly affected (Dolphin, 1992), in contrast to striatal voltage-gated  $\text{Na}^{+}$  channels which appear to be inactivated by phosphorylation (Schiffmann et al., 1998). Effects of phosphorylation on inward rectifier  $\text{K}^{+}$  channels are varied, depending on the particular circumstances and system of study (Inoue and Imanaga, 1995; Koumi et al., 1995; Takano et al., 1995). Pharmacological inhibition of PP-1/PP-2A results in increased current through NMDA receptors (Wang et al., 1994) and  $\text{P}_4$  purine receptors (Pintor et al., 1997). Thus, PP-1 and the regulation of PP-1 by inhibitor-1 have the potential to greatly impact neuronal function by the direct dephosphorylation of various ion channels.

The effects of Cdk5 on ion channel function are less well-characterized. Nonetheless, numerous studies in the past decade suggest an important role for Cdk5 in the direct regulation of various ion channels. Cdk5 phosphorylates and activates transient receptor potential vanilloid 1 (TRPV1) (Pareek et al., 2007). Phosphorylation of the  $\alpha 1C$  subunit of L-type voltage-gated  $Ca^{2+}$  channels at Ser783 by Cdk5 inhibits  $Ca^{2+}$  flux and insulin secretion by pancreatic  $\beta$  cells (Wei et al., 2005a). P/Q-type voltage-gated  $Ca^{2+}$  channels involved in neurotransmitter release are similarly affected (Tomizawa et al., 2002). Finally, phosphorylation of the NR2A subunit of the NMDA receptor by Cdk5 at Ser1232 is thought to be important in mediating long-term potentiation (Li et al., 2001) and the death of CA1 pyramidal neurons following ischemic injury (Wang et al., 2003).

Given the importance of PP-1 and Cdk5 to ion channel function, we undertook an electrophysiological characterization of constitutive inhibitor-1 knockout mice and conditional Cdk5 knockout mice at the whole-cell level. Because ~90 % of inhibitor-1 in the hippocampal formation is concentrated in the granule cells of the dentate gyrus (Chapter 4), they were the focus of the inhibitor-1 studies. Recordings from conditional Cdk5 knockout mice were performed in CA1 pyramidal neurons to provide a link to the enhanced contextual fear and spatial learning observed in these mice (Hawasli et al., manuscript submitted).

## Experimental Procedures

### *Drugs and reagents*

All drugs and reagents were from Sigma, except where indicated. 6,7-dinitroquinoxaline-2,3-dione (DNQX) was purchased from Tocris.

### *Slice preparation*

Paratransverse hippocampal slices were prepared from inhibitor-1 wild-type or constitutive knockout mice (3-6 weeks) (Allen et al., 2000) for the inhibitor-1 studies and from conditional Cdk5 knockout mice (10-12 weeks) 2-4 weeks after induction of knockout by 15 daily intraperitoneal injections of 66.7 mg/kg hydroxytamoxifen (Ammar H. Hawasli, UT Southwestern Medical Center) for the Cdk5 studies. Littermate males dosed with the same regimen of hydroxytamoxifen, but lacking the Cre transgene, served as controls for the Cdk5 studies.

Halothane-anesthetized male mice were subjected to intracardiac perfusion with chilled artificial cerebrospinal fluid (ACSF, 125 mM NaCl, 25 mM glucose, 25 mM NaHCO<sub>3</sub>, 2.5 mM KCl, 1.25 mM NaH<sub>2</sub>PO<sub>4</sub>, 2 mM CaCl<sub>2</sub>, 1 mM MgCl<sub>2</sub>, pH 7.4) or cutting saline (200 mM sucrose, 3 mM KCl, 1.4 mM NaH<sub>2</sub>PO<sub>4</sub>, 26 mM NaHCO<sub>3</sub>, 2 mM MgCl<sub>2</sub>, 2 mM CaCl<sub>2</sub>, 10 mM glucose) for the inhibitor-1 and Cdk5 studies, respectively. Slices (300 µm) were prepared in the perfusion solution using a vibratome and recovered at 34°C for 20 min in an interface

chamber containing ACSF constantly bubbled with 95% O<sub>2</sub> / 5% CO<sub>2</sub>, then held at room temperature. Kynurenic acid (2 mM) was included in the recovery chamber for the Cdk5 studies to prevent excitotoxicity in the aged slices. For recording, slices were visualized with a Zeiss microscope (Oberkochen, Germany) equipped with differential interference optics.

#### *Current-clamp recordings*

Whole-cell, current-clamp recordings were made at room temperature from the soma of dentate GCs using a BVC-700 amplifier (Dagan, Minneapolis, MN). Patch-clamp electrodes (3-4 MΩ) were fabricated from thick-walled borosilicate glass. The intracellular solution consisted of 115 mM potassium gluconate, 20 mM KCl, 10 mM sodium phosphocreatine, 10 mM 4-(2-hydroxyethyl)-1-piperazineethanesulfonic acid (HEPES), 2 mM Mg-ATP, 0.3 mM Na-GTP, and 0.1 mM ethylene glycol-bis(2-aminoethyl ether)-N,N,N',N'-tetraacetic acid (EGTA), pH 7.3, with 0.1% biocytin for subsequent visualization by Douglas A. Meyer (UT Southwestern Medical Center) as in (**Supplemental Figure 5.1**). Recordings were performed in ACSF containing 2 mM kynurenic acid, 2 μM SR95531, and 1 μM atropine sulfate.

GCs were generally held at -71 mV; cells resting at > -58 mV upon break-in were not used. Input resistance and action potential properties were determined from 600-ms step pulses. Trains of 0.1-ms step pulses lasting for one

second were used in the analysis of train frequency breakpoint, and current intensity was chosen to be 25 pA higher than that required for a faithful response to a 40-Hz train. Simulated excitatory postsynaptic currents (sEPSCs), with a rise time of 0.2 ms and a decay time of 6 ms, were injected into the soma via the recording pipette and were followed 400 ms later by a 5-ms step pulse to verify accurate bridge balance and capacitance compensation. sEPSC intensity was chosen as that required for a 5-mV deflection in membrane potential from rest. For the roscovitine studies, spike ratio and action potential threshold were determined from 600-ms step pulses, in which current intensity was chosen as that required for approximately five action potentials immediately after break-in.

#### *Voltage-clamp recordings*

Whole-cell, voltage-clamp recordings were made at 32°C from the soma of CA1 pyramidal neurons using a BVC-700 amplifier (Dagan, Minneapolis, MN). Patch-clamp electrodes (3-5 M $\Omega$ ) were fabricated from thick-walled borosilicate glass. The intracellular solution consisted of 110 mM D-gluconic acid, 110 mM CsOH, 20 mM CsCl, 10 mM disodium phosphocreatine, 0.3 mM Na-GTP, 2 mM Mg-ATP, 10 mM HEPES, 0.5 mM EGTA, and 5 mM lidocaine N-ethylbromide with 0.1% biocytin. Recordings were performed in ACSF containing 2  $\mu$ M SR95531, 1  $\mu$ M atropine, 50  $\mu$ M NiCl<sub>2</sub>, and 10  $\mu$ M nimodipine.

CA1 pyramidal neurons resting at  $> -55$  mV upon break-in were not used. A stimulating electrode made of two intertwined strands of 4  $\mu$ m coated stainless steel wire was placed in the stratum radiatum to elicit excitatory postsynaptic currents (EPSCs). EPSCs were evoked at 0.05 Hz using a BSI-950 biphasic stimulus isolator (Dagan, Minneapolis, MN), and stimulus intensity was chosen to elicit 125-150 pA EPSCs at a holding potential of -70 mV. Prior to each sweep, a -5 mV step pulse was injected to assess and control for series resistance. NMDA receptor-mediated EPSCs were isolated with 20  $\mu$ M DNQX.

#### *Data analysis*

Data were converted using an ITC-18 interface (Instrutech, Port Washington, NY) and analyzed using custom macros running under Igor Pro 5.0 (WaveMetrics, Lake Oswego, OR). Input resistance was only calculated from responses to -10, -5, 0, and +5 pA current injections to avoid errors from rectification. Action potential properties were defined from the first action potential observed in response to a step pulse of current near rheobase. Action potential half-widths were calculated as the width of the action potential at a voltage halfway between the threshold and the peak voltage, in which threshold was defined as the voltage at which the first derivative of the action potential reached 30 mV/ms. Train frequency breakpoints were defined as the minimum frequency of stimulation required to induce at least one failure, or a voltage

deflection in which the peak voltage was less than 0 mV. Oscillatory behavior was quantified as the average deviation in membrane potential over 14 s in the absence of action potentials. Responses to sEPSCs were integrated for quantitation. For the roscovitine studies, spike ratios were calculated as the number of action potentials elicited by a 600-ms step pulse at defined times after break-in to that immediately after break-in. Action potential thresholds were defined from the first elicited action potential as above.

Data analysis for the Cdk5 studies was performed by Ammar H. Hawasli (UT Southwestern Medical Center). In addition to calculation of the NMDA/AMPA ratio via isolation of the NMDA-receptor current with DNQX, NMDA/AMPA ratios were also calculated in the absence of DNQX, where the NMDA receptor component was defined as the area of the +40 mV EPSC from 45 ms to 350 ms and the AMPA receptor component as the area of the -70 mV EPSC from 0 ms to 44 ms. Decay constants ( $\tau$ ) were calculated with a single-exponential fit.

## Results

### *Characterization of dentate GCs from inhibitor-1 knockout mice*

A number of passive and active electrical properties were evaluated, including input resistance, action potential half-width and maximum derivative, train frequency breakpoint, subthreshold membrane potential oscillations, and

voltage-dependent amplification of responses to simulated synaptic input. The input resistance of the GCs was quite high, in the range of hundreds of megaohms (**Figure 5.1**). Previously reported input resistance values, calculated from whole-cell patch clamp (Ambrogini et al., 2004; Liu et al., 1996; Lubke et al., 1998; Staley et al., 1992) or perforated patch-clamp (Spruston and Johnston, 1992) methods, vary from 200 to 6000 M $\Omega$ . Apparently, the properties of granule cells vary with location (Wang et al., 2000), maturity of the neuron (Ambrogini et al., 2004), and age of the animal (Liu et al., 1996). Input resistances calculated from sharp electrode recordings are much lower (~50 M $\Omega$ ) (Fricke and Prince, 1984; Staley et al., 1992), likely due to electrode-associated leak conductances (Staley et al., 1992). The median action potential half-width was 1.35 ms, larger than the reported value of 0.87 ms (Lubke et al., 1998). Any of the aforementioned factors could account for the difference in action potential half-width. The maximum derivative of action potentials generally fell between 250 and 500 mV/ms (**Figure 5.2**), reasonably consistent with a previous report (Ambrogini et al., 2004).

Dentate GCs are remarkable for their ability to faithfully respond to high-frequency trains of stimuli, in contrast to prolonged step pulses. All cells were capable of repetitive firing in response to 40-Hz trains, but eventually faltered as higher and higher frequencies were tested. The median train frequency breakpoint, or the minimum frequency at which failures appeared, was 100 Hz for wild-type GCs (**Figure 5.3**). None of the ten recorded wild-type cells faltered



below 75 Hz. In contrast, three of the six recorded knockout cells faltered below 75 Hz, with one cell exhibiting failures at a frequency as low as 50 Hz.

As has been observed in subicular neurons (Cooper et al., 2003; Mattia et al., 1997), GCs demonstrated near-threshold membrane potential oscillations (**Figure 5.4**), likely as a result of subthreshold activation of voltage-gated Na<sup>+</sup> channels. They also displayed voltage-dependent amplification of responses to simulated synaptic input (**Figure 5.5**), a phenomenon demonstrated to be dependent on boosting of voltage-gated Na<sup>+</sup> channels in neocortical (Gonzalez-Burgos and Barrionuevo, 2001; Stuart and Sakmann, 1995) and subicular neurons (Cooper et al., 2003).

While knockout of inhibitor-1 caused several properties of the GCs, including input resistance, action potential maximum derivative, membrane potential oscillations, and voltage-dependent amplification of sEPSCs, to perhaps trend towards a change, these differences were not significant because of the low *n*. More GCs from inhibitor-1 knockout mice would have to be recorded before a judgement can be made. The most promising difference was observed in the analysis of train frequency breakpoint. This difference reached significance ( $p < 0.05$ ) by a student's unpaired *t* test. Unfortunately, the number of inhibitor-1 knockout mice available was limiting at the time these recordings were conducted.

### *Effects of Cdk5 inhibition on GC excitability*

In an effort to identify an electrophysiological measure that might be affected by Cdk5-dependent regulation of inhibitor-1 in dentate GCs, we pharmacologically inhibited Cdk5 with roscovitine. Intracellular application of roscovitine (1  $\mu$ M) caused GCs to become more excitable. Action potential frequency in response to a defined step pulse increased in a time-dependent manner upon wash-in of roscovitine, in contrast to firing threshold, which decreased (**Figure 5.6**). Fifteen minutes after break-in, the firing rate increased by  $3.6 \pm 0.3$ -fold, and the threshold decreased by  $4.8 \pm 1.5$  mV.

### *Examination of EPSC components in CA1 pyramidal neurons from conditional Cdk5 knockout mice*

Current-voltage relations for CA1 pyramidal neurons from control and conditional Cdk5 knockout mice were largely indistinguishable, except at +40 mV (**Figure 5.7A**). Here cells from knockout animals displayed larger synaptically-evoked EPSCs, despite no change in the reversal potential. In addition, NMDA/AMPA EPSC ratios were  $1.4 \pm 0.2$ -fold larger in cells from conditional knockout mice (**Figure 5.7B**), in spite of equivalent AMPA receptor-mediated whole-cell currents ( $3601 \pm 400$  vs.  $3800 \pm 313$ ). Calculation of the NMDA/AMPA ratio using an alternative method without the use of the AMPA

receptor antagonist DNQX yielded similar results (**Figure 5.7C**). These data suggest that loss of Cdk5 results in larger NMDA receptor-mediated currents.

In the adult hippocampal Schaffer collateral pathway, NMDA receptor-mediated current occurs predominantly through receptor complexes consisting of NR1 and NR2A or NR2B subunits (Monyer et al., 1994). Relative subunit contributions to the increased NMDA receptor-mediated current were determined by measuring sensitivity to the NR2B-selective inhibitor ifenprodil (Chenard and Menniti, 1999). Ifenprodil-sensitive currents were  $3.2 \pm 0.5$ -fold greater in cells from conditional Cdk5 knockout mice (**Figure 5.7D**). NR1/NR2B-mediated currents exhibit a longer decay constant than NR1/NR2A-mediated currents (Vicini et al., 1998). Consistent with this fact, the decay constant ( $\tau$ ) for NMDA receptor-mediated currents was longer in knockout ( $74.2 \pm 7.2$  ms) than in control ( $51.5 \pm 4.7$  ms) mice (**Figure 5.7D**).

## Discussion

In the rat, approximately one million dentate GCs innervate some 300,000 CA3 pyramidal neurons via mossy fibers (Amaral et al., 1990). Spike transmission, or the firing of a postsynaptic cell in response to the firing of a presynaptic cell, occurs in response to trains of spikes, but not a single spike of the GC (Henze et al., 2002). Furthermore, the probability of spike transmission varies with the frequency of granule cell firing, with 100-Hz firing resulting in a

probability greater than 0.8. Thus, the ability of GCs to transmit information to CA3 neurons is critically dependent on their ability to rapidly fire trains of action potentials. Our train frequency breakpoint assay is a measure of this ability. The lower train frequency breakpoint observed in GCs lacking inhibitor-1 suggests that the efficacy with which these cells communicate with target CA3 neurons may be reduced.

Roscovitine affects neuronal function in a number of known and unknown ways unrelated to its inhibition of Cdk5. Specifically, it has been shown to increase P/Q-type calcium tail currents when applied extracellularly, but not intracellularly (Yan et al., 2002). Recently, similar effects were observed for N- and R-type ( $EC_{50} = 54 \mu M$ ), but not L-type, voltage-gated calcium channels (Buraei et al., 2005; Buraei et al., 2007). While the deactivation kinetics were not altered, bath-applied roscovitine also rapidly inactivated voltage-gated potassium channels ( $EC_{50} = 23 \mu M$ ) (Buraei et al., 2007). Thus, experiments employing roscovitine as a means of inhibition of Cdk5 must be interpreted carefully. Nonetheless, the effects of roscovitine on GC excitability are interesting, especially considering the fact that roscovitine was applied intracellularly at a low concentration ( $1 \mu M$ ). As of yet, no side effects from intracellular administration have been reported. Studies employing other Cdk5 inhibitors, such as indolinone A, will be helpful in determining whether roscovitine acted via a Cdk5-dependent mechanism.

The results from the Cdk5 studies correlate well with a number of observations regarding the conditional loss of Cdk5 (Hawasli et al., manuscript submitted): 1) Mice display superior performance in hippocampal-dependent learning tasks, including contextual fear memory and water maze reversal learning. 2) Long-term potentiation (LTP) is enhanced. 3) NMDA/AMPA field excitatory postsynaptic potential (EPSP) ratios are larger. 4) Hippocampal NR2B protein levels are increased. 5) The enhanced LTP is reversed by the NR2B-selective antagonist ifenprodil and the general NMDA receptor antagonist 2-amino-5-phosphonopentanoic acid (AP5). Thus, the enhanced NMDA receptor-mediated currents and NR2B-dependent components observed at the whole-cell level contribute to a novel mechanism by which Cdk5 regulates NR2B-containing NMDA receptors.

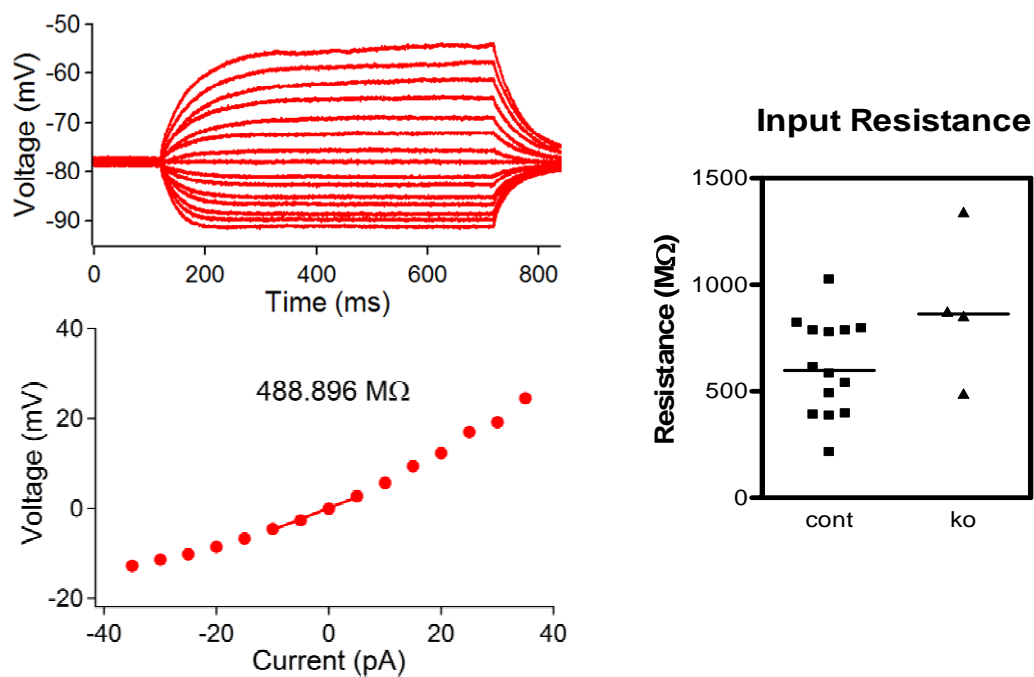


**Figure 5.1. Input resistance.** Example voltage responses of a GC to step current injections (top left) quantitated as a voltage-current relationship (bottom left). Input resistance of GCs from inhibitor-1 control (cont) and knockout (ko) mice in a scatter plot with a median bar (right).

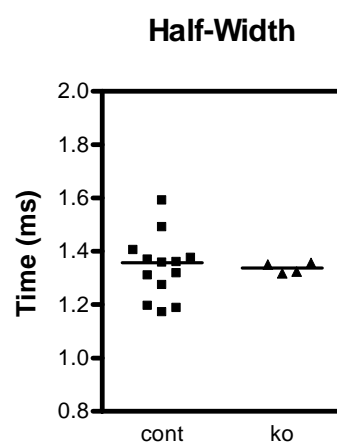


**Figure 5.2. Action potential properties.** Scatter plots with median bars depicting the half-width (left) and maximum derivative (right) of action potentials derived from GCs of inhibitor-1 cont and ko mice.

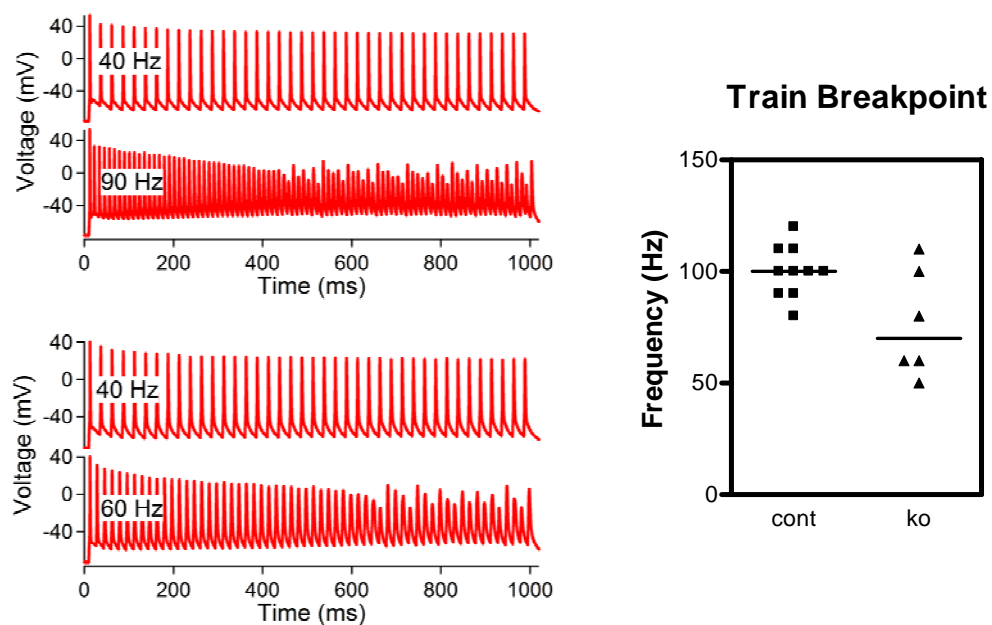


**Figure 5.3. Train frequency breakpoint.** Example traces of the voltage response of GCs from inhibitor-1 cont (top left) and ko (bottom left) mice to high frequency stimulation. Scatter plot with a median bar depicting the minimum frequency of stimulation at which action potentials falter for each group (right).  $p < 0.05$ , student's unpaired  $t$  test,  $n = 6-10$ .



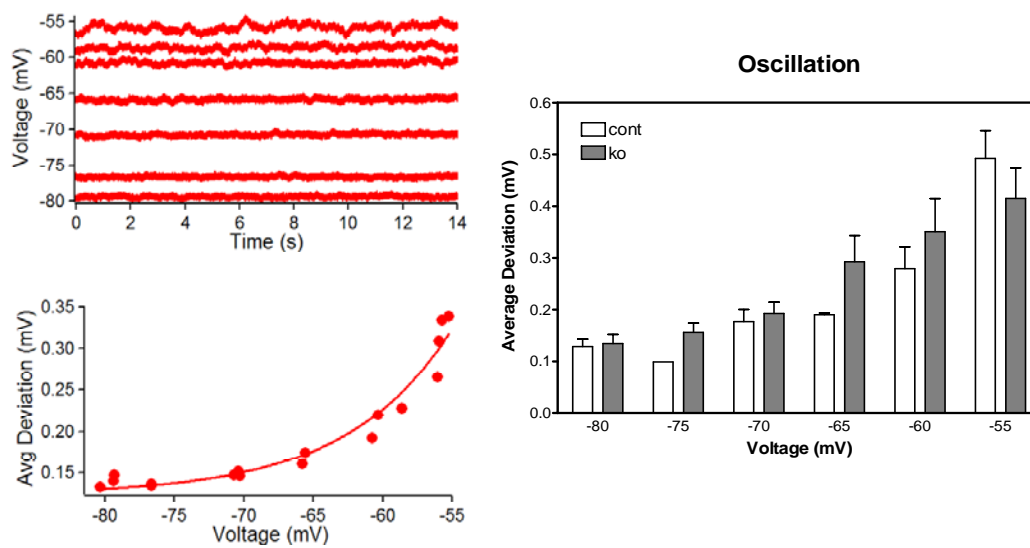


**Figure 5.4. Membrane potential oscillations.** Example oscillatory behavior of a GC held at different potentials (top left) quantitated as average deviation (bottom left). Graph depicting subthreshold membrane potential oscillations of inhibitor-1 cont and ko GCs held at different potentials (right).

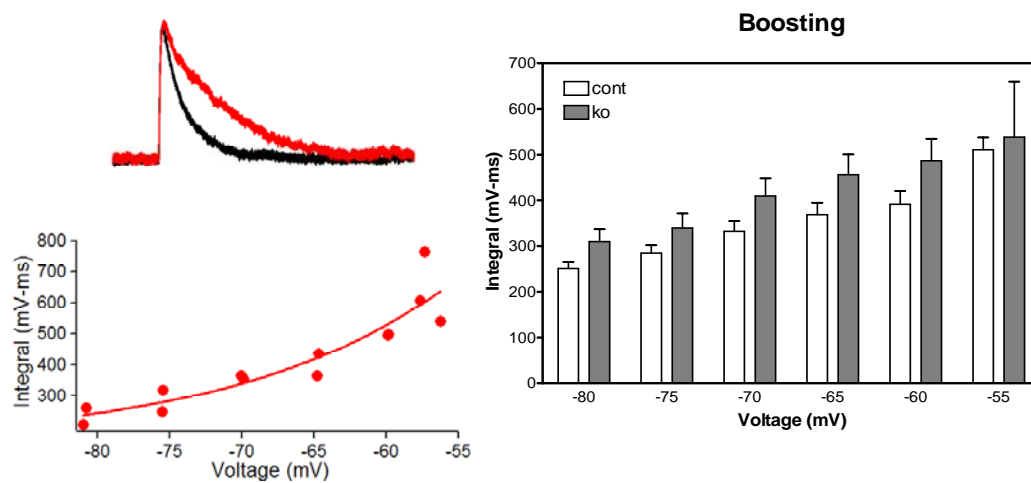


**Figure 5.5. Voltage-dependent amplification of responses to simulated synaptic input.** Example voltage response of a GC held at two different potentials to a subthreshold simulated synaptic input (top left). Graph depicting the integrated voltage response of an example GC (bottom left) and the average responses of inhibitor-1 cont and ko GCs held at different potentials (right).

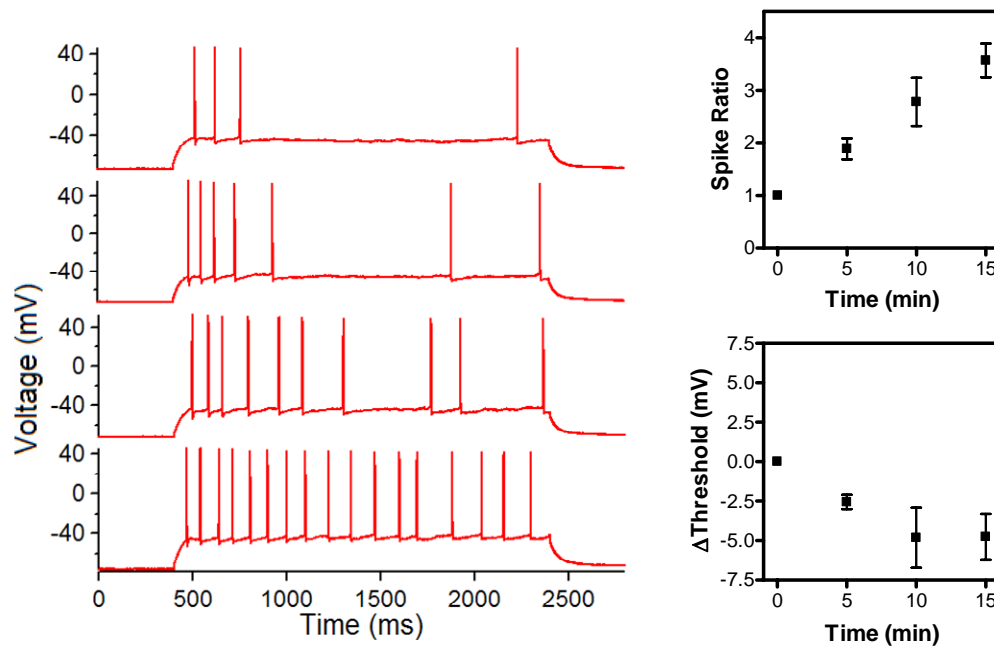


**Figure 5.6. Effects of roscovitine on GC excitability.** Successive traces depicting spiking behavior of an example GC upon intracellular application of 1  $\mu$ M roscovitine (left). Graphs depicting the ratio of the number of spikes at various times after break-in to that immediately after break-in (top right,  $p < 0.01$ , one-way ANOVA) and the change in action potential threshold with time (bottom right,  $p < 0.05$ , Kruskal-Wallis test).

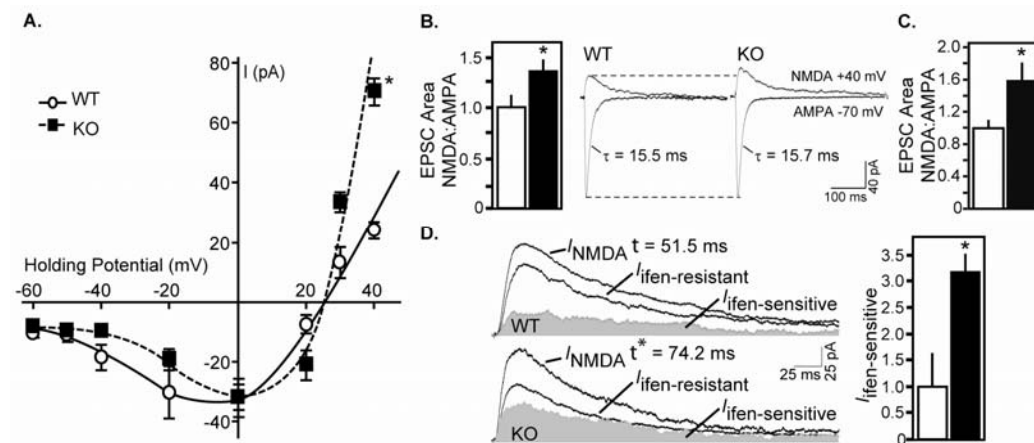


**Figure 5.7. Effects of loss of Cdk5 on NMDA receptor currents.** **A**,  $I$ - $V$  relationship for CA1 pyramidal neurons from wild-type (wt) and conditional Cdk5 knockout (ko) mice. **B**, Whole cell NMDA:AMPA EPSC charge ratio with representative traces. AMPA- and NMDA-mediated EPSCs were measured at  $-70$  mV and  $+40$  mV/ $20$   $\mu\text{M}$  DNQX, respectively,  $n = 7$ - $10$  cells,  $5$ - $7$  mice/genotype. **C**, Alternative whole cell NMDA:AMPA EPSC charge ratio. AMPA- and NMDA-mediated EPSCs were measured at  $-70$  mV ( $0$  ms –  $44$  ms) and  $+40$  mV ( $45$  ms –  $350$  ms), respectively,  $n = 6$ - $8$  cells,  $5$ - $7$  mice/genotype. **D**, Effect of ifenprodil (ifen) on whole-cell NMDAR-mediated EPSCs. Representative traces of NMDAR-mediated EPSCs before ( $I_{\text{NMDA}}$ ) and after ( $I_{\text{ifen-resistant}}$ )  $10$   $\mu\text{M}$  ifenprodil are shown.  $I_{\text{ifen-sensitive}}$  represents area between  $I_{\text{NMDA}}$  and  $I_{\text{ifen-resistant}}$  traces, normalized to  $I_{\text{NMDA}}$ .  $\tau$  for  $I_{\text{NMDA}}$  is shown,  $n = 6$ - $8$  cells,  $6$ - $7$  mice/genotype ( $+60$  mV/ $20$   $\mu\text{M}$  DNQX). \*  $p < 0.05$ , student's  $t$  test,  $\square$  = wt and  $\blacksquare$  = ko.



**Supplemental Figure 5.1. Biocytin stains of dentate granule cells.** Shown are the the somas and dendritic arbors of four dentate granule cells filled with biocytin during whole-cell patch clamp analysis.

## APPENDIX A

### DATAPRO MACROS FOR USE IN IGOR

```
#pragma rtGlobals=1          // Use modern global access method.
#include <ANOVA>

menu "Chan"
    "PosthocInputR", PosthocInputR()
end

function PosthocInputR ()
    variable/g Rexecution // to keep track of how many times function has been run
    string list, deltaVno, inputIno, deltaVmno, inputImno, fit_deltaVmno
    string theWave, adtheWave, IRtext, sweeplist, currentlist, sweeptime
    variable index=0, o=0, abbrev1, abbrev2
    variable pulseavg, baseavg, IR
    prompt list, "Enter sweep numbers as ranges, or separated by commas"
    doprompt "Input Resistance", list
    if (V_Flag)

        return -1
    endif
    do
        if (index == 0)                // is this the first wave?
            print itemsinlist(list, ",")
            make/o/N=(itemsinlist(list, ",")) deltaV           // create deltaV wave
            make/o/N=(itemsinlist(list, ",")) inputI           // create input current wave
            make/o/N=1 deltaVm
            make/o/N=1 inputIm
        endif
        theWave = StringFromList (index, list, ",")
        for (;stringmatch (theWave, "*-*") == 1;) // for loop b/c possibility of multiple ranges
            sscanf theWave, "%f-%f", abbrev1, abbrev2 // assign start and stop of range
            do
                list = list + "," + num2str(abbrev1) // add individual sweeps of range to list
                abbrev1 += 1
            while (abbrev1 <= abbrev2) // until last sweep in range
            list = removefromlist (theWave, list, ",") // remove range from list
            print list
            theWave = StringFromList (index, list, ",") // reassign theWave
            print theWave
            redimension/n=(itemsinlist(list, ",")) deltaV // adjust # points in waves
            redimension/n=(itemsinlist(list, ",")) inputI // adjust # points in waves
            endfor
        adtheWave = "ad1_" + theWave
    
```

```

if (strlen(theWave) == 0)
    break // ran out of waves
endif
if (index == 0) // is this the first wave?
    display $adtheWave
    currentlist = ""
else
    appendtograph $adtheWave
endif
wavestats/q/r=(0,100) $adtheWave
baseavg = v_avg
wavestats/q/r=(600,700) $adtheWave
pulseavg = v_avg
if (pulseavg > -100) // make sure pulseavg not maxed out
    deltaV [index] = pulseavg - baseavg
    wave/t stimhistory = stimhistory
    inputI [index] = str2num(stimhistory [(str2num(theWave))][4])
    currentlist += stimhistory [(str2num(theWave))][4] // for textbox of currents
    currentlist += " "
// 4 spaces to separate
    if ((-12 < str2num(stimhistory [(str2num(theWave))][4])) & (str2num(stimhistory
        [(str2num(theWave))][4]) < 8))
        if (o!=0)
            redimension/n=(o+1) deltaVm
            redimension/n=(o+1) inputIm
        endif
        deltaVm [o] = pulseavg - baseavg
        inputIm [o] = str2num(stimhistory [(str2num(theWave))][4])
        o+=1
    endif
endif
else
    removefromgraph $adtheWave // exclude out-of-bounds wave from appended sweeps
    list = removefromlist (theWave, list, ",") // remove out-of-bounds wave from list
    index -= 1 // to account for item removal from list
    redimension/n=(itemsinlist(list, ",")) deltaV, inputI // get rid of extra data point
endif
index += 1 // next wave
while (1)
    currentlist = Sortlist(currentlist, " ", 2) // sort current list into numerical order
    currentlist = "pulses " + currentlist
    currentlist += " pA"
    ModifyGraph gfSize=7
    ModifyGraph lblMargin(left)=5
    ModifyGraph lblMargin(bottom)=1
    deltaVno = "deltaV" + num2str(Rexecution)
    inputIno = "inputI" + num2str(Rexecution)
    duplicate deltaV $deltaVno
    duplicate inputI $inputIno
    display $deltaVno vs $inputIno // inputR graph
    ModifyGraph mode=3,marker=19 // scatterplot

```

```

curvefit line deltaVm /x=inputim /d
fit_deltaVmno = "fit_deltaVm" + num2str(Rexecution)
duplicate fit_deltaVm $fit_deltaVmno
appendtograph $fit_deltaVmno
ModifyGraph gfSize=7
ModifyGraph lblMargin(left)=4
ModifyGraph lblMargin(bottom)=6
wave w_coef = w_coef
IR=(w_coef[1])*1000 // convert inputR (slope) to MOhms

sprintf IRtext, "%g M\F'Symbol'W", IR          // for textbox
list = Sortlist(list, "", 2)                  // sort sweeplist

sprintf sweeplist, "Sweeps %s", list          // for textbox
theWave = StringFromList (0, list, ",") // determine first sweep to record time
sweepTime = stimhistory [(str2num(theWave))][8] // time of first sweep
TextBox/C/N=text1/F=0/A=MT/E=0 IRtext        // inputR value in MOhms
TextBox/C/N=text4/X=5.00/Y=15/F=0/A=MT/E=0 sweepTime // time
Label bottom "pA" // for inputR graph
Label left "mV" // for inputR graph
Rexecution+=1
end

```

### macro MaxDerivative2(startsweep,endsweep)

```

variable pointnumber,startsweep,endsweep, threshold, halfY, vmax, maxloc, vmax2, halfx1,
    halfxavg, halfx2, halfwidth
variable/g o
string thiswave
string base

o=startsweep
base=bname1
pointnumber=0
    sprintf thiswave "%s%d",base, o
    print thiswave
    dowindow/K changraph
    chanwindow()
    display/HOST=chanwindow $thiswave
dowindow changraph

do
    sprintf thiswave "%s%d",base, o

    duplicate/o $thiswave diffwave
    differentiate diffwave
    wavestats/q diffwave
    vmax=V_max
    maxloc=V_maxloc

```



```

lidocainediff[pointnumber]=vmax //display maxderiv in table

findlevel/q diffwave, 30 //find threshold
duplicate/o $thiswave vlevelY //find Y corresponding to X threshold
Threshold=vlevelY(V_levelx) //find Y corresponding to X threshold
lidocainethresh[pointnumber]=threshold //display threshold in table
wavestats/q $thiswave
vmax2=V_max //peak of curve
halfY=((vmax2-threshold)/2)+threshold //Y halfway b/w threshold and peak
findlevel/q $thiswave,halfY //left point at halfy
halfx1=V_levelx
findlevel/q/t=10 $thiswave, halfY //avg point at halfy
halfxavg=V_levelx
halfx2=(halfxavg*2)-halfx1 //right point at halfy
halfwidth= halfx2-halfx1
print halfY
print halfx1
print halfxavg
print halfx2
print halfwidth
lidocainehalfwidth[pointnumber]=halfwidth //display halfwidth in table
diffwave=-vmax+10 //move into view

o+=1
pointnumber+=1
while (o<=endsweep)
end

window chanwindow()
string base
base=bname1
sprintf thiswave "%s%d",base, o
dowindow/f changraph
display $thiswave
appendtograph diffwave
ModifyGraph rgb(diffwave)=(0,0,0) //change color
wavestats/q $thiswave
SetAxis bottom V_maxloc-10,V_maxloc+10 //zoom in
end

macro KillGraphs (except)
string except, graphexcept, theGraph
graphexcept = "graph" + except
string allgraphs = winlist ("graph*",",", "win:1")
variable index=0
do
    theGraph = StringFromList (index, allgraphs)
    if (stringmatch (theGraph, graphexcept) == 0)

```

```

        dowindow/k $theGraph
    endif
    if (strlen(allgraphs) == 0)
        break
    endif
    index += 1
while (1)
end

```

```

macro KillAllGraphs ()
string theGraph
string allgraphs = winlist ("graph*",";", "win:1")
variable index=0
do
    theGraph = StringFromList (index, allgraphs)
    dowindow/k $theGraph
    if (strlen(allgraphs) == 0)
        break
    endif
    index += 1
while (1)
end

```

```

macro KillAllTables ()
string theTable
string alltables = winlist ("table*",";", "win:2")
variable index=0
do
    theTable = StringFromList (index, alltables)
    dowindow/k $theTable
    if (strlen(alltables) == 0)
        break
    endif
    index += 1
while (1)
end

```

```

menu "Chan"
    "ActiveProperties", ActiveProperties()
end

```

### function ActiveProperties()

```

// be sure to killwaves threshold, maxderiv, halfwidth, APsweep1ist, APtimelist before starting
variable thresh, halfY, halfx1, halfxavg, halfx2, halfw, sweepno
string Aptime
svar newwave1

```

```

duplicate/o $newwave1 diffwave
differentiate diffwave

```

```

findlevel/q diffwave, 30 //find X at which deriv is 30 (threshold)
duplicate/o $newwave1 vlevelY //for correct syntax in next step
thresh=vlevelY(V_levelx) //find Y corresponding to X threshold
if (waveexists(Threshold)==0)
    make/n=1 Threshold
    Threshold[0]=thresh
    edit threshold
else
    DoWindow/f ActivePropSummary
    redimension/n=((numpts(Threshold)+1)) Threshold
    Threshold[(numpts(Threshold)-1)]=thresh
endif

wavestats/q diffwave
if (waveexists(MaxDeriv)==0)
    make/n=1 MaxDeriv
    MaxDeriv[0]=V_max
    appendtotable MaxDeriv
else
    redimension/n=((numpts(MaxDeriv)+1)) MaxDeriv
    MaxDeriv[(numpts(MaxDeriv)-1)]=V_max
endif

wavestats/q $newwave1
halfY=((V_max-thresh)/2)+thresh //Y halfway b/w threshold and peak
findlevel/q $newwave1,halfY //left point at halfy
halfx1=V_levelx
findlevel/q/t=10 $newwave1, halfY //avg point at halfy
halfxavg=V_levelx
halfx2=(halfxavg*2)-halfx1 //right point at halfy
halfw= halfx2-halfx1
print halfxavg
if (waveexists(HalfWidth)==0)
    make/n=1 HalfWidth
    HalfWidth[0]=halfw
    appendtotable HalfWidth
else
    redimension/n=((numpts(HalfWidth)+1)) Halfwidth
    HalfWidth[(numpts(HalfWidth)-1)]=halfw
endif

sscanf newwave1, "ad1_%f", sweepno
if (waveexists(APSweepList)==0)
    make/n=1 APSweepList
    APSweepList[0]=sweepno
    appendtotable APSweepList
else
    redimension/n=((numpts(APSweepList)+1)) APSweepList
    APSweepList[(numpts(APSweepList)-1)]=sweepno
endif

```

```

wave/t stimhistory = stimhistory
APtime=stimhistory[sweepno][8]
if (waveexists(APtimeList)==0)
    make/t/n=1 APtimeList
    APtimeList[0]=APtime
    appendtotable APtimeList
    ModifyTable size=8,alignment=1
    DoWindow/C/T ActivePropSummary,"Active Properties"
else
    redimension/n=((numpts(APtimeList)+1)) APtimeList
    APtimeList[(numpts(APtimeList)-1)]=APtime
endif

end

Function APButton(ctrlName) : ButtonControl
    String ctrlName
    Execute "ActiveProperties()"
End

menu "Chan"
    "DentateInputR", DentateInputR()
end

function DentateInputR()
    variable increment, firstIR, pointno
    variable IR, i, change, j
    NVAR IRinitial
    string IRtext="", changetext=""

    dowindow/f adc_daccontrol
    PopupMenu dacpopup_0 mode=3
    douupdate

    i=0

    dowindow/k Input_Resistance
    NVAR Multdac0
    Multdac0 = 1 //sets multiplier to 1
    NVAR dplong
    dplong = 600
    increment=5
    if (waveexists(deltaV)==0)
        firstIR=0 // variable firstIR is 0 if this is first IR measure for exp
    else
        firstIR=1 // otherwise firstIR is 1
    endif
end

```

```

do

    if (i==0)                                // if first cycle, make waves
        make/o/n=1 baselineAvg
        make/o/n=1 baselineSD
        make/o/n=1 pulseAvg
        make/o/n=1 pulseSD
        make/o/n=1 CurrentInjection
        make/o/n=1 deltaV
    else
        redimension/n=(i+1) baselineAvg      // otherwise, make waves longer
        redimension/n=(i+1) baselineSD
        redimension/n=(i+1) pulseAvg
        redimension/n=(i+1) pulseSD
        redimension/n=(i+1) CurrentInjection
        redimension/n=(i+1) deltaV
    endif

    NVAR dpdur
    dpdur=600
    NVAR dphigh
    dphigh=-5-i*increment // start at -5pA and go down by "increments"
    CurrentInjection[i]=dphigh
    doupdate
    //sets duration of long pulse to 600 ms
    // sets amplitude of long pulse to -200 pA
    dodataacq() //acquires data
    SaveStimHistory(0) // writes to history table

    SVAR newwave1
    wavestats/q/r=(0,100) $newwave1
    baselineAvg[i]=v_avg
    baselineSD[i]=v_sdev

    wavestats/q/r=(600,700) $newwave1
    pulseAvg[i]=v_avg
    pulseSD[i]=v_sdev

    i+=1

while ((pulseAvg[i-1]>-88) && (i<15) && HaltProcedures()<1) // while cell is more + than
    88 and spacebar not pressed

    j=i
    i=1

do

    redimension/n=(j+1) baselineAvg
    redimension/n=(j+1) baselineSD

```

```

redimension/n=(j+1) pulseAvg
redimension/n=(j+1) pulseSD
redimension/n=(j+1) CurrentInjection
redimension/n=(j+1) deltaV

NVAR dpdur
dpdur=600
NVAR dphigh
dphigh=-5+i*increment // start at -5pA and go up by "increments"
CurrentInjection[j]=dphigh
douupdate
dodataacq() //acquires data
SaveStimHistory(0) // writes to history table

SVAR newwave1
wavestats/q/r=(0,100) $newwave1
baselineAvg[j]=v_avg
baselineSD[j]=v_sdev

wavestats/q/r=(600,700) $newwave1
pulseAvg[j]=v_avg
pulseSD[j]=v_sdev

j+=1
i+=1
duplicate/o $newwave1 diffwave // to find action potentials
differentiate diffwave
findlevel/q diffwave, 40

while ((V_flag==1) && (j<30) && HaltProcedures()<1) // no action potentials and 30
rounds max

deltaV=pulseAvg-baselineAvg
display deltaV vs currentinjection as ""
dowindow/c/f Input_Resistance
ModifyGraph mode=3
ModifyGraph rgb(deltaV)=(0,0,0)
label left "mV"
label bottom "pA"
pointno=umpnts(deltaV)
pointno-=2
CurveFit/q line deltaV[,pointno] /X=CurrentInjection /D
wave w_coef=w_coef
IR=(w_coef[1])*1000 // convert to MOhms
sprintf IRtext, "%g M\F'Symbol'W", IR // for textbox
TextBox/C/N=text1/F=0/A=MT/E=0/y=4 IRtext // inputR value in MOhms
if (firstIR==0) // if first IR measure for exp
    IRinitial=IR // define global variable IRinitial for memory
else
    change=(IR/IRinitial) // otherwise calculate change

```

```

        change*=100                // as a percentage
        sprintf changetext, "%g"change
        changetext += "% of initial"
    endif
    TextBox/C/N=text2/F=0/A=MT/E=0/y=12 changetext        // %change from initial
end

Function DGIR(ctrlName) : ButtonControl
    String ctrlName
    Execute "DentateInputR()"
End

menu "Chan"
    "Oscillations", Oscillatn()
end

function Oscillatn()
    variable/g oscexecution
    string list, sweeptime, peaknos, voltagenos
    string theWave, adtheWave, sweeplist, currentlist
    variable index=0, abbrev1, abbrev2
    prompt list, "Enter sweep numbers as ranges, or separated by commas"
    doprompt "Oscillations", list
    if (V_Flag)
        return -1
    endif
    do
        if (index == 0)                // is this the first wave?
            make/o/N=(itemsinlist(list, ",")) peak        // create peak wave
            make/o/N=(itemsinlist(list, ",")) voltage        // create voltage wave
        endif
        theWave = StringFromList (index, list, ",")
        for (;stringmatch (theWave, "*-*") == 1;)    // for loop b/c possibility of multiple ranges
            sscanf theWave, "%f-%f", abbrev1, abbrev2 // assign start and stop of range
            do
                list = list + "," + num2str(abbrev1)    // add individual sweeps of range to list
                abbrev1 += 1
            while (abbrev1 <= abbrev2)                // until last sweep in range
            list = removefromlist (theWave, list, ",")    // remove range from list
            print list
            theWave = StringFromList (index, list, ",")    // reassign theWave
            redimension/n=(itemsinlist(list, ",")) peak    // adjust # points in waves
            redimension/n=(itemsinlist(list, ",")) voltage    // adjust # points in waves
            endfor
        adtheWave = "ad1_" + theWave
        if (strlen(theWave) == 0)
            break        // ran out of waves
        endif
        if (index == 0)                // is this the first wave?

```

```

        display $adtheWave
        ModifyGraph gfSize=7
        ModifyGraph lblPos(left)=27
        ModifyGraph lblMargin(bottom)=6
    else
        appendtograph $adtheWave
    endif
    wavestats/q $adtheWave
    voltage[index]=V_avg
    duplicate/o $adtheWave predoscill // curvefit destination wave (next step) must already exist
    curvefit/q poly 3, $adtheWave /d=predoscill
    duplicate/o $adtheWave dupWave // cannot use $string in function
    duplicate/o $adtheWave difference // wave has to exist before using in function
    difference = dupwave - predoscill
    wavestats/q difference
    peak[index]=V_adev
    index +=1
while (1) // until break above

    peaknos = "peak" + num2str(oscexecution)
    print peaknos
    voltagenos = "voltage" + num2str(oscexecution)
    duplicate/o peak $peaknos
    duplicate/o voltage $voltagenos
    display $peaknos vs $voltagenos
    ModifyGraph mode=3,marker=19
    K0 = 0;K1 = 7.067;K2 = -.0526
    CurveFit/G exp $peaknos /X=$voltagenos /D
    Label bottom "mV"
    Label left "Avg Dev"
    ModifyGraph gfSize=7
    ModifyGraph lblMargin(left)=4
    ModifyGraph lblMargin(bottom)=6
    theWave = StringFromList (0, list, ",") // determine first sweep to record time
    wave/t stimhistory = stimhistory
    sweeptime = stimhistory [(str2num(theWave))][8] // time of first sweep
    TextBox/C/N=text4/Y=15.00/F=0/A=MT/E=0 sweeptime // time
    TextBox/C/N=text1/F=0/A=MT/E=0 num2str(k2)
    oscexecution+=1
end

menu "Chan"
"PlotforLayout", PlotforLayout()
end

function PlotforLayout()
    svar newwave1=newwave1
    nvar newsweep
    wave/t stimhistory

```



```

string gainz, currentz, wavenom, commentz, thyme, newsweepstr
duplicate/o $newwave1 $newwave1+"copy"
display $newwave1+"copy"
ModifyGraph gfSize=7
ModifyGraph lblMargin(left)=4
ModifyGraph lblMargin(bottom)=6

```

```

    gainz=stimhistory[newsweep][1]
    currentz=stimhistory[newsweep][4]
    wavenom=stimhistory[newsweep][0]
    Commentz=stimhistory[newsweep][7]
    thyme=stimhistory[newsweep][8]
    newsweepstr=num2str(newswEEP)

    TextBox/C/N=text1/f=0 wavenom
    if (cmpstr(wavenom,"StepPulse_DAC")!=0)
        TextBox/C/N=text3/f=0/y=25 gainz
        TextBox/C/N=text2/f=0 ""
    else
        TextBox/C/N=text2/f=0/y=25 currentz
        TextBox/C/N=text3/f=0 ""
    endif
    TextBox/C/N=text4/f=0/y=50 thyme
    TextBox/C/N=text5/f=0/y=75 newsweepstr

```

```

end

```

```

function PlotLButton(ctrlName) : ButtonControl
    string ctrlName
    execute "PlotforLayout()"
end

```

```

menu "Chan"
    "StackedPlot", StackedPlots()
end

```

```

function StackedPlots()
    svar newwave1=newwave1
    nvar newsweep
    wave/t stimhistory
    string gainz, currentz, wavenom, commentz, thyme, newsweepstr
    dowindow/b databrowser
    AppendToGraph/L=left2 $newwave1
    ModifyGraph lblPos(left2)=27
    ModifyGraph axisEnab(left2)={0,0.48},freePos(left2)=0
    ModifyGraph axisEnab(left)={0.52,1}
    ModifyGraph lblMargin(left)=4
    ModifyGraph lblMargin(bottom)=6

```

```

gainz=stimhistory[newsweep][1]
currentz=stimhistory[newsweep][4]
wavenom=stimhistory[newsweep][0]
Commentz=stimhistory[newsweep][7]
thyme=stimhistory[newsweep][8]
newsweepstr=num2str(newsweep)

TextBox/C/N=text3/y=15
TextBox/C/N=text2/y=15
TextBox/C/N=text4/y=25
TextBox/C/N=text5/y=37.5

TextBox/C/N=text6/f=0/y=55 wavenom
if (cmpstr(wavenom,"StepPulse_DAC")!=0)
    TextBox/C/N=text7/f=0/y=67.5 Gainz
    TextBox/C/N=text8/f=0 ""
else
    TextBox/C/N=text8/f=0/y=67.5 Currentz
    TextBox/C/N=text7/f=0 ""
endif
TextBox/C/N=text9/f=0/y=80 thyme
TextBox/C/N=text10/f=0/y=92.5 newsweepstr
end

function StackButton(ctrlName) : ButtonControl
    string ctrlName
    execute "StackedPlots()"
end

menu "Chan"
    "Boosting", Boostin()
end

function Boostin()
    string list, areawno, holdIno, boostpeakno
    string theWave, adtheWave, sweeplist, sweeptime
    variable/g boostexecution
    variable index=0, abbrev1, abbrev2, baseline
    prompt list, "Enter sweep numbers as ranges, or separated by commas"
    doprompt "Boosting", list
    if (V_Flag)
        return -1
    endif
    print boostexecution
    do
        if (index == 0)                                // is this the first wave?
            print itemsinlist(list, ",")
            make/o/N=(itemsinlist(list, ",")) areaw          // create area wave

```

```

        make/o/N=(itemsinlist(list, ",")) holdI           // create holding current wave
        make/o/N=(itemsinlist(list, ",")) boostpeak       // create peak wave
    endif
    theWave = StringFromList (index, list, ",")
    for (;stringmatch (theWave, "*_*") == 1;) // for loop b/c possibility of multiple ranges
        sscanf theWave, "%f-%f", abbrev1, abbrev2 // assign start and stop of range
    do
        list = list + "," + num2str(abbrev1) // add individual sweeps of range to list
        abbrev1 += 1
        while (abbrev1 <= abbrev2) // until last sweep in range
            list = removefromlist (theWave, list, ",") // remove range from list
            print list
            theWave = StringFromList (index, list, ",") // reassign theWave
            print theWave
            redimension/n=(itemsinlist(list, ",")) areaw // adjust # points in waves
            redimension/n=(itemsinlist(list, ",")) holdI // adjust # points in waves
            redimension/n=(itemsinlist(list, ",")) boostpeak
        endfor
        adtheWave = "ad1_" + theWave
        if (strlen(theWave) == 0)
            break // ran out of waves
        endif

        wavestats/q/r=(0,60) $adtheWave
        baseline = v_avg
        wavestats/q $adtheWave
        boostpeak[index] = v_max - baseline
        duplicate/o $adtheWave, tempwave
        tempwave-=baseline
        areaw[index] = area(tempwave, 60, 400)
        holdI[index] = v_avg
        index += 1 // next wave
    while (1)
        areawno = "areaw" + num2str(boostexecution)
        print areawno
        holdIno = "holdI" + num2str(boostexecution)
        duplicate/o areaw $areawno
        duplicate/o holdI $holdIno
        display $areawno vs $holdIno
        ModifyGraph mode=3,marker=19 // scatterplot
        K0 = 0;K1 = 5783.8;K2 = -.04
        Curvefit/g exp $areawno /x=$holdIno /d

        list = Sortlist(list, ",", 2) // sort sweep list
        sprintf sweeplist, "Sweeps %s", list // for textbox
        theWave = StringFromList (0, list, ",") // determine first sweep to record time
        TextBox/C/N=text1/F=0/A=MT/E=0 num2str(k2)
        wave/t stimhistory = stimhistory
        sweeptime = stimhistory [(str2num(theWave))][8] // time of first sweep
        TextBox/C/N=text4/Y=15.00/F=0/A=MT/E=0 sweeptime // time

```

```

Label bottom "mV"
Label left "EPSP Integral"
ModifyGraph gfSize=7
ModifyGraph lblMargin(left)=4
ModifyGraph lblMargin(bottom)=6

boostpeakno = "boostpeak" + num2str(boostexecution)
duplicate/o boostpeak $boostpeakno
display $boostpeakno vs $holdIno
ModifyGraph mode=3,marker=19      // scatterplot
K0 = 0;K1 = 9.04;K2 = -.0059
Curvefit/g exp $boostpeakno /x=$holdIno /d
TextBox/C/N=text1/F=0/A=MT/E=0 num2str(k2)
TextBox/C/N=text4/Y=15.00/F=0/A=MT/E=0 sweeptime      // time
Label bottom "mV"
Label left "Peak"
ModifyGraph gfSize=7
ModifyGraph lblMargin(left)=4
ModifyGraph lblMargin(bottom)=6
boostexecution+=1
end

```

## BIBLIOGRAPHY

- Allen PB, Hvalby O, Jensen V, Errington ML, Ramsay M, Chaudhry FA, Bliss TV, Storm-Mathisen J, Morris RG, Andersen P, Greengard P. Protein phosphatase-1 regulation in the induction of long-term potentiation: heterogeneous molecular mechanisms. *J. Neurosci.* (2000) **20**:3537-3543.
- Amaral DG, Ishizuka N, Claiborne B. Neurons, numbers and the hippocampal network. *Prog. Brain Res.* (1990) **83**:1-11.
- Ambrogini P, Lattanzi D, Ciuffoli S, Agostini D, Bertini L, Stocchi V, Santi S, Cuppini R. Morpho-functional characterization of neuronal cells at different stages of maturation in granule cell layer of adult rat dentate gyrus. *Brain Res.* (2004) **1017**:21-31.
- Barbas H, Gustafson EL, Greengard P. Comparison of the immunocytochemical localization of DARPP-32 and I-1 in the amygdala and hippocampus of the rhesus monkey. *J. Comp. Neurol.* (1993) **334**:1-18.
- Baumann K, Mandelkow EM, Biernat J, Piwnica-Worms H, Mandelkow E. Abnormal Alzheimer-like phosphorylation of tau-protein by cyclin-dependent kinases cdk2 and cdk5. *FEBS Lett.* (1993) **336**:417-424.
- Bayer SA, Brunner RL, Hine R, Altman J. Behavioural effects of interference with the postnatal acquisition of hippocampal granule cells. *Nature: New biology* (1973) **242**:222-224.
- Bernath S. Calcium-independent release of amino acid neurotransmitters: fact or artifact? *Prog. Neurobiol.* (1992) **38**:57-91.
- Beullens M, Van Eynde A, Vulsteke V, Connor J, Shenolikar S, Stalmans W, Bollen M. Molecular determinants of nuclear protein phosphatase-1 regulation by NIPP-1. *J. Biol. Chem.* (1999) **274**:14053-14061.
- Bialojan C, Takai A. Inhibitory effect of a marine-sponge toxin, okadaic acid, on protein phosphatases. Specificity and kinetics. *Biochem. J.* (1988) **256**:283-290.
- Bibb JA, Chen J, Taylor JR, Svenningsson P, Nishi A, Snyder GL, Yan Z, Sagawa ZK, Ouimet CC, Nairn AC, Nestler EJ, Greengard P. Effects of

chronic exposure to cocaine are regulated by the neuronal protein Cdk5. *Nature* (2001a) **410**:376-380.

Bibb JA, da Cruz e Silva EF. Identification of posttranslational modification sites by site-directed mutagenesis. In: Hemmings, HC, Jr., editor. *Regulatory protein modification: techniques and protocols*. Totowa, N. J.: Humana Press (1997), p 275-307.

Bibb JA, Nishi A, O'Callaghan JP, Ule J, Lan M, Snyder GL, Horiuchi A, Saito T, Hisanaga S, Czernik AJ, Nairn AC, Greengard P. Phosphorylation of protein phosphatase inhibitor-1 by Cdk5. *J. Biol. Chem.* (2001b) **276**:14490-14497.

Bibb JA, Snyder GL, Nishi A, Yan Z, Meijer L, Fienberg AA, Tsai LH, Kwon YT, Girault JA, Czernik AJ, Haganir RL, Hemmings HC, Jr., Nairn AC, Greengard P. Phosphorylation of DARPP-32 by Cdk5 modulates dopamine signalling in neurons. *Nature* (1999) **402**:669-671.

Bito H, Deisseroth K, Tsien RW. CREB phosphorylation and dephosphorylation: a  $\text{Ca}^{2+}$ - and stimulus duration-dependent switch for hippocampal gene expression. *Cell* (1996) **87**:1203-1214.

Blank T, Nijholt I, Teichert U, Kugler H, Behrsing H, Fienberg A, Greengard P, Spiess J. The phosphoprotein DARPP-32 mediates cAMP-dependent potentiation of striatal N-methyl-D-aspartate responses. *Proc. Natl Acad. Sci. USA* (1997) **94**:14859-14864.

Blitzer RD, Connor JH, Brown GP, Wong T, Shenolikar S, Iyengar R, Landau EM. Gating of CaMKII by cAMP-regulated protein phosphatase activity during LTP. *Science* (1998) **280**:1940-1942.

Blitzer RD, Wong T, Nouranifar R, Iyengar R, Landau EM. Postsynaptic cAMP pathway gates early LTP in hippocampal CA1 region. *Neuron* (1995) **15**:1403-1414.

Bollen M. Combinatorial control of protein phosphatase-1. *Trends Biochem. Sci.* (2001) **26**:426-431.

Brown GP, Blitzer RD, Connor JH, Wong T, Shenolikar S, Iyengar R, Landau EM. Long-term potentiation induced by theta frequency stimulation is regulated by a protein phosphatase-1-operated gate. *J. Neurosci.* (2000) **20**:7880-7887.

- Brown M, Jacobs T, Eickholt B, Ferrari G, Teo M, Monfries C, Qi RZ, Leung T, Lim L, Hall C. Alpha2-chimaerin, cyclin-dependent Kinase 5/p35, and its target collapsin response mediator protein-2 are essential components in semaphorin 3A-induced growth-cone collapse. *J. Neurosci.* (2004) **24**:8994-9004.
- Buraei Z, Anghelescu M, Elmslie KS. Slowed N-type calcium channel (CaV2.2) deactivation by the cyclin-dependent kinase inhibitor roscovitine. *Biophys. J.* (2005) **89**:1681-1691.
- Buraei Z, Schofield G, Elmslie KS. Roscovitine differentially affects CaV2 and Kv channels by binding to the open state. *Neuropharmacology* (2007) **52**:883-894.
- Campbell DG, Morrice NA. Identification of protein phosphorylation sites by a combination of mass spectrometry and solid phase Edman sequencing. *J. Biomol. Tech.* (2002) **13**:119-130.
- Cepeda C, Levine MS. Where do you think you are going? The NMDA-D1 receptor trap. *Sci STKE* (2006) **2006**:pe20.
- Chae T, Kwon YT, Bronson R, Dikkes P, Li E, Tsai LH. Mice lacking p35, a neuronal specific activator of Cdk5, display cortical lamination defects, seizures, and adult lethality. *Neuron* (1997) **18**:29-42.
- Chenard BL, Menniti FS. Antagonists selective for NMDA receptors containing the NR2B subunit. *Curr. Pharm. Des.* (1999) **5**:381-404.
- Cheng K, Li Z, Fu WY, Wang JH, Fu AK, Ip NY. Pctaire1 interacts with p35 and is a novel substrate for Cdk5/p35. *J. Biol. Chem.* (2002) **277**:31988-31993.
- Cheung ZH, Chin WH, Chen Y, Ng YP, Ip NY. Cdk5 Is Involved in BDNF-Stimulated Dendritic Growth in Hippocampal Neurons. *PLoS biology* (2007) **5**:e63.
- Chyan CL, Tang TC, Chen Y, Liu H, Lin FM, Liu CK, Hsieh MJ, Shiao MS, Huang H, Lin TH. Letter to the editor: backbone 1H, 15N, and 13C resonance assignments of inhibitor-1--a protein inhibitor of protein phosphatase-1. *J. Biomol. NMR* (2001) **21**:287-288.
- Cohen P. The regulation of protein function by multisite phosphorylation--a 25 year update. *Trends Biochem. Sci.* (2000) **25**:596-601.

- Cohen P. The structure and regulation of protein phosphatases. *Annu. Rev. Biochem.* (1989) **58**:453-508.
- Cohen P, Alemany S, Hemmings BA, Resink TJ, Stralfors P, Tung HY. Protein phosphatase-1 and protein phosphatase-2A from rabbit skeletal muscle. *Methods Enzymol.* (1988) **159**:390-408.
- Cohen PT. Protein phosphatase 1--targeted in many directions. *J. Cell Sci.* (2002) **115**:241-256.
- Connor JH, Weiser DC, Li S, Hallenbeck JM, Shenolikar S. Growth arrest and DNA damage-inducible protein GADD34 assembles a novel signaling complex containing protein phosphatase 1 and inhibitor 1. *Mol. Cell. Biol.* (2001) **21**:6841-6850.
- Cooper DC, Moore SJ, Staff NP, Spruston N. Psychostimulant-induced plasticity of intrinsic neuronal excitability in ventral subiculum. *J. Neurosci.* (2003) **23**:9937-9946.
- Czernik AJ, Mathers J, Mische SM. Phosphorylation state-specific antibodies. In: Hemmings, HC, Jr., editor. *Regulatory protein modification: techniques and protocols*. Totowa, N.J.: Humana Press (1997), p 219-250.
- Dhavan R, Tsai LH. A decade of CDK5. *Nature reviews* (2001) **2**:749-759.
- Dolphin AC. The effect of phosphatase inhibitors and agents increasing cyclic-AMP-dependent phosphorylation on calcium channel currents in cultured rat dorsal root ganglion neurones: interaction with the effect of G protein activation. *Pflugers Arch.* (1992) **421**:138-145.
- Dorofeeva NA, Tikhonov DB, Barygin OI, Tikhonova TB, Salnikov YI, Magazanik LG. Action of extracellular divalent cations on native alpha-amino-3-hydroxy-5-methylisoxazole-4-propionate (AMPA) receptors. *J. Neurochem.* (2005) **95**:1704-1712.
- Eisch AJ, Harburg GC. Opiates, psychostimulants, and adult hippocampal neurogenesis: Insights for addiction and stem cell biology. *Hippocampus* (2006) **16**:271-286.
- El-Armouche A, Pamminer T, Ditz D, Zolk O, Eschenhagen T. Decreased protein and phosphorylation level of the protein phosphatase inhibitor-1 in failing human hearts. *Cardiovasc. Res.* (2004) **61**:87-93.



- El-Armouche A, Rau T, Zolk O, Ditz D, Pamminger T, Zimmermann WH, Jackel E, Harding SE, Boknik P, Neumann J, Eschenhagen T. Evidence for protein phosphatase inhibitor-1 playing an amplifier role in beta-adrenergic signaling in cardiac myocytes. *FASEB J.* (2003) **17**:437-439.
- Elbrecht A, DiRenzo J, Smith RG, Shenolikar S. Molecular cloning of protein phosphatase inhibitor-1 and its expression in rat and rabbit tissues. *J. Biol. Chem.* (1990) **265**:13415-13418.
- Emerich DF, Walsh TJ. Hyperactivity following intradentate injection of colchicine: a role for dopamine systems in the nucleus accumbens. *Pharmacol. Biochem. Behav.* (1990) **37**:149-154.
- Endo S, Zhou X, Connor J, Wang B, Shenolikar S. Multiple structural elements define the specificity of recombinant human inhibitor-1 as a protein phosphatase-1 inhibitor. *Biochemistry (Mosc).* (1996) **35**:5220-5228.
- Fischer A, Sananbenesi F, Schrick C, Spiess J, Radulovic J. Cyclin-dependent kinase 5 is required for associative learning. *J. Neurosci.* (2002) **22**:3700-3707.
- Fischer A, Sananbenesi F, Schrick C, Spiess J, Radulovic J. Regulation of contextual fear conditioning by baseline and inducible septo-hippocampal cyclin-dependent kinase 5. *Neuropharmacology* (2003) **44**:1089-1099.
- Fletcher AI, Shuang R, Giovannucci DR, Zhang L, Bittner MA, Stuenkel EL. Regulation of exocytosis by cyclin-dependent kinase 5 via phosphorylation of Munc18. *J. Biol. Chem.* (1999) **274**:4027-4035.
- Floyd SR, Porro EB, Slepnev VI, Ochoa GC, Tsai LH, De Camilli P. Amphiphysin 1 binds the cyclin-dependent kinase (cdk) 5 regulatory subunit p35 and is phosphorylated by cdk5 and cdc2. *J. Biol. Chem.* (2001) **276**:8104-8110.
- Foulkes JG, Strada SJ, Henderson PJ, Cohen P. A kinetic analysis of the effects of inhibitor-1 and inhibitor-2 on the activity of protein phosphatase-1. *Eur. J. Biochem.* (1983) **132**:309-313.
- Fricke RA, Prince DA. Electrophysiology of dentate gyrus granule cells. *J. Neurophysiol.* (1984) **51**:195-209.
- Fu AK, Fu WY, Ng AK, Chien WW, Ng YP, Wang JH, Ip NY. Cyclin-dependent kinase 5 phosphorylates signal transducer and activator of transcription 3

- and regulates its transcriptional activity. *Proc. Natl Acad. Sci. USA* (2004) **101**:6728-6733.
- Fu WY, Chen Y, Sahin M, Zhao XS, Shi L, Bikoff JB, Lai KO, Yung WH, Fu AK, Greenberg ME, Ip NY. Cdk5 regulates EphA4-mediated dendritic spine retraction through an ephexin1-dependent mechanism. *Nat. Neurosci.* (2007) **10**:67-76.
- Fu WY, Wang JH, Ip NY. Expression of Cdk5 and its activators in NT2 cells during neuronal differentiation. *J. Neurochem.* (2002) **81**:646-654.
- Gavazzo P, Mazzolini M, Tedesco M, Marchetti C. Nickel differentially affects NMDA receptor channels in developing cultured rat neurons. *Brain Res.* (2006) **1078**:71-79.
- Genoux D, Haditsch U, Knobloch M, Michalon A, Storm D, Mansuy IM. Protein phosphatase 1 is a molecular constraint on learning and memory. *Nature* (2002) **418**:970-975.
- Gillardon F, Schratzenholz A, Sommer B. Investigating the neuroprotective mechanism of action of a CDK5 inhibitor by phosphoproteome analysis. *J. Cell. Biochem.* (2005a) **95**:817-826.
- Gillardon F, Steinlein P, Burger E, Hildebrandt T, Gerner C. Phosphoproteome and transcriptome analysis of the neuronal response to a CDK5 inhibitor. *Proteomics* (2005b) **5**:1299-1307.
- Gonzalez-Burgos G, Barrionuevo G. Voltage-gated sodium channels shape subthreshold EPSPs in layer 5 pyramidal neurons from rat prefrontal cortex. *J. Neurophysiol.* (2001) **86**:1671-1684.
- Graham ME, Ruma-Haynes P, Capes-Davis AG, Dunn JM, Tan TC, Valova VA, Robinson PJ, Jeffrey PL. Multisite phosphorylation of doublecortin by cyclin-dependent kinase 5. *Biochem. J.* (2004) **381**:471-481.
- Gupta RC, Mishra S, Rastogi S, Imai M, Habib O, Sabbah HN. Cardiac SR-coupled PP1 activity and expression are increased and inhibitor 1 protein expression is decreased in failing hearts. *Am. J. Physiol. Heart Circ. Physiol.* (2003) **285**:H2373-2381.
- Gupta RC, Mishra S, Yang XP, Sabbah HN. Reduced inhibitor 1 and 2 activity is associated with increased protein phosphatase type 1 activity in left

- ventricular myocardium of one-kidney, one-clip hypertensive rats. *Mol. Cell. Biochem.* (2005) **269**:49-57.
- Gupta RC, Neumann J, Watanabe AM, Lesch M, Sabbah HN. Evidence for presence and hormonal regulation of protein phosphatase inhibitor-1 in ventricular cardiomyocyte. *Am. J. Physiol.* (1996) **270**:H1159-1164.
- Gustafson EL, Girault JA, Hemmings HC, Jr., Nairn AC, Greengard P. Immunocytochemical localization of phosphatase inhibitor-1 in rat brain. *J Comp Neurol* (1991) **310**:170-188.
- Hagiwara M, Alberts A, Brindle P, Meinkoth J, Feramisco J, Deng T, Karin M, Shenolikar S, Montminy M. Transcriptional attenuation following cAMP induction requires PP-1-mediated dephosphorylation of CREB. *Cell* (1992) **70**:105-113.
- Harada T, Morooka T, Ogawa S, Nishida E. ERK induces p35, a neuron-specific activator of Cdk5, through induction of Egr1. *Nat. Cell Biol.* (2001) **3**:453-459.
- Harburg GC, Hall FS, Harrist AV, Sora I, Uhl GR, Eisch AJ. Knockout of the mu opioid receptor enhances the survival of adult-generated hippocampal granule cell neurons. *Neuroscience* (2007) **144**:77-87.
- Hastings NB, Gould E. Rapid extension of axons into the CA3 region by adult-generated granule cells. *J. Comp. Neurol.* (1999) **413**:146-154.
- Hawasli AH, Benavides DR, Nguyen C, Kansy JW, Hayashi K, Chambon P, Greengard P, Powell CM, Cooper DC, Bibb JA. Cyclin-dependent kinase 5 governs learning and synaptic plasticity via regulation of NMDA receptor degradation. *Nat. Neurosci.* (manuscript submitted).
- Hayashi K, Pan Y, Shu H, Ohshima T, Kansy JW, White CL, 3rd, Tamminga CA, Sobel A, Curmi PA, Mikoshiba K, Bibb JA. Phosphorylation of the tubulin-binding protein, stathmin, by Cdk5 and MAP kinases in the brain. *J. Neurochem.* (2006) **99**:237-250.
- Hemmings HC, Jr., Greengard P. DARPP-32, a dopamine- and adenosine 3':5'-monophosphate-regulated phosphoprotein: regional, tissue, and phylogenetic distribution. *J. Neurosci.* (1986) **6**:1469-1481.
- Hemmings HC, Jr., Nairn AC, Greengard P. DARPP-32, a dopamine- and adenosine 3':5'-monophosphate-regulated neuronal phosphoprotein. II.

- Comparison of the kinetics of phosphorylation of DARPP-32 and phosphatase inhibitor 1. *J. Biol. Chem.* (1984) **259**:14491-14497.
- Henze DA, Wittner L, Buzsaki G. Single granule cells reliably discharge targets in the hippocampal CA3 network in vivo. *Nat. Neurosci.* (2002) **5**:790-795.
- Herzig S, Neumann J. Effects of serine/threonine protein phosphatases on ion channels in excitable membranes. *Physiol. Rev.* (2000) **80**:173-210.
- Hisanaga S, Saito T. The regulation of cyclin-dependent kinase 5 activity through the metabolism of p35 or p39 Cdk5 activator. *Neurosignals* (2003) **12**:221-229.
- Holmberg CI, Tran SE, Eriksson JE, Sistonen L. Multisite phosphorylation provides sophisticated regulation of transcription factors. *Trends Biochem. Sci.* (2002) **27**:619-627.
- Hooks MS, Kalivas PW. The role of mesoaccumbens--pallidal circuitry in novelty-induced behavioral activation. *Neuroscience* (1995) **64**:587-597.
- Huang FL, Glinsmann WH. Separation and characterization of two phosphorylase phosphatase inhibitors from rabbit skeletal muscle. *Eur. J. Biochem.* (1976) **70**:419-426.
- Ingebritsen TS, Cohen P. Protein phosphatases: properties and role in cellular regulation. *Science* (1983) **221**:331-338.
- Inoue M, Imanaga I. Phosphatase is responsible for run down, and probably G protein-mediated inhibition of inwardly rectifying K<sup>+</sup> currents in guinea pig chromaffin cells. *J. Gen. Physiol.* (1995) **105**:249-266.
- Kaczmarek LK, Jennings KR, Strumwasser F, Nairn AC, Walter U, Wilson FD, Greengard P. Microinjection of catalytic subunit of cyclic AMP-dependent protein kinase enhances calcium action potentials of bag cell neurons in cell culture. *Proc. Natl. Acad. Sci. U.S.A.* (1980) **77**:7487-7491.
- Kamei H, Saito T, Ozawa M, Fujita Y, Asada A, Bibb JA, Saido TC, Sorimachi H, Hisanaga S. Suppression of calpain-dependent cleavage of the CDK5 activator p35 to p25 by site-specific phosphorylation. *J. Biol. Chem.* (2007) **282**:1687-1694.

- Kansy JW, Daubner SC, Nishi A, Sotogaku N, Lloyd MD, Nguyen C, Lu L, Haycock JW, Hope BT, Fitzpatrick PF, Bibb JA. Identification of tyrosine hydroxylase as a physiological substrate for Cdk5. *J. Neurochem.* (2004) **91**:374-384.
- Kerokoski P, Suuronen T, Salminen A, Soininen H, Pirttilä T. Both N-methyl-D-aspartate (NMDA) and non-NMDA receptors mediate glutamate-induced cleavage of the cyclin-dependent kinase 5 (cdk5) activator p35 in cultured rat hippocampal neurons. *Neurosci. Lett.* (2004) **368**:181-185.
- Kerokoski P, Suuronen T, Salminen A, Soininen H, Pirttilä T. Influence of phosphorylation of p35, an activator of cyclin-dependent kinase 5 (cdk5), on the proteolysis of p35. *Brain Res. Mol. Brain Res.* (2002) **106**:50-56.
- Kesavapany S, Lau KF, McLoughlin DM, Brownlee J, Ackerley S, Leigh PN, Shaw CE, Miller CC. p35/cdk5 binds and phosphorylates beta-catenin and regulates beta-catenin/presenilin-1 interaction. *Eur. J. Neurosci.* (2001) **13**:241-247.
- Keshvara L, Magdaleno S, Benhayon D, Curran T. Cyclin-dependent kinase 5 phosphorylates disabled 1 independently of Reelin signaling. *J. Neurosci.* (2002) **22**:4869-4877.
- Kesner RP, Lee I, Gilbert P. A behavioral assessment of hippocampal function based on a subregional analysis. *Rev. Neurosci.* (2004) **15**:333-351.
- Ko J, Humbert S, Bronson RT, Takahashi S, Kulkarni AB, Li E, Tsai LH. p35 and p39 are essential for cyclin-dependent kinase 5 function during neurodevelopment. *J. Neurosci.* (2001) **21**:6758-6771.
- Koumi S, Wasserstrom JA, Ten Eick RE. Beta-adrenergic and cholinergic modulation of inward rectifier K<sup>+</sup> channel function and phosphorylation in guinea-pig ventricle. *The Journal of physiology* (1995) **486** ( Pt 3):661-678.
- Kusakawa G, Saito T, Onuki R, Ishiguro K, Kishimoto T, Hisanaga S. Calpain-dependent proteolytic cleavage of the p35 cyclin-dependent kinase 5 activator to p25. *J. Biol. Chem.* (2000) **275**:17166-17172.
- Kwiatkowski AP, Shell DJ, King MM. The role of autophosphorylation in activation of the type II calmodulin-dependent protein kinase. *J. Biol. Chem.* (1988) **263**:6484-6486.

- Kwon YG, Huang HB, Desdouits F, Girault JA, Greengard P, Nairn AC. Characterization of the interaction between DARPP-32 and protein phosphatase 1 (PP-1): DARPP-32 peptides antagonize the interaction of PP-1 with binding proteins. *Proc. Natl Acad. Sci. USA* (1997) **94**:3536-3541.
- Kwon YT, Gupta A, Zhou Y, Nikolic M, Tsai LH. Regulation of N-cadherin-mediated adhesion by the p35-Cdk5 kinase. *Curr. Biol.* (2000) **10**:363-372.
- Lagace DC, Fischer SJ, Eisch AJ. Gender and endogenous levels of estradiol do not influence adult hippocampal neurogenesis in mice. *Hippocampus* (2007) **17**:175-180.
- Lee I, Hunsaker MR, Kesner RP. The role of hippocampal subregions in detecting spatial novelty. *Behav. Neurosci.* (2005) **119**:145-153.
- Lee MS, Kwon YT, Li M, Peng J, Friedlander RM, Tsai LH. Neurotoxicity induces cleavage of p35 to p25 by calpain. *Nature* (2000) **405**:360-364.
- Lemaire V, Aourousseau C, Le Moal M, Abrous DN. Behavioural trait of reactivity to novelty is related to hippocampal neurogenesis. *Eur. J. Neurosci.* (1999) **11**:4006-4014.
- Leuner B, Gould E, Shors TJ. Is there a link between adult neurogenesis and learning? *Hippocampus* (2006) **16**:216-224.
- Leussis MP, Bolivar VJ. Habituation in rodents: a review of behavior, neurobiology, and genetics. *Neurosci. Biobehav. Rev.* (2006) **30**:1045-1064.
- Lew J, Beaudette K, Litwin CM, Wang JH. Purification and characterization of a novel proline-directed protein kinase from bovine brain. *J. Biol. Chem.* (1992) **267**:13383-13390.
- Lew J, Huang QQ, Qi Z, Winkfein RJ, Aebersold R, Hunt T, Wang JH. A brain-specific activator of cyclin-dependent kinase 5. *Nature* (1994) **371**:423-426.
- Li BS, Sun MK, Zhang L, Takahashi S, Ma W, Vinade L, Kulkarni AB, Brady RO, Pant HC. Regulation of NMDA receptors by cyclin-dependent kinase-5. *Proc. Natl Acad. Sci. USA* (2001) **98**:12742-12747.

- Li BS, Zhang L, Takahashi S, Ma W, Jaffe H, Kulkarni AB, Pant HC. Cyclin-dependent kinase 5 prevents neuronal apoptosis by negative regulation of c-Jun N-terminal kinase 3. *EMBO J.* (2002) **21**:324-333.
- Li Z, David G, Hung KW, DePinho RA, Fu AK, Ip NY. Cdk5/p35 phosphorylates mSds3 and regulates mSds3-mediated repression of transcription. *J. Biol. Chem.* (2004) **279**:54438-54444.
- Lilja L, Meister B, Berggren PO, Bark C. DARPP-32 and inhibitor-1 are expressed in pancreatic beta-cells. *Biochem. Biophys. Res. Commun.* (2005) **329**:673-677.
- Lilja L, Yang SN, Webb DL, Juntti-Berggren L, Berggren PO, Bark C. Cyclin-dependent kinase 5 promotes insulin exocytosis. *J. Biol. Chem.* (2001) **276**:34199-34205.
- Lisman J. A mechanism for the Hebb and the anti-Hebb processes underlying learning and memory. *Proc. Natl Acad. Sci. USA* (1989) **86**:9574-9578.
- Lisman JE, Zhabotinsky AM. A model of synaptic memory: a CaMKII/PP1 switch that potentiates transmission by organizing an AMPA receptor anchoring assembly. *Neuron* (2001) **31**:191-201.
- Liu F, Ma XH, Ule J, Bibb JA, Nishi A, DeMaggio AJ, Yan Z, Nairn AC, Greengard P. Regulation of cyclin-dependent kinase 5 and casein kinase 1 by metabotropic glutamate receptors. *Proc. Natl Acad. Sci. USA* (2001) **98**:11062-11068.
- Liu J, Brautigan DL. Glycogen synthase association with the striated muscle glycogen-targeting subunit of protein phosphatase-1. Synthase activation involves scaffolding regulated by beta-adrenergic signaling. *J. Biol. Chem.* (2000) **275**:26074-26081.
- Liu XY, Chu XP, Mao LM, Wang M, Lan HX, Li MH, Zhang GC, Parelkar NK, Fibuch EE, Haines M, Neve KA, Liu F, Xiong ZG, Wang JQ. Modulation of D2R-NR2B interactions in response to cocaine. *Neuron* (2006) **52**:897-909.
- Liu YB, Lio PA, Pasternak JF, Trommer BL. Developmental changes in membrane properties and postsynaptic currents of granule cells in rat dentate gyrus. *J. Neurophysiol.* (1996) **76**:1074-1088.

- Lowenstein PR, Shering AF, MacDougall LK, Cohen P. Immunolocalisation of protein phosphatase inhibitor-1 in the cerebral cortex of the rat, cat and ferret. *Brain Res.* (1995) **676**:80-92.
- Lubke J, Frotscher M, Spruston N. Specialized electrophysiological properties of anatomically identified neurons in the hilar region of the rat fascia dentata. *J. Neurophysiol.* (1998) **79**:1518-1534.
- MacDougall LK, Campbell DG, Hubbard MJ, Cohen P. Partial structure and hormonal regulation of rabbit liver inhibitor-1; distribution of inhibitor-1 and inhibitor-2 in rabbit and rat tissues. *Biochim. Biophys. Acta* (1989) **1010**:218-226.
- Manfroid I, Martial JA, Muller M. Inhibition of protein phosphatase PP1 in GH3B6, but not in GH3 cells, activates the MEK/ERK/c-fos pathway and the human prolactin promoter, involving the coactivator CPB/p300. *Mol. Endocrinol.* (2001) **15**:625-637.
- Markakis EA, Gage FH. Adult-generated neurons in the dentate gyrus send axonal projections to field CA3 and are surrounded by synaptic vesicles. *J. Comp. Neurol.* (1999) **406**:449-460.
- Matsubara M, Kusubata M, Ishiguro K, Uchida T, Titani K, Taniguchi H. Site-specific phosphorylation of synapsin I by mitogen-activated protein kinase and Cdk5 and its effects on physiological functions. *J. Biol. Chem.* (1996) **271**:21108-21113.
- Mattia D, Kawasaki H, Avoli M. Repetitive firing and oscillatory activity of pyramidal-like bursting neurons in the rat subiculum. *Exp. Brain Res.* (1997) **114**:507-517.
- McAvoy T, Allen PB, Obaishi H, Nakanishi H, Takai Y, Greengard P, Nairn AC, Hemmings HC, Jr. Regulation of neurabin I interaction with protein phosphatase 1 by phosphorylation. *Biochemistry (Mosc.)*. (1999) **38**:12943-12949.
- Meijer L, Borgne A, Mulner O, Chong JP, Blow JJ, Inagaki N, Inagaki M, Delcros JG, Moulinoux JP. Biochemical and cellular effects of roscovitine, a potent and selective inhibitor of the cyclin-dependent kinases cdc2, cdk2 and cdk5. *Eur. J. Biochem.* (1997) **243**:527-536.



- Mitchell SN, Yee BK, Feldon J, Gray JA, Rawlins JN. Activation of the retrohippocampal region in the rat causes dopamine release in the nucleus accumbens: disruption by fornix section. *Eur. J. Pharmacol.* (2000) **407**:131-138.
- Mogenson GJ, Nielsen M. A study of the contribution of hippocampal-accumbens-subpallidal projections to locomotor activity. *Behav. Neural Biol.* (1984) **42**:38-51.
- Monyer H, Burnashev N, Laurie DJ, Sakmann B, Seeburg PH. Developmental and regional expression in the rat brain and functional properties of four NMDA receptors. *Neuron* (1994) **12**:529-540.
- Morabito MA, Sheng M, Tsai LH. Cyclin-dependent kinase 5 phosphorylates the N-terminal domain of the postsynaptic density protein PSD-95 in neurons. *J. Neurosci.* (2004) **24**:865-876.
- Morfini G, Szebenyi G, Brown H, Pant HC, Pigino G, DeBoer S, Beffert U, Brady ST. A novel CDK5-dependent pathway for regulating GSK3 activity and kinesin-driven motility in neurons. *EMBO J.* (2004) **23**:2235-2245.
- Morishita W, Connor JH, Xia H, Quinlan EM, Shenolikar S, Malenka RC. Regulation of synaptic strength by protein phosphatase 1. *Neuron* (2001) **32**:1133-1148.
- Moy LY, Tsai LH. Cyclin-dependent kinase 5 phosphorylates serine 31 of tyrosine hydroxylase and regulates its stability. *J. Biol. Chem.* (2004) **279**:54487-54493.
- Mulkey RM, Endo S, Shenolikar S, Malenka RC. Involvement of a calcineurin/inhibitor-1 phosphatase cascade in hippocampal long-term depression. *Nature* (1994) **369**:486-488.
- Nath R, Davis M, Probert AW, Kupina NC, Ren X, Schielke GP, Wang KK. Processing of cdk5 activator p35 to its truncated form (p25) by calpain in acutely injured neuronal cells. *Biochem. Biophys. Res. Commun.* (2000) **274**:16-21.
- Neumann J, Gupta RC, Schmitz W, Scholz H, Nairn AC, Watanabe AM. Evidence for isoproterenol-induced phosphorylation of phosphatase inhibitor-1 in the intact heart. *Circ. Res.* (1991) **69**:1450-1457.

- Nguyen C, Bibb JA. Cdk5 and the mystery of synaptic vesicle endocytosis. *J. Cell Biol.* (2003) **163**:697-699.
- Nguyen MD, Lariviere RC, Julien JP. Deregulation of Cdk5 in a mouse model of ALS: toxicity alleviated by perikaryal neurofilament inclusions. *Neuron* (2001) **30**:135-147.
- Niethammer M, Smith DS, Ayala R, Peng J, Ko J, Lee MS, Morabito M, Tsai LH. NUDEL is a novel Cdk5 substrate that associates with LIS1 and cytoplasmic dynein. *Neuron* (2000) **28**:697-711.
- Nimmo GA, Cohen P. The regulation of glycogen metabolism. Purification and characterisation of protein phosphatase inhibitor-1 from rabbit skeletal muscle. *Eur. J. Biochem.* (1978) **87**:341-351.
- Nishi A, Bibb JA, Matsuyama S, Hamada M, Higashi H, Nairn AC, Greengard P. Regulation of DARPP-32 dephosphorylation at PKA- and Cdk5-sites by NMDA and AMPA receptors: distinct roles of calcineurin and protein phosphatase-2A. *J. Neurochem.* (2002) **81**:832-841.
- Nishi A, Bibb JA, Snyder GL, Higashi H, Nairn AC, Greengard P. Amplification of dopaminergic signaling by a positive feedback loop. *Proc. Natl Acad. Sci. USA* (2000) **97**:12840-12845.
- Nishi A, Snyder GL, Nairn AC, Greengard P. Role of calcineurin and protein phosphatase-2A in the regulation of DARPP-32 dephosphorylation in neostriatal neurons. *J. Neurochem.* (1999) **72**:2015-2021.
- Ohshima T, Suzuki H, Morimura T, Ogawa M, Mikoshiba K. Modulation of Reelin signaling by Cyclin-dependent kinase 5. *Brain Res.* (2007) **1140**:84-95.
- Ohshima T, Ward JM, Huh CG, Longenecker G, Veeranna, Pant HC, Brady RO, Martin LJ, Kulkarni AB. Targeted disruption of the cyclin-dependent kinase 5 gene results in abnormal corticogenesis, neuronal pathology and perinatal death. *Proc. Natl Acad. Sci. USA* (1996) **93**:11173-11178.
- Ono K, Fozzard HA. Two phosphatase sites on the Ca<sup>2+</sup> channel affecting different kinetic functions. *The Journal of physiology* (1993) **470**:73-84.
- Paglini G, Pigino G, Kunda P, Morfini G, Maccioni R, Quiroga S, Ferreira A, Caceres A. Evidence for the participation of the neuron-specific CDK5

- activator P35 during laminin-enhanced axonal growth. *J. Neurosci.* (1998) **18**:9858-9869.
- Pareek TK, Keller J, Kesavapany S, Agarwal N, Kuner R, Pant HC, Iadarola MJ, Brady RO, Kulkarni AB. Cyclin-dependent kinase 5 modulates nociceptive signaling through direct phosphorylation of transient receptor potential vanilloid 1. *Proc. Natl Acad. Sci. USA* (2007) **104**:660-665.
- Patrick GN, Zhou P, Kwon YT, Howley PM, Tsai LH. p35, the neuronal-specific activator of cyclin-dependent kinase 5 (Cdk5) is degraded by the ubiquitin-proteasome pathway. *J. Biol. Chem.* (1998) **273**:24057-24064.
- Patrick GN, Zukerberg L, Nikolic M, de la Monte S, Dikkes P, Tsai LH. Conversion of p35 to p25 deregulates Cdk5 activity and promotes neurodegeneration. *Nature* (1999) **402**:615-622.
- Patzke H, Tsai LH. Calpain-mediated cleavage of the cyclin-dependent kinase-5 activator p39 to p29. *J. Biol. Chem.* (2002) **277**:8054-8060.
- Perchenet L, Clement-Chomienne O. External nickel blocks human Kv1.5 channels stably expressed in CHO cells. *J. Membr. Biol.* (2001) **183**:51-60.
- Piccolino M, Pignatelli A. Calcium-independent synaptic transmission: artifact or fact? *Trends Neurosci.* (1996) **19**:120-125.
- Pigino G, Paglini G, Ulloa L, Avila J, Caceres A. Analysis of the expression, distribution and function of cyclin dependent kinase 5 (cdk5) in developing cerebellar macroneurons. *J. Cell Sci.* (1997) **110** ( Pt 2):257-270.
- Pintor J, Gualix J, Miras-Portugal MT. Dinucleotide receptor modulation by protein kinases (protein kinases A and C) and protein phosphatases in rat brain synaptic terminals. *J. Neurochem.* (1997) **68**:2552-2557.
- Raber J, Rola R, LeFevour A, Morhardt D, Curley J, Mizumatsu S, VandenBerg SR, Fike JR. Radiation-induced cognitive impairments are associated with changes in indicators of hippocampal neurogenesis. *Radiat. Res.* (2004) **162**:39-47.
- Roberson ED, Sweatt JD. Transient activation of cyclic AMP-dependent protein kinase during hippocampal long-term potentiation. *J. Biol. Chem.* (1996) **271**:30436-30441.

- Rola R, Raber J, Rizk A, Otsuka S, VandenBerg SR, Morhardt DR, Fike JR. Radiation-induced impairment of hippocampal neurogenesis is associated with cognitive deficits in young mice. *Exp. Neurol.* (2004) **188**:316-330.
- Rosales JL, Lee KY. Extraneuronal roles of cyclin-dependent kinase 5. *Bioessays* (2006) **28**:1023-1034.
- Sahin B, Shu H, Fernandez J, El-Armouche A, Molkentin JD, Nairn AC, Bibb JA. Phosphorylation of protein phosphatase inhibitor-1 by protein kinase C. *J. Biol. Chem.* (2006) **281**:24322-24335.
- Saito T, Ishiguro K, Onuki R, Nagai Y, Kishimoto T, Hisanaga S. Okadaic acid-stimulated degradation of p35, an activator of CDK5, by proteasome in cultured neurons. *Biochem. Biophys. Res. Commun.* (1998) **252**:775-778.
- Saito T, Onuki R, Fujita Y, Kusakawa G, Ishiguro K, Bibb JA, Kishimoto T, Hisanaga S. Developmental regulation of the proteolysis of the p35 cyclin-dependent kinase 5 activator by phosphorylation. *J. Neurosci.* (2003) **23**:1189-1197.
- Sakagami H, Ebina K, Kondo H. Localization of phosphatase inhibitor-1 mRNA in the developing and adult rat brain in comparison with that of protein phosphatase-1 mRNAs. *Brain Res. Mol. Brain Res.* (1994) **25**:7-18.
- Sasaki Y, Cheng C, Uchida Y, Nakajima O, Ohshima T, Yagi T, Taniguchi M, Nakayama T, Kishida R, Kudo Y, Ohno S, Nakamura F, Goshima Y. Fyn and Cdk5 mediate semaphorin-3A signaling, which is involved in regulation of dendrite orientation in cerebral cortex. *Neuron* (2002) **35**:907-920.
- Sato K, Zhu YS, Saito T, Yotsumoto K, Asada A, Hasegawa M, Hisanaga S. Regulation of the membrane association and kinase activity of Cdk5-p35 by phosphorylation of p35. *J. Neurosci. Res.* (manuscript submitted).
- Schiffmann SN, Desdouits F, Menu R, Greengard P, Vincent JD, Vanderhaeghen JJ, Girault JA. Modulation of the voltage-gated sodium current in rat striatal neurons by DARPP-32, an inhibitor of protein phosphatase. *Eur. J. Neurosci.* (1998) **10**:1312-1320.
- Schnell SA, Staines WA, Wessendorf MW. Reduction of lipofuscin-like autofluorescence in fluorescently labeled tissue. *J. Histochem. Cytochem.* (1999) **47**:719-730.

- Sharma P, Sharma M, Amin ND, Albers RW, Pant HC. Regulation of cyclin-dependent kinase 5 catalytic activity by phosphorylation. *Proc. Natl Acad. Sci. USA* (1999) **96**:11156-11160.
- Sharma P, Veeranna, Sharma M, Amin ND, Sihag RK, Grant P, Ahn N, Kulkarni AB, Pant HC. Phosphorylation of MEK1 by cdk5/p35 down-regulates the mitogen-activated protein kinase pathway. *J. Biol. Chem.* (2002) **277**:528-534.
- Sheng S, Perry CJ, Kleyman TR. External nickel inhibits epithelial sodium channel by binding to histidine residues within the extracellular domains of alpha and gamma subunits and reducing channel open probability. *J. Biol. Chem.* (2002) **277**:50098-50111.
- Shenolikar S, Nairn AC. Protein phosphatases: recent progress. *Adv. Second Messenger Phosphoprotein Res.* (1991) **23**:1-121.
- Shors TJ, Miesegaes G, Beylin A, Zhao M, Rydel T, Gould E. Neurogenesis in the adult is involved in the formation of trace memories. *Nature* (2001) **410**:372-376.
- Shors TJ, Townsend DA, Zhao M, Kozorovitskiy Y, Gould E. Neurogenesis may relate to some but not all types of hippocampal-dependent learning. *Hippocampus* (2002) **12**:578-584.
- Shuang R, Zhang L, Fletcher A, Groblewski GE, Pevsner J, Stuenkel EL. Regulation of Munc-18/syntaxin 1A interaction by cyclin-dependent kinase 5 in nerve endings. *J. Biol. Chem.* (1998) **273**:4957-4966.
- Sikes S, Shenolikar S. Protein phosphatase inhibitor-1, an amplifier of cAMP signals. *Cellscience Reviews* (2005) **2**.
- Snyder GL, Fienberg AA, Huganir RL, Greengard P. A dopamine/D1 receptor/protein kinase A/dopamine- and cAMP-regulated phosphoprotein (Mr 32 kDa)/protein phosphatase-1 pathway regulates dephosphorylation of the NMDA receptor. *J. Neurosci.* (1998) **18**:10297-10303.
- Snyder GL, Girault JA, Chen JY, Czernik AJ, Kebabian JW, Nathanson JA, Greengard P. Phosphorylation of DARPP-32 and protein phosphatase inhibitor-1 in rat choroid plexus: regulation by factors other than dopamine. *J. Neurosci.* (1992) **12**:3071-3083.

- Snyder JS, Hong NS, McDonald RJ, Wojtowicz JM. A role for adult neurogenesis in spatial long-term memory. *Neuroscience* (2005) **130**:843-852.
- Spruston N, Johnston D. Perforated patch-clamp analysis of the passive membrane properties of three classes of hippocampal neurons. *J. Neurophysiol.* (1992) **67**:508-529.
- Staley KJ, Otis TS, Mody I. Membrane properties of dentate gyrus granule cells: comparison of sharp microelectrode and whole-cell recordings. *J. Neurophysiol.* (1992) **67**:1346-1358.
- Stanfield BB, Trice JE. Evidence that granule cells generated in the dentate gyrus of adult rats extend axonal projections. *Exp. Brain Res.* (1988) **72**:399-406.
- Staruschenko A, Dorofeeva NA, Bolshakov KV, Stockand JD. Subunit-dependent cadmium and nickel inhibition of acid-sensing ion channels. *J. Neurobiol.* (2006) **67**:97-107.
- Stockand J, Sultan A, Molony D, DuBose T, Jr., Sansom S. Interactions of cadmium and nickel with K channels of vascular smooth muscle. *Toxicol. Appl. Pharmacol.* (1993) **121**:30-35.
- Strack S, Choi S, Lovinger DM, Colbran RJ. Translocation of autophosphorylated calcium/calmodulin-dependent protein kinase II to the postsynaptic density. *J. Biol. Chem.* (1997) **272**:13467-13470.
- Stuart G, Sakmann B. Amplification of EPSPs by axosomatic sodium channels in neocortical pyramidal neurons. *Neuron* (1995) **15**:1065-1076.
- Takano K, Stanfield PR, Nakajima S, Nakajima Y. Protein kinase C-mediated inhibition of an inward rectifier potassium channel by substance P in nucleus basalis neurons. *Neuron* (1995) **14**:999-1008.
- Tan TC, Valova VA, Malladi CS, Graham ME, Berven LA, Jupp OJ, Hansra G, McClure SJ, Sarcevic B, Boadle RA, Larsen MR, Cousin MA, Robinson PJ. Cdk5 is essential for synaptic vesicle endocytosis. *Nat. Cell Biol.* (2003) **5**:701-710.
- Tanaka T, Serneo FF, Tseng HC, Kulkarni AB, Tsai LH, Gleeson JG. Cdk5 phosphorylation of doublecortin ser297 regulates its effect on neuronal migration. *Neuron* (2004) **41**:215-227.

- Tang D, Wang JH. Cyclin-dependent kinase 5 (Cdk5) and neuron-specific Cdk5 activators. *Prog. Cell Cycle Res.* (1996) **2**:205-216.
- Tang D, Yeung J, Lee KY, Matsushita M, Matsui H, Tomizawa K, Hatase O, Wang JH. An isoform of the neuronal cyclin-dependent kinase 5 (Cdk5) activator. *J. Biol. Chem.* (1995) **270**:26897-26903.
- Tomizawa K, Ohta J, Matsushita M, Moriwaki A, Li ST, Takei K, Matsui H. Cdk5/p35 regulates neurotransmitter release through phosphorylation and downregulation of P/Q-type voltage-dependent calcium channel activity. *J. Neurosci.* (2002) **22**:2590-2597.
- Tomizawa K, Sunada S, Lu YF, Oda Y, Kinuta M, Ohshima T, Saito T, Wei FY, Matsushita M, Li ST, Tsutsui K, Hisanaga S, Mikoshiba K, Takei K, Matsui H. Cophosphorylation of amphiphysin I and dynamin I by Cdk5 regulates clathrin-mediated endocytosis of synaptic vesicles. *J. Cell Biol.* (2003) **163**:813-824.
- Tsai LH, Delalle I, Caviness VS, Jr., Chae T, Harlow E. p35 is a neural-specific regulatory subunit of cyclin-dependent kinase 5. *Nature* (1994) **371**:419-423.
- van Praag H, Christie BR, Sejnowski TJ, Gage FH. Running enhances neurogenesis, learning, and long-term potentiation in mice. *Proc. Natl Acad. Sci. USA* (1999) **96**:13427-13431.
- Vander Mierde D, Scheuner D, Quintens R, Patel R, Song B, Tsukamoto K, Beullens M, Kaufman RJ, Bollen M, Schuit FC. Glucose activates a protein phosphatase-1-mediated signaling pathway to enhance overall translation in pancreatic beta-cells. *Endocrinology* (2007) **148**:609-617.
- Vicini S, Wang JF, Li JH, Zhu WJ, Wang YH, Luo JH, Wolfe BB, Grayson DR. Functional and pharmacological differences between recombinant N-methyl-D-aspartate receptors. *J. Neurophysiol.* (1998) **79**:555-566.
- Wang J, Liu S, Fu Y, Wang JH, Lu Y. Cdk5 activation induces hippocampal CA1 cell death by directly phosphorylating NMDA receptors. *Nat. Neurosci.* (2003) **6**:1039-1047.
- Wang LY, Orser BA, Brautigan DL, MacDonald JF. Regulation of NMDA receptors in cultured hippocampal neurons by protein phosphatases 1 and 2A. *Nature* (1994) **369**:230-232.

- Wang S, Scott BW, Wojtowicz JM. Heterogenous properties of dentate granule neurons in the adult rat. *J. Neurobiol.* (2000) **42**:248-257.
- Wei FY, Nagashima K, Ohshima T, Saheki Y, Lu YF, Matsushita M, Yamada Y, Mikoshiba K, Seino Y, Matsui H, Tomizawa K. Cdk5-dependent regulation of glucose-stimulated insulin secretion. *Nat. Med.* (2005a) **11**:1104-1108.
- Wei FY, Tomizawa K, Ohshima T, Asada A, Saito T, Nguyen C, Bibb JA, Ishiguro K, Kulkarni AB, Pant HC, Mikoshiba K, Matsui H, Hisanaga S. Control of cyclin-dependent kinase 5 (Cdk5) activity by glutamatergic regulation of p35 stability. *J. Neurochem.* (2005b) **93**:502-512.
- Weiser DC, Sikes S, Li S, Shenolikar S. The inhibitor-1 C terminus facilitates hormonal regulation of cellular protein phosphatase-1: functional implications for inhibitor-1 isoforms. *J. Biol. Chem.* (2004) **279**:48904-48914.
- Weishaupt JH, Kussmaul L, Grotzsch P, Heckel A, Rohde G, Romig H, Bahr M, Gillardon F. Inhibition of CDK5 is protective in necrotic and apoptotic paradigms of neuronal cell death and prevents mitochondrial dysfunction. *Mol. Cell. Neurosci.* (2003) **24**:489-502.
- Winder DG, Sweatt JD. Roles of serine/threonine phosphatases in hippocampal synaptic plasticity. *Nature Reviews Neuroscience* (2001) **2**:461-474.
- Woo NH, Abel T, Nguyen PV. Genetic and pharmacological demonstration of a role for cyclic AMP-dependent protein kinase-mediated suppression of protein phosphatases in gating the expression of late LTP. *Eur. J. Neurosci.* (2002) **16**:1871-1876.
- Xie Z, Sanada K, Samuels BA, Shih H, Tsai LH. Serine 732 phosphorylation of FAK by Cdk5 is important for microtubule organization, nuclear movement, and neuronal migration. *Cell* (2003) **114**:469-482.
- Yan Z, Chi P, Bibb JA, Ryan TA, Greengard P. Roscovitine: a novel regulator of P/Q-type calcium channels and transmitter release in central neurons. *The Journal of physiology* (2002) **540**:761-770.
- Yan Z, Hsieh-Wilson L, Feng J, Tomizawa K, Allen PB, Fienberg AA, Nairn AC, Greengard P. Protein phosphatase 1 modulation of neostriatal AMPA



- channels: regulation by DARPP-32 and spinophilin. *Nat. Neurosci.* (1999) **2**:13-17.
- Yang XJ. Multisite protein modification and intramolecular signaling. *Oncogene* (2005) **24**:1653-1662.
- Zachariou V, Benoit-Marand M, Allen PB, Ingrassia P, Fienberg AA, Gonon F, Greengard P, Picciotto MR. Reduction of cocaine place preference in mice lacking the protein phosphatase 1 inhibitors DARPP 32 or Inhibitor 1. *Biol. Psychiatry* (2002) **51**:612-620.
- Zhang J, Krishnamurthy PK, Johnson GV. Cdk5 phosphorylates p53 and regulates its activity. *J. Neurochem.* (2002) **81**:307-313.
- Zhao C, Teng EM, Summers RG, Jr., Ming GL, Gage FH. Distinct morphological stages of dentate granule neuron maturation in the adult mouse hippocampus. *J. Neurosci.* (2006) **26**:3-11.
- Zhen X, Goswami S, Abdali SA, Gil M, Bakshi K, Friedman E. Regulation of cyclin-dependent kinase 5 and calcium/calmodulin-dependent protein kinase II by phosphatidylinositol-linked dopamine receptor in rat brain. *Mol. Pharmacol.* (2004) **66**:1500-1507.
- Zhu YS, Saito T, Asada A, Maekawa S, Hisanaga S. Activation of latent cyclin-dependent kinase 5 (Cdk5)-p35 complexes by membrane dissociation. *J. Neurochem.* (2005) **94**:1535-1545.
- Zukerberg LR, Patrick GN, Nikolic M, Humbert S, Wu CL, Lanier LM, Gertler FB, Vidal M, Van Etten RA, Tsai LH. Cables links Cdk5 and c-Abl and facilitates Cdk5 tyrosine phosphorylation, kinase upregulation, and neurite outgrowth. *Neuron* (2000) **26**:633-646.

## VITAE



Chan Nguyen was born in Houston, Texas, on February 7, 1983, the daughter of Tu C. Tran and Tien L. Nguyen. After completing her work at Mustang High School, Mustang, Oklahoma in 1997, she attended the University of Oklahoma, where she majored in biochemistry and graduated *summa cum laude* with the degree of Bachelor of Science in May, 2000.

She spent the next ten months in the Graduate Program in Biomedical Sciences at the University of Oklahoma Health Sciences Center. In March, 2001 she entered the Medical Scientist Training Program at the University of Texas Southwestern Medical Center at Dallas. She plans to marry Huy D. Pham on June 2, 2007.

Permanent Address: 4031 Willow Leaf Ct  
Dallas, TX 75212